INTEGRATIVE ANALYSIS OF THE EPIGENETIC MODIFICATIONS IN A BREAST CANCER CELL LINE TREATED WITH A BIOACTIVE EXTRACT OF *BIDENS PILOSA*.

PIRWANA KHOLOFELO CHOKOE

THESIS

Submitted in fulfilment of the requirements for the degree of

Doctor of Philosophy

in

Biochemistry

in the

Faculty of Science and Agriculture

(School of Molecular and Life Sciences)

at the

University of Limpopo.

SUPERVISOR: Prof. LJ Mampuru

CO-SUPERVISOR: Prof. C Pheiffer (South African Medical Research Council)

2021

DECLARATION

I, Pirwana Kholofelo Chokoe, declare that **Integrative analysis of the epigenetic modifications in a breast cancer cell line treated with a bioactive extract of *Bidens pilosa*** has not been previously submitted by me for a degree at this or any other University, that it is my work in design and execution, and that all material contained herein has been duly acknowledged.

P.K Chokoe (Ms) — 16 August 2021

Initials and Surname (Title) — Date

Signature

DEDICATION

To my children; Phuti, Mmatlou, Mosa and Phenyo. May you never grow too old to broaden your horizons.

ACKNOWLEDGEMENTS

My parents, siblings and friends; your unwavering support was and is everything. Thank you.

Thank you to the staff and students of UL's Department of Biochemistry, Microbiology and Biotechnology who assisted in various aspects of this project.

I am eternally grateful to SAMRC's BRIP students and staff members. You were all ever eager to assist in the laboratory and in analysis of results. I am very grateful to the members of the epigenetics group who spent endless hours with me in the laboratory, your commitment to seeing one another's projects to fruition is worthy of commendation.

The following people deserve a special mention for their involvement in the execution of experiments and analysis of data: Prof. Vusi Mbazima (UL), Prof. Peter Masoko (UL), Mr Mashoto Matotoka (UL), Dr Sylvia Riedel (SAMRC), Dr Tarryn Willmer (SAMRC), Dr Stephanie Dias (SAMRC), Dr Babalwa Jack (SAMRC), Ms Ruzayda Van Aarde (SAMRC), Mr Thendo Mabuda (SAMRC), Mr Yoonus Abrahams (SAMRC), Mr Nkoana Mongalo (UNISA) and Mr Sol Nety (UNISA). Thank you all for the hard work you put into this study.

To my supervisor, Prof. Leseilane Mampuru and co-supervisor, Prof. Carmen Pheiffer, I thank you for your mentorship. It was a long bumpy ride and you never gave up on the project. I appreciate you support.

Thank you to SAMRC and UL for funding the study as well as for providing facilities and equipment to complete this work.

Lastly, I am eternally thankful to the Almighty, who continues to protect, sustain and bless me and mine.

TABLE OF CONTENTS

DECLARATION ii
DEDICATION iii
ACKNOWLEDGEMENTS iv
TABLE OF CONTENTS v
LIST OF FIGURES ix
LIST OF TABLES xi
LIST OF ABBREVIATIONS xii
ABSTRACT xiv
CHAPTER 1 1
1.1 INTRODUCTION 1
1.2 LITERATURE REVIEW 2
1.2.1 BREAST CANCER 2
1.2.1.1 Breast Cancer Biomarkers 3
1.2.1.2 Classification of Breast Cancer Cells 4
1.2.1.3 Hormone Receptor Status 4
1.2.1.4 Invasive and Metastatic Breast Cancer 5
1.2.2 GENES OF INTEREST IN BREAST CANCER 5
1.2.2.1 Breast cancer susceptibility proteins 6
1.2.2.2 Epithelial cadherin 7
1.2.2.3 Mutations in Breast Cells 8
1.2.3 EPIGENETIC MODIFICATIONS 8
1.2.4 METHYLATION 9
1.2.4.1 DNA Methylation in Normal Cells 10
1.2.4.2 The Role of CpG Islands 10
1.2.4.3 DNA Methyltransferases 11
1.2.4.4 Global DNA Methylation 12
1.2.4.5 Methylation Patterns in Cancer 12

1.2.4.6 Methylation in Breast Cancer 13
1.2.5 TELOMERASE ACTIVITY 14
1.2.6 BREAST CANCER TREATMENT 14
1.2.7 APOPTOSIS – Programmed Cell Death 15
1.2.8 MEDICINAL PLANTS 17
1.2.8.1 *Bidens pilosa* 18
1.3 MOTIVATION FOR THE STUDY 19
1.4 HYPOTHESIS 20
1.5 AIM 20
1.5.1 Objectives 20
CHAPTER 2 21
MATERIALS AND METHODS 21
2.1 MATERIALS 21
2.1.1 Equipment 21
2.1.2 Chemicals, Kits, Cells and Culture Media 21
2.2 METHODS 23
2.2.1 Collection and preparation of fractions 23
2.2.2 TLC analysis of phytoconstituents 25
2.2.3 TLC-DPPH antioxidant screening 25
2.2.4. DPPH radical-scavenging activity assay 25
2.2.5 Folin-Ciocalteu phenolic content assay 26
2.2.6 Folin-Ciocalteu tannin content assay 26
2.2.7 Aluminium chloride flavonoid content assay 27
2.2.8 Gas chromatography-mass spectrometry 27
2.2.9 Cell culture and maintenance 28
2.2.10 MTT cell viability assay 28
2.2.11 Mitochondrial membrane potential assay 29

2.2.12 Annexin V and dead cell assay 29
2.2.13 Cell cycle analysis 30
2.2.14 Isolation of RNA, DNA and protein 31
2.2.15 DNase treatment of RNA samples 32
2.2.16 Nucleic acid concentration and purity determination 32
2.2.17 Human Breast Cancer RT^2 Profiler PCR Array 33
2.2.18 Quantification of proteins 34
2.2.19 Western blot analysis 34
2.2.20 Global DNA methylation analysis 35
2.2.21 PCR primer design for pyrosequencing 36
2.2.22 Bisulfite conversion 37
2.2.23 PCR amplification of bisulfite-converted DNA 38
2.2.24 Pyrosequencing 39
2.2.25 Verification of PCR primers with control methylated DNA 40
2.2.26 Telomerase PCR ELISA 41
2.2.27 Statistical Analysis 42
CHAPTER 3 43
RESULTS 43
3.1 Phytochemical and TLC-DPPH antioxidant screening 43
3.2 Quantification of antioxidant activity 45
3.3 Quantification of the total phenolic content 46
3.4 Quantification of the total tannin content 47
3.5 Quantification of the total flavonoid content 48
3.6 Characterisation of *B. pilosa* fractions 49
3.7 Determination of cytotoxicity 58
3.8 Evaluation of mitochondrial membrane depolarisation 61
3.9 Detection of apoptosis 64

3.10 Cell cycle distribution analysis 65
3.11 Gene expression analysis 66
3.12 Evaluation of BRCA1 protein expression 69
3.13 Quantification of global methylation 71
3.14 Confirmation of the quality of bisulfite-converted amplicons 72
3.15 Analysis of CpG site methylation on *BRCA*1, *BRCA*2 and *CDH*1 73
3.16 Verification of pyrosequencing primers 76
3.17 Analysis of telomerase activity 77
CHAPTER 4 78
DISCUSSION AND CONCLUSION 78
4.1 General Discussion 78
4.2 Integration and analysis 88
4.3 Novelty and significance 88
4.4 Strengths and limitations 89
4.5 Future work 91
4.6 Conclusion 92
REFERENCES 93
APPENDIX A 121
GC-MS CHROMATOGRAMS 121

LIST OF FIGURES

Figure1.1: BRCA1 transcriptional complexes.

Figure 1.2: A schematic representation of the intrinsic and extrinsic apoptotic pathways.

Figure 1.3: Bidens pilosa.

Figure 2.1: Fractionation scheme of *Bidens pilosa* leaves.

Figure 2.2: Schematic representation of location and number of analysed CpG sites upstream of the transcription start site on *BRCA*1, *BRCA*2 and *CDH*1.

Figure 3.1: Thin layer chromatography profile of the crude methanol extract and six fractions of *Bidens pilosa* developed in CEF (5:4:1, v/v/v).

Figure 3.2: DPPH radical scavenging activity of the crude methanol extract and the six fractions of *Bidens pilosa.*

Figure 3.3: Total phenolic content of the crude methanol extract and six fractions of *Bidens pilosa*.

Figure 3.4: Tannin content of the crude methanol extract and six fractions of *Bidens pilosa*.

Figure 3.5: Flavonoid content of the crude methanol extract and six fractions of *Bidens pilosa*.

Figure 3.6: The effect of *Bidens pilosa* and its fractions on viability of MCF-7 cells.

Figure 3.7: The effect of the chloroform fraction of *Bidens pilosa* on viability of MCF-7 cells.

Figure 3.8A: The effect of the chloroform fraction of *Bidens pilosa* on depolarization of MCF-7 mitochondrial membranes after 12 hours.

Figure 3.8B: The effect of the chloroform fraction of *Bidens pilosa* on depolarization of MCF-7 mitochondrial membranes after 24 hours.

Figure 3.9: The effect of the chloroform fraction of *Bidens pilosa* on MCF-7 cell death.

Figure 3.10: The effect of the chloroform fraction of *Bidens pilosa* on MCF-7 cell division cycle.
Figure 3.11: Scatter plot of gene expression in MCF-7 cells treated with the chloroform fraction of *B. pilosa*.
Figure 3.12: Effect of the chloroform fraction of *B. pilosa* on BRCA1 protein expression in MCF-7 cells.
Figure 3.13: Global DNA methylation levels in MCF-7 cells treated with the chloroform fraction of *B. pilosa*.
Figure 3.14: Agarose gels of bisulfite-converted amplicons.
Figure 3.15A: *BRCA*1 CpG site methylation in *B. pilosa* chloroform fraction-treated MCF-7 cells.
Figure 3.15B: *BRCA*2 CpG site methylation in *B. pilosa* chloroform fraction-treated MCF-7 cells.
Figure 3.15C: *CDH*1 CpG site methylation in *B. pilosa* chloroform fraction-treated MCF-7 cells.
Figure 3.16: Conversion efficiency of *BRCA*1, *BRCA*2 and *CDH*1 pyrosequencing primers.
Figure 3.17: Telomerase activity in MCF-7 cells treated with the chloroform fraction of *B. pilosa*.

LIST OF TABLES

Table 2.1: Pyrosequencing primer sequences for *BRCA*1, *BRCA*2 and *CDH*1.

Table 2.2: PCR conditions for bisulfite-converted DNA samples.

Table 2.3: PCR conditions for amplification of bisulfite-converted DNA.

Table 2.4: PCR conditions for telomere repeat amplification protocol (TRAP) reaction.

Table 3.1: Major chemical compounds identified in the crude methanol extract of *Bidens pilosa*.

Table 3.2: Major chemical compounds identified in the hexane fraction of the crude methanol extract of *Bidens pilosa*.

Table 3.3: Major chemical compounds identified in the chloroform fraction of the crude methanol extract of *Bidens pilosa*.

Table 3.4: Major chemical compounds identified in the ethyl acetate fraction of the crude methanol extract of *Bidens pilosa*.

Table 3.5: Major chemical compounds identified in the butanol fraction of the crude methanol extract of *Bidens pilosa*.

Table 3.6: Major chemical compounds identified in the 65% methanol fraction of the crude methanol extract of *Bidens pilosa*.

Table 3.7: Major chemical compounds identified in the water fraction of the crude methanol extract of *Bidens pilosa*.

Table 3.8: Major chemical compounds identified in more than one fraction of *B. pilosa.*

Table 3.9: Differentially expressed genes in MCF-7 cells treated with the chloroform fraction of *B. pilosa.*

LIST OF ABBREVIATIONS

°C	Degrees centigrade (Celsius)
%	Percentage
ANOVA	One-way analysis of variance
ATCC	American Type Culture Collection
ATP	Adenosine triphosphate
BCA	Bicinchoninic acid
BRCA1	Breast cancer susceptibility type 1
BRCA2	Breast cancer susceptibility type 2
CDH1	E-cadherin
cDNA	Complementary deoxyribonucleic acid
CEF	Chloroform: ethyl acetate: formic acid
CO_2	Carbon dioxide
CpG	Cytidine-phosphate-guanosine
C_T	Threshold cycle
DMSO	Dimethyl sulfoxide
DMEM	Dulbecco's Modified Eagle's Medium
DNA	Deoxyribonucleic acid
DNMT	DNA methyltransferases
DPPH	2,2-Diphenyl-1-picryl-hydrazyl
dsDNA	Double-stranded deoxyribonucleic acid
EDTA	Ethylenediaminetetraacetic acid
EGFR	Epidermal growth factor receptor
ER	Oestrogen receptor
FBS	Foetal bovine serum
G_0	Gap 0
G_1	Gap 1
G_2	Gap 2
GAE	Gallic acid equivalents
GC-MS	Gas chromatography-mass spectrometry
HER2	Human epithelial receptor 2
M phase	Mitotic phase

mg	Milligram
mi-RNA	Micro RNA
ml	Millilitre
mm	Millimetre
mRNA	Messenger ribonucleic acid
MTT	3-(4,5-dimethylthiazol-2-yl)-2,5-diphenyl tetrazolium bromide
nm	Nanometre
PBS	Phosphate-buffered saline
PCR	Polymerase chain reaction
PR	Progesterone receptor
QE	Quercetin equivalents
RNA	Ribonucleic acid
RPM	Revolutions per minute
RSA	Republic of South Africa
TBS	Tris-buffered saline
TLC	Thin layer chromatography
USA	United States of America
µM	Micromolar
µg	Microgram
µl	Microlitre
UK	United Kingdom
UV	Ultraviolet
Vis	Visible
w/v	Weight per volume

ABSTRACT

Breast cancer is the leading cause of female deaths in the world. Varying types of therapy options are available, yet these conventional treatments for the malignancy are known to have numerous side effects. Similar to other diseases, herbal remedies are being explored as alternative treatment options as well as starting points for development of new drugs to treat breast cancer. *Bidens pilosa* is a weed distributed throughout the world with known medicinal properties. Its anti-cancer activity has been established in various cancers. This study aimed to investigate the epigenetic patterns affected by a bioactive extract of *B. pilosa* in breast cancer. A crude methanol extract of *B. pilosa* was fractionated with *n*-hexane, chloroform, ethyl acetate, *n*-butanol, 65% methanol and water. Healing properties of plants are often an attribute of the presence of phenolic compounds within the plant and the sub-fractions of the methanol extract of *B. pilosa* were, therefore, assayed for these compounds. The water sub-fraction showed the highest content of total phenolic compounds, however, when the sub-fractions were analysed for the presence of two classes of specific phenolic compounds, the butanol sub-fraction boasted the highest concentration of flavonoids and tannins, affording it superior antioxidant activity in a quantitative DPPH assay. Distribution of the antioxidant compounds in TLC-DPPH analysis also supported this finding. Despite its high antioxidant compound content, cytotoxicity of the butanol sub-fraction in MCF-7 breast cancer cells was not impressive in the MTT viability assay. Treatment with varying concentrations of the chloroform sub-fraction resulted in a better dose- and time-dependent decrease in cell viability of MCF-7 cells than all the other sub-fractions as well as the crude methanol extract. Analysis of breast cancer genes affected by the chloroform sub-fraction on the Human Breast Cancer RT^2 Profiler PCR array showed repression in *BRCA*1 and *BRCA*2, genes classified as tumour suppressors. Bisulfite pyrosequencing showed no significant modification in methylation of selected CpG islands within the promoter regions of both genes. Results of the array also showed decreased expression of *CDH*1 which is associated with invasiveness and aggression of tumours. Its investigated CpG island was also shown not to be differentially methylated by treatment of the cells with the chloroform sub-fraction of the extract. As a well-appreciated biomarker for breast cancer risk, BRCA1 protein expression was further investigated. Western blot analysis showed parallel findings to those of the PCR array, with down-regulation of BRCA1 within 24

hours of treatment of MCF-7 cells with the sub-fraction. Repression of the *BRCA* genes is strongly linked to arrest of cells at the G_2/M phase of the cell division cycle, and this was therefore also assessed. Treatment of MCF-7 cells with the chloroform sub-fraction effected a dose-dependent accumulation of cells at the G_2/M phase of the cell cycle as determined by flow cytometry. Results of global DNA methylation analysis showed an increase in chromosomal instability by a significantly reduced level of methylation of the genome. This hypomethylation also supports arrest of the cells at the G_2/M phase of the cell cycle, as cells accumulate at this checkpoint, awaiting repair to prevent segregation of broken chromosomes during mitosis. However, the lack of BRCA1 suggests that repair proteins were not recruited to the sites of repair and the cells were consequently directed to apoptosis. Analysis of the effect of the chloroform sub-fraction of the methanol extract of *B. pilosa* in the Mitopotential assay showed an increase in the number of dead cells with depolarised mitochondrial membranes, alluding to the intrinsic mode of apoptotic cell death in MCF-7 cells treated with the sub-fraction. Down-regulation of BRCA1 is further associated with telomerase inactivation in cancer cells. Treatment of MCF-7 cells with the chloroform sub-fraction reduced telomerase activity within 24 hours of treatment, with an absence of activity following treatment with 100 and 125 μg/ml of the sub-fraction. This lack of telomerase activity resulted in shortened telomeres which limit proliferative ability of the cells. Characterisation of the six sub-fractions of the methanol extract of *B. pilosa* with GC-MS showed an abundance of fatty acids in the chloroform sub-fraction, specifically α-linolenic acid, palmitic acid and linoleic acid. Palmitic acid is alleged to play a role in down-regulation of BRCA1 and its abundance in this sub-fraction leads to the conclusion that palmitic acid may be responsible for the decreased expression of BRCA1 in MCF-7 breast cancer cells. The down-regulation results in hypomethylation of the genome leading to cell cycle arrest at the G_2/M checkpoint and subsequent apoptosis as a result of this repression of BRCA1. Repression of BRCA1 also leads to inactivation of telomerase, inhibiting cell proliferation. Taken together, the observed antioxidant activity and pro-apoptotic potential attributed to epigenetic modifications validate *B. pilosa* as an anticancer agent. Our findings merit the plant for use in development of potential breast cancer drugs.

CHAPTER 1

1.1 INTRODUCTION

Breast cancer is the most common cancer in women and the leading cause of cancer-related deaths in the global female population (Sung *et al*. 2021). It has been shown that with early detection many women survive the malignancies, yet, there is still a high risk of recurrence following treatment (Bezerra *et al*. 2018; Ginsburg *et al*. 2020). Breast cancer treatment depends on the stage of the cancer and may involve therapeutic radiation, chemotherapy, hormone therapy, exploitation of the immune system in targeted therapy and immunotherapy or the lesion may require surgical removal in a lumpectomy or mastectomy (Benson, Jatoi, and Toi 2016; García-Aranda and Redondo 2019; Greenlee *et al*. 2017; Waks and Winer 2019). Most often, a combination of these therapies is required to achieve optimum outcome (Esteva *et al*. 2019; Núñez *et al*. 2016). Patients who receive neoadjuvant chemotherapy before a lumpectomy have better operation outcomes and fewer of them require follow-up surgery (Landercasper *et al*. 2017). However, among many side effects of these conventional therapies, patients undergoing chemotherapy and radiation therapy often complain of dizziness, loss of appetite, hair loss, diarrhoea, bleeding and bruising (Odle 2014; Ohnishi and Takeda 2015; Olver *et al*. 2018). This then necessitates the administration of more drugs to alleviate or mask these side effects.

Due to the adverse side effects of conventional medicines, there is a need for safer treatment options. These therapies are often offered by plant extracts as they have proven to be safer, easier to access, and are cost effective (Sen and Samanta 2014; van Wyk and Prinsloo 2018). In recent years, many people have slowly reverted to seeking healing from natural products because they have become more socially acceptable and are known to have fewer side effects than conventional synthetic drugs (Raimi *et al*. 2020). Plants and their isolated bioactive compounds have been shown to have good biological activity against a myriad of diseases including breast cancer (Levitsky and Dembitsky 2015; Mainasara, Abu Bakar, and Linatoc 2018; Onyancha *et al*. 2018; Prabhu *et al*. 2012; Richard *et al*. 2015). Still, much research is required to validate the current applications of medicinal plants as well as exploiting other plants for possible therapeutic use.

Bidens pilosa is an herb that has widely accepted medicinal use and has been found to have inhibitory action against cancer cells (Arroyo *et al*. 2010; Kumari *et al*. 2009; Raimi *et al*. 2020; Xuan and Khanh 2016). The therapeutic effect of plants on the genetic mechanisms involved in cancer are an active are of research. However, since cancer is a result of both genetic and epigenetic modifications to the genome, this study aimed to investigate if *B. pilosa* effects any epigenetic alterations in breast cancer cells that could contribute to treating the malignancy.

1.2 LITERATURE REVIEW

1.2.1 BREAST CANCER

The South African National Cancer Registry is the most comprehensive database containing pathology-based cancer data in the country, with 80 000 new cancer cases added to the repository every year (NCR, 2012). According to the NRC, breast cancer is the most prevalent cancer in South African women, followed closely by cervical cancer (NCR, 2014).

Developed regions of the world have been shown to have higher incidences of breast cancer (Ginsburg *et al*. 2020). This may be because all forms of cancer are under-reported in developing countries, like South Africa, due to poor cancer surveillance systems as well as few healthcare services available to the greater proportion of the population (Hopkins and Mkuzi 2018; Kruger and Apffelstaedt 2007). In these developing countries, women with medical cover and those of generally high socioeconomic status seemingly detect their breast cancer earlier and therefore begin treatment timeously, resulting in a more favourable outcome than their poorer counterparts (Desantis, Jemal, and Ward 2010; Ginsburg *et al*. 2020).

Numerous factors in developing countries have contributed to the increasing burden of breast cancer on healthcare systems. In Africa, race, age group and socioeconomic status have shown to be variables that play an important role in breast cancer detection and survival (Espina, McKenzie, and Dos-Santos-Silva 2017). It was reported that African and African-American women have an earlier onset of breast cancer than white women and that the cancer is less aggressive in the latter (Bertrand *et al*. 2020; Demicheli *et al*. 2007).

Prompt detection and early therapy leads to appreciable survival rates in women with breast cancer (Coleman 2017). Screening programmes for early detection of breast cancer include breast self-examination, a clinical breast examination as well as mammography (Bleyer and Welch 2012). Clinical breast examination has always been preferred as an inexpensive alternative to mammography and is reported to detect many cancers that are also detected by mammography (Alba *et al*. 2018).

Self-screening, together with mammography, are early detection methods that can save many women form the agony of surgery and extended corrective therapies. Another mode of early detection of breast cancer that is gaining momentum is the use of biomarkers that lead to or are a result of the tumour (Fang *et al*. 2011).

1.2.1.1 Breast Cancer Biomarkers

Tumour-specific biomarkers facilitate diagnosis and treatment of the malignancy at the pre-invasive stage (Misek and Kim 2011; Tsai and Baylin 2011). This then gives room for more therapy options without the need for surgery that would be most likely if the cancer were detected at a later stage. Furthermore, it allows better survival of patients. Biomarkers useful in breast cancer screening can be in the form of micro RNAs (mi-RNAs), serum proteins, ductal proteins, antibodies released in response to the tumour as well as methylated DNA (Hamam *et al.* 2017; Bhat *et al.* 2019). Due to the stability of DNA, methylation data can be obtained by extracting DNA from body fluids and analysing epigenetic markers (Misek and Kim 2011). Tracing these markers facilitates detection of tumour initiation, progression and metastasis. Detection of methylated DNA in serum has proven to be an invaluable tool for early intervention in cancer therapy (Zhang *et al*. 2016).

Circulating mi-RNAs are short sequences of non-coding, single-stranded RNA (O'Brien et al. 2015). These RNA sequences are less than 23 nucleotides long and play a pivotal role in gene regulation by degrading the 3′ untranslated region of target mRNA, repressing translation (Hamam *et al.*, 2017). In breast cancer, mi-RNAs are able to silence tumour suppressor genes or activate oncogenes. MiR-21 is a mi-RNA that is highly expressed in breast cancer and has been linked to tumour progression

as it targets mRNA encoding proteins involved in tumour suppression (Zhang *et al*. 2016). Similarly, MiR-155 targets BRCA1 and silences it interfering with DNA repair during the cell division cycle (Mattiske *et al.* 2012). Together with a panel of other mi-RNAs, both these mi-RNAs can be used to detect early stage breast cancer.

1.2.1.2 Classification of Breast Cancer Cells

Breast cancer begins when a few cells in the breast become abnormal and multiply to form a lesion or tumour in the breast tissue. The tumour usually begins in the milk ducts (ductal cancer) which is common in both men and women (Visser *et al*. 2019). It may also begin in milk-producing glands (lobular cancer) (Rakha *et al*. 2010). Men have little or no lobular tissue, therefore this type of breast cancer is less common in the male population. In fact, male breast cancer only makes up 1% of all breast cancers worldwide (Senger, Adams, and Kanthan 2017).

Early breast cancer is relatively painless, and progresses to form a noticeable lump, changes in breast shape or size, nipple discharge and changes in nipple morphology (Koo *et al*. 2017). The skin of the breast may also change and become itchy and scaly. The next stage of breast cancer may involve metastasis into surrounding tissue and to distal organs (Liu and Cao 2016).

Breast cancer is heterogeneous. It consists of an array of molecular subtypes, various cellular compositions and patients present with different clinical behaviour (Engels *et al*. 2016; Song *et al.* 2012). Furthermore, different subtypes of breast cancer have distinct biological characteristics and will therefore respond differently to treatment (Waks and Winer 2019). It is therefore important to classify tumours according to their size, grade, nodal involvement as well as hormone receptor status for accurate prognosis (Ahmed 2016).

1.2.1.3 Hormone Receptor Status

Breast cancer cells are categorized based on gene expression, most notably the expression of oestrogen receptors (ER) and progesterone receptors (PGR) as well as

human epithelial receptor 2 (HER2) (Waks and Winer 2019). Cells expressing ER and/or PGR are known as luminal cells. Cells only expressing HER2 with neither ER nor PGR expression are known as HER2 positive cells, while those expressing none of the receptors are termed triple negative breast cancer cells (Voduc *et al*. 2010). Luminal cell lines have been shown to be less aggressive than HER2 positive cells, with triple negative cells being the most aggressive and their tumours having the worst prognosis (Januškevičienė and Petrikaitė 2019; Turashvili and Brogi 2017). Luminal cells are also more differentiated and have tight cell-cell junctions, making them less likely to migrate or metastasize (Ahmed 2016).

1.2.1.4 Invasive and Metastatic Breast Cancer

Breast cancer cells retain the morphology and function of normal breast cells (Eslami Amirabadi *et al*. 2019). Still, various genetic and epigenetic changes gradually manifest within breast epithelial cells to promote malignancies. Invasive breast cancer occurs when malignant tumour cells spread from the duct to the stroma of the adjacent tissue (Chan and Lim 2010). A significant histological change occurring during this transition is a loss of an external layer of myoepithelial cells as well as the basement membrane. The myoepethelial barrier is known to introduce protease inhibitors and other components of the extracellular matrix to the lesion that may also assist in tumour suppression (Rohilla *et al*. 2015). These molecules act as paracrine and autocrine tumour suppressors as well as regulators of invasion, angiogenesis and metastasis (Al Nemer 2017).

Metastatic breast cancer, also known as stage IV cancer, occurs in almost 30% of all breast cancers and accounts for 90% of breast cancer deaths (Chaffer and Weinberg 2011; Chen *et al*. 2018). Cells that migrate from the tumour spread to the liver, brain, bones and/or lungs to begin other tumours in the new location (Chen *et al*. 2018; Ishay-Ronen and Christofori 2019).

1.2.2 GENES OF INTEREST IN BREAST CANCER

Breast cancer prognosis has been shown to be strongly reliant on the hormone receptor status of the tumour, with each receptor giving the tumour characteristics that

can be used to predict progression and select suitable therapy (Bae *et al*. 2015; Jonasson *et al*. 2016; Tang *et al*. 2019). The three hormone receptors, ER, PGR and HER2, assist in decision making for breast cancer patients (Feeley *et al*. 2014). ER/PGR-positive tumours metastasize; however, patients have been shown to survive longer and the tumour responds more effectively to various forms of therapy than in ER/PGR-negative tumours (Li *et al.* 2014). Further, ER/PGR positive tumours have less risk of recurrence if identified early and have caused less deaths following adjuvant therapy, which cannot be said for tumours with a negative ER/PGR status (Murata *et al*. 2019; Sestak *et al*. 2013).

The breast cancer susceptibility type 1 and type 2 proteins (BRCA1 and BRCA2) are responsible for many inherited breast cancers, with women carrying an inherited *BRCA1* mutation having a higher probability of developing the disease at some point in their life (Speight and Tischkowitz 2017). Although *BRCA* mutations are rare in sporadic cancer, expression of the *BRCA* genes decrease in 30% breast cancers (Zhu *et al.* 2015; Blows *et al.* 2010; De Leeneer *et al.* 2012). In epithelial ovarian cancer, low expression and absence of BRCA1 was shown to be a predictor of good clinical response to chemotherapy, therefore a favourable prognostic factor (Carser *et al*. 2011).

1.2.2.1 Breast cancer susceptibility proteins

BRCA1 and *2* encode the breast cancer type 1 and type 2 susceptibility proteins, nuclear phosphoproteins that are involved in repair of double stranded DNA breaks (Huen, Sy, and Chen 2010). Both proteins fall in the tumour suppressor family of proteins as their expression is associated with prevention of dysregulated cell proliferation and resultant tumourigenesis (Henderson 2012). The proteins interact with other tumour suppressor proteins, DNA damage sensors and signal transducers to form a multi-unit complex termed BRCA1-associated surveillance complex (BASC) (Rosen 2013). This complex interacts with RNA polymerase II as well as histone deacetylases and play an important part in transcription, repair of double stranded DNA breaks as well as DNA recombination (Savage and Harkin 2015).

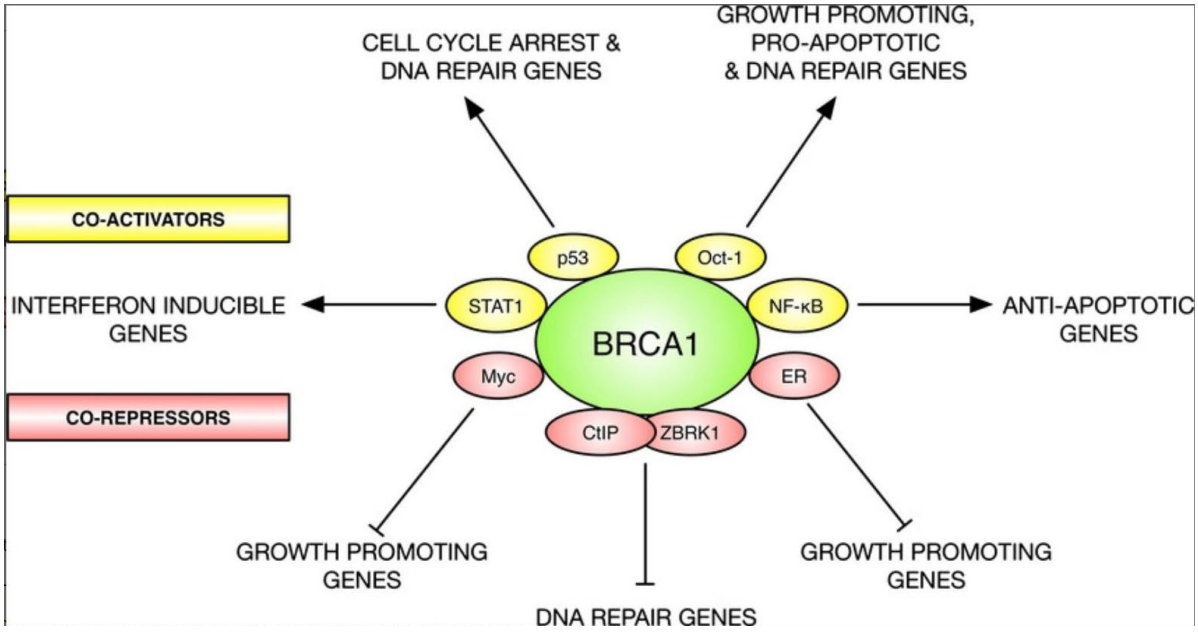

Figure1.1: **BRCA1 transcriptional complexes.** BRCA1 forms transcription complexes with the ability to either co-repress or co-activate genes involved in various cellular processes (Savage and Harkin 2015).

1.2.2.2 Epithelial cadherin

*CDH*1 encodes the calcium-regulated adhesion molecule, epithelial cadherin (E-cadherin). E-cadherin is a protein that is expressed in breast tissue and is associated with cell-to-cell adhesion in normal adult epithelial cells (Gall and Frampton 2013). It is classified as a tumour suppressor gene and reduction of its expression causes differentiation and invasiveness in human tumours (Wendt *et al*. 2011). Cells that lose E-cadherin undergo epithelial-to-mesenchymal transition wherein polarised epithelial cells undergo numerous modifications to give them the mesenchymal phenotype (Loh *et al*. 2019). These non-polarised mesenchymal cells are invasive and migrate to other organs to initiate formation of new tumours (Gall and Frampton 2013).

Downregulation of *CHD*1 is also associated with Loss of E-cadherin is known to occur very early in carcinogenesis although its effects are only observed later during tumour progression (Wendt *et al*. 2011). It is reported that this loss is not only due to genetic alterations but also from modifications at the epigenetic level. Promoter hypermethylation plays a pivotal role in silencing *CDH*1 in breast cancer and this down-regulation is associated with poor prognosis, i.e. larger tumours, high

histological grade and metastasis; as well as poor overall survival (Loh *et al*. 2019; Tan *et al.* 2015; Wong *et al*. 2018).

1.2.2.3 Mutations in Breast Cells

It is important to identify risk factors for breast cancer and this is an active area of medical research. Mutations in critical genes controlling cell growth and DNA repair can often go unrepaired, resulting in unregulated growth of affected cells. These mutations may be inherited or somatic (occurring during development). Somatic mutations occur in various genes but only in specific cells. On the contrary, inherited mutations are present in virtually all cells in the body and increase the risk of various cancers from birth.

Mutations in *BRCA*1 and *BRCA*2 genes are inherited and are used as markers in predicting ovarian and breast cancer risk for cancer in women (Shinjo and Kondo 2015; Stefansson *et al.* 2012). Mutations in these two genes are inherited in an autosomal dominant pattern, with a single copy of a faulty gene inherited from either parent sufficient to increase cancer risk (Rosen 2013). *BRCA* genes are high penetrance genes; i.e. mutations in these genes increase the chances of developing cancer (Sadeghi *et al*. 2020). Low and moderate penetrance genes do not have much influence on cancer risk, unless in addition to other mutated genes.

Although inherited mutations are very common, breast cancers are mostly caused by somatic mutations acquired during development (Vos, Moelans, and van Diest 2017). The cancer is not inherited, but the risk. The status of the mutation has been linked to treatment type.

1.2.3 EPIGENETIC MODIFICATIONS

Cumulative discoveries have demonstrated how various modifications of the genome can alter gene expression without changing the sequence of nucleotides, culminating in tumour formation (Davalos and Esteller 2010; Dawson and Kouzarides 2012; Drake and Søreide 2019; Park and Han 2019). These epigenetic changes are heritable, yet reversible, and can involve DNA or RNA as well as proteins associated with

packaging, replication, transcription, translation or repair of nucleic acids (Virani *et al*. 2012).

Analogous to genetic modifications, epigenetic changes are a consequence of DNA damage, oxidative stress, diet, aging and environmental elements (Franco *et al*. 2008; Varela-Rey *et al*. 2012; Ziech *et al.* 2011). Manifestations of these factors lead to progressive silencing or activation of specific genes (Sandoval and Esteller 2012). Epigenetic alterations that have been thoroughly studied include methylation, acetylation and phosphorylation of the genome (Burger, Ketley, and Gullerova 2019; Moore, Le, and Fan 2013; Nowsheen *et al*. 2014; Orouji and Utikal 2018; Rousseaux and Khochbin 2015).

1.2.4 METHYLATION

DNA methylation is donation of a methyl group to the 5′ position of a cytosine residue (5mC) (Shinjo and Kondo 2015). This covalent attachment occurs on a cytosine-guanine (CG) dinucleotide, prevalent in promoter regions on a nucleotide sequence (Vos *et a*l. 2017). The clustering of CG dinucleotides has made these regions well-known as CpG islands, regions usually exceeding 200 base pairs in length containing more than 50 % content of CG dinucleotides (Babenko *et al*. 2017; Kowal *et al*. 2020).

Addition of a methyl moiety onto a nucleotide introduces an obstacle to transcription factors and polymerases, therefore DNA methylation at CpG islands is associated with repression of gene expression or gene silencing (Kakumani, Ahmad, and Devabhaktuni 2012). The methyl group of 5mC is situated in the major groove of the DNA double helix (Rao *et al*. 2018). This positioning, indeed, disrupts binding of transcription factors and inhibits gene expression. The methyl group can also recruit protein families whose function is to repress transcription by inhibiting the binding of transcription factors as well (Moore *et al.* 2013).

Patterns of methylation are usually stable and heritable. Together with these heritable manifestations, certain environmental conditions can trigger the onset of further modifications (Han *et al*. 2016). DNA methyltransferases (DNMTs) are enzymes responsible for induction of methyl group transfers triggered by environmental insults

(Wang, Chen, and Shen 2014). Some of these transferases induce novel methylation marks while others enforce existing methylation patterns (Zhang *et al*. 2020).

1.2.4.1 DNA Methylation in Normal Cells

During normal development, mandatory methylation of CpG regions in the genome occurs. This serves to control growth of the embryo, transcription of DNA, inactivation of the X chromosome in females as well as determination of gene mapping (Cotton *et al*. 2015; Li *et al*. 2018). Many CpG islands in promoter regions remain unmethylated, while repetitive sequences in the genome are hypermethylated to ensure stability of chromosomes, i.e. prevent transposition of the elements (Zheng *et al*. 2017).

Although many methods have been developed to evaluate DNA methylation; they all use either affinity purification of methylated DNA, digestion of DNA with methylation-sensitive restriction enzymes or bisulfite conversion. In affinity purification methods, a monoclonal antibody specific to methylated cytosine is used to purify methylated DNA through immunoprecipitation (Bock *et al*. 2010; Robinson *et al*. 2010). With this technique, the density of methylation in a specific region of DNA is quantified. Restriction-enzyme based methylation analysis measures the extent of methylation by either enriching for methylated or unmethylated DNA (Hashimoto *et al*. 2007). A comparison is then made with a (un)methylated DNA control digested with the same methylation-sensitive restriction enzyme (Hua *et al.* 2011).

Treatment of genomic DNA with sodium bisulfite causes deamination of unmethylated cytosine residues to uracil and PCR amplification of the DNA results in substitution of the uracil nucleotides with thymine (Delaney, Garg, and Yung 2015). The degree of methylation can then be measured with sequencing methods, often pyrosequencing (Kumar, Dalan, and Carless 2020).

1.2.4.2 The Role of CpG Islands

The mammalian genome has DNA sequences with a high frequency of CpG base pairs that somehow escape the mandatory methylation observed throughout the rest of the genome (Hughes, Kelley, and Klose 2020). The sequences have been shown

to be associated with promoters in constitutively expressed genes and of genes with tissue specific expression (Ehrlich, Baribault, and Ehrlich 2020). This is consistent with the co-localisation of CpG islands with gene-rich sequences of the genome. CpG islands that are found outside transcription start sites have led to discoveries of promoters of genes that are evidently expressed at certain development stages (Li *et al*. 2018; Moore *et al*. 2013).

It is necessary to analyse the mode by which CpG islands remain hypomethylated. A mechanism by which CpG islands remain unmethylated has been hypothesized as involving transcription factors (Zhu *et al*. 2017). Bound transcription factors on the DNA strand impede association of DNA methyltransferases with the nucleic acid thus preventing methylation of cytosines. Due to the regulatory potential of CpG islands on promoter regions, they have gained much attention in various areas of medical research (Goren *et al*. 2006). The transcriptional repression instigated by methylation of CpG islands is a crucial aspect associated with tumour initiation and progression, as silencing of tumour suppressor genes can be attributed, in part, to acquisition of methyl moieties on CpG islands (Manoochehri *et al*. 2016; Vos *et al*. 2017).

1.2.4.3 DNA Methyltransferases

The initiation and progression of cancer takes place over years and methylation of CpG residues within promoter regions is accepted to occur early in the initiation stages of the neoplasm through the action of various DNA methyltransferases (DNMT) (Zhang *et al.* 2020). The DNMT3 family of methyltransferases methylates CpG sites through *de novo* methylation while the DNMT1 family maintains methylation during DNA replication (Gujar, Weisenberger, and Liang 2019). DNMT3b is active during implantation and early embryogenesis and DNMT3a plays a significant role during late development of the embryo as well and during cell differentiation (Chen and Zhang 2020; Yagi et al. 2020). During DNA replication, it is the responsibility of DNMT1 to retain the integrity of the methylation pattern at CpG sites during the S-phase of the cell cycle (Loo *et al*. 2018; Schneider *et al*. 2013).

It has been shown that demethylation of a methylated CpG island on a promoter sequence restores expression of the gene while remethylation induces repression (De

Biase et al. 2020; Ketkar et al. 2020). Mutations in DNMT3b that result in loss of methylation function support the hypothesis that hypomethylation of the genome results in chromosome instability, as many tumours with mutated DNMT3b have rearranged chromosomes (Kim *et al*. 2013; Shah and Licht 2011; Siraj *et al*. 2019).

1.2.4.4 Global DNA Methylation

Half of the human genome is composed of repetitive elements. In non-cancerous tissue, these intergenic regions are hypermethylated, protecting chromatin from digestion by endonucleases (Kaw and Blumenthal 2010; Si *et al.* 2009). Repetitive sequences close to centromeres are important for the key role that they play in chromosome stability (Barra and Fachinetti 2018). These regions keep the DNA molecule packaged into heterochromatin during sister chromatid association. Hypomethylation of the CpG sequences in these tandem repeats causes decondensation of heterochromatin and may lead to translocation and amplification of genes involved in tumour initiation (Ehrlich 2002; Rajshekar *et al*. 2018).

Methylation of the entire genome is important in the development and progression of cancer, and is termed a cancer methylome fingerprint (Gómez *et al*. 2015; Kulis *et al*. 2015). In many cancers, global methylation decreases due to the loss of methyl groups at repetitive sequences and introns (Zheng *et al*. 2017). These methylation changes occurring away from promoter regions are mostly evident in repetitive elements in distal regulatory regions within the genome (Cho *et al*. 2010; Gujar *et al*. 2019; Zhu *et al*. 2011). A decrease in global DNA methylation was one of the first epigenetic alterations to be identified in human cancer tissue and the extent of global methylation has been shown to be indicative of the extent of tumour progression in virtually all cancer cell types (Ehrlich 2009; Sandoval and Esteller 2012).

1.2.4.5 Methylation Patterns in Cancer

In cancer, hypomethylation of the genome is prominent (Ehrlich 2009). Global hypomethylation leads to expression of genes that promote development and growth of tumours, while hypermethylation at certain CpG islands will silence genes that repress tumour development (tumour suppressor genes) (Kuchiba *et al*. 2014;

Spencer *et al*. 2017). Hypomethylation has also been hypothesized to favour genomic instability by playing a significant role in chromosomal instability and abnormal chromosome structure (Nishida *et al.* 2012; Kawano *et al.* 2014).

Methylation of promoter regions in certain genes is a known marker for cancer. There are specific methylation biomarkers for individual cancer types, and these occur at designated sites of the genome. The growth arrest and DNA-damage-inducible protein alpha (*GADD*45a) is an important biomarker in differentiating benign prostate cancer from the malignant disease as methylation of the gene is significantly higher in malignant patients (Reis *et al*. 2015). Similarly, hypermethylation at the promoter region of the tumour suppressor gene, E-cadherin (*CDH*1), is known to be associated with progression of breast cancer and is used as a biomarker for the malignancies (Asiaf *et al*. 2014).

1.2.4.6 Methylation in Breast Cancer

Early stages of breast cancer initiation involve both genetic and epigenetic manifestations (Pasculli, Barbano, and Parrella 2018). The most prominent epigenetic modifications driving initiation and progression of breast carcinomas are DNA methylation, histone modifications and non-coding RNAs (Bhat *et al*. 2019; Lewis, Jordan, and Tollefsbol 2018). Initially, changes in methylation patterns occur as well as the post-translational modification of proteins bound to DNA (Park and Han 2019). Increased methylation in CpG regions (promoters) of some genes, e.g. *BRCA*1, is associated with increased risk of breast cancer (Zhang and Long 2015). This has been reported in genes mostly associated with cell cycle regulation, DNA repair, apoptosis, metastasis, cell adhesion, cell-signalling and transcription regulation (Agrawal, Murphy, and Agrawal 2007; Beetch *et al*. 2020; Fang *et al*. 2011; Hung *et al*. 2018; Kobayashi *et al*. 2013). On the contrary, increased methylation in sequences away from promoters decreases risk of breast cancer by increasing genome stability (Cho *et al*. 2010).

Mutations in the *BRCA*1 gene were one of the first anomalies to be associated with a risk of breast cancer (Sadeghi *et al.* 2020). Moreover, hypermethylation at the gene's promoter region has also been identified and thoroughly studied (Cai *et al*. 2014; Vos

et al. 2017; Zhu *et al*. 2015). Methylation in this region has been associated with an increase in the early onset of breast cancer, making this particular promoter an important biomarker for early detection of malignancies (Carser *et al*. 2011).

1.2.5 TELOMERASE ACTIVITY

In mammalian cells, the ends of chromosomes contain TTAGGG hexameric repeats called telomeres (Rosen 2013). These are conserved, repetitive sequences of DNA at the end of linear chromosomes that confer protection against genomic instability caused by the gradual loss of nucleotides during DNA replication (Günes and Rudolph 2013). Telomeres function to keep the integrity of the genome during replication, however, each replication cycle results in shortening of the telomeres as DNA polymerase cannot replicate the very ends of the DNA strand (Koziel and Herbert 2015). In all cells telomerase, an RNA-dependent DNA polymerase, is employed to elongate the extreme ends of DNA (Günes and Rudolph 2013). Activity of this enzyme is tightly regulated and is only observed in cells that are constantly replicating, e.g. germ cells, and very rarely in somatic cells (Can Akincilar, Unal and Tergaonkar, 2016). In cancer cells, however, telomerase is reactivated, giving the cells unlimited proliferative ability (Tong *et al*. 2015).

Numerous synthetic telomerase inhibitors have been developed, albeit with significant toxicity (Röth, Harley, and Baerlocher 2010). Imetelstat, a synthetic telomerase inhibiting compound, has been investigated in breast cancer and it potentiates the effects of paclitaxel and trastuzumab in mammary tumours (Koziel and Herbert 2015; Röth *et al*. 2010). Inhibiting the activity of telomerase is one of the many attempts at treating malignancies by targeting epigenetic manifestations.

1.2.6 BREAST CANCER TREATMENT

Breast cancer survival has increased substantially in the past 40 years by 40%, with metastasis risk decreasing by 80% (Jemal *et al*., 2017). This is attributed to implementation of earlier screening methods as well as better modes of treatment for the malignancy. A special contributing factor to better survival rates for breast cancer patients is adjuvant radiotherapy, adjuvant chemotherapy as well as adjuvant

endocrine therapy (Cheng *et al*. 2015; Jurrius *et al*. 2020). Yet, once breast cancer has metastasized, treatment can include surgery, chemotherapy, radiation, hormonal therapy or targeted therapy (Song *et al*. 2012). The main treatment is surgery, then it is necessary to determine which patients will benefit from further therapy, i.e. chemotherapy, hormone therapy and radiation therapy, but treatment is always aimed maximum benefit for the patient (Esserman and Yau 2015).

Cancer research has expanded into investigating drugs with the potential to correct epigenetic aberrations, specifically reactivation of silenced tumour suppressor genes (Bhat *et al*. 2019). The main advantage of epigenetic treatment is the reversibility of epigenetic manifestations in the genome. Reversal of epigenetic anomalies is often achieved by demethylating agents that remove the methyl moieties bound to cytosine nucleotides on promoters of tumour suppressor genes (Xu *et al*. 2010). These demethylating agents must demonstrate anticancer activity *in vitro*, attributed to induction of apoptosis.

1.2.7 APOPTOSIS – Programmed Cell Death

There are numerous events that can lead to the destruction or death of cells. Certain assaults, both chemical and physical, cause destruction of cells in mechanisms specific to the particular injury. Some modes of cell death, however, are regulated and play significant roles in development in multicellular organisms (Fuchs and Steller 2011; De Paepe *et al.* 2019). They occur inevitably as part of homeostatic fine-tuning in the growth of organisms. These forms of regulated cell death can either be a result of external disturbances to the cellular environment or they are part of an predictable built-in mechanism that controls development (Voss and Strasser 2020). Innate molecular mechanisms of self-destruction are observed in many diseases and disorders such as autoimmune disorders and cancer (Volpe *et al.* 2018; Favaloro *et al.* 2012).

The most common mode of regulated cell death is apoptosis or programmed cell death, where cells employ their own cellular machinery for self-destruction and resultant debris is ingested by neighbouring cells (phagocytosis) for lysosomal degradation (Nainu, Shiratsuchi, and Nakanishi 2017; Sierra *et al*. 2010). Apoptosis

can be induced by disturbances in the cellular environment, either intracellularly or extracellularly.

Intrinsic apoptosis, mostly occurs due to a defective cell cycle, production of excess reactive oxygen species and diminished growth requirements that often lead to irreparable DNA damage (Green and Llambi 2015; Nguyen, Willmore, and Tayabali 2013). Intrinsic apoptosis is marked most notably by the irreversible permeabilisation of the outer mitochondrial membrane, while the plasma membrane remains intact (Galluzzi *et al.* 2018). Increased permeability of the outer membranes of mitochondria occurs as a results of a decrease in the mitochondrial membrane potential, an electrical/chemical gradient (Gottlieb *et al*. 2003). Permeability of the mitochondrial membrane leads to release of cytochrome c into the cytosol which then initiates a cascade of reactions that result in apoptosis (Zorova *et al*. 2018).

On the other hand, the extrinsic mode of apoptosis does not involve disturbances to the mitochondrial membrane, but rather the plasma membrane(Green and Llambi 2015). This suggests that the extrinsic pathway of apoptosis is triggered by external assaults to the cell, activating plasma membrane receptors involved in programmed cell death (Loreto *et al.* 2014). These receptors are known as death receptors. Signals identified by death receptors are often produced by cytotoxic T cells in response to damaged or infected cells (Pfeffer and Singh 2018). The ligands bind to tumour necrosis factor family death receptors which in turn bind to adaptor proteins to form a death domain (Goldar *et al*. 2015). A cascade of events follows upon binding of the death domain to procaspases that eventually culminates in cell death (Green and Llambi 2015).

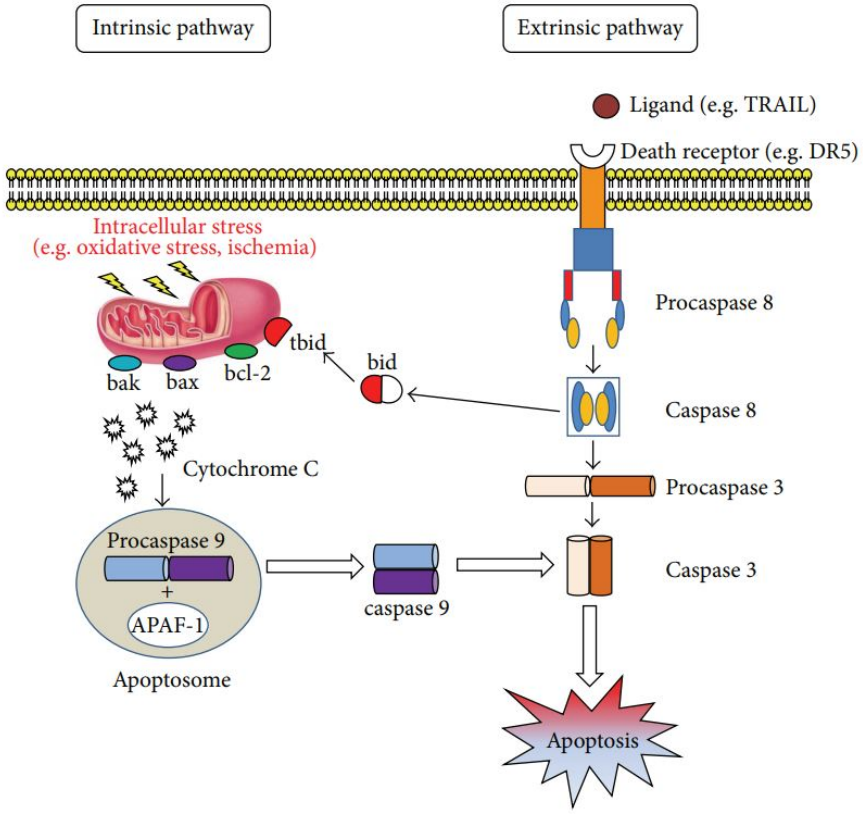

Figure 1.2: **A schematic representation of the intrinsic and extrinsic apoptotic pathways.** (Loreto *et al*. 2014).

1.2.8 MEDICINAL PLANTS

Plants have been used for countless applications by man and animals since the beginning of time. Mankind has been using plants for food, shelter, clothing, as well as for medicinal purposes; with a great deal of knowledge on medicinal plants being passed down generations over the years (van Wyk and Prinsloo 2018).

Plants synthesize secondary metabolites (phytochemicals or phytocompounds) that are key players in environmental adaptation, unlike primary metabolites, that are required for basic functions, i.e. cell growth, respiration and reproduction (Cheynier 2012). Phytocompounds protect plants from various biotic and abiotic assaults, including ultra-violet light, pathogens and herbivores (Lee and Min 2019). Phytochemicals contain medically relevant classes of compounds, especially the flavonoids (phenolic compounds), sesquiterpenoids and diterpenoids (terpenoids) (Shaikh and Patil 2020).

Phenolic compounds are a widespread group of phytochemicals possessing an aromatic ring with one or more hydroxyl groups and are responsible for the colour and taste of plants (Ozcan *et al*. 2014). Phenolics have significant radical-scavenging activity, making them good antioxidants (Olas 2018; Roleira *et al*. 2015). These compounds can be divided further into phenolic acids, flavonoids, tannins and stilbenes. Flavonoids are low molecular weight compounds consisting of 15 carbon atoms (Palma 2017). They are the most abundant phenolic compounds in the human diet and are prevalent in fruits, vegetables, wine and tea (Cheynier 2012). Tannins are of higher molecular weights and are known to confer a myriad of health benefits in humans including antibacterial, anti-inflammatory, anti-oxidative and anticancer activity (Cai *et al*. 2017; Wahyuni *et al*. 2020). Tannins are also abundant in fruits, vegetables and cocoa, giving many plants their bitter taste (Soares *et al*. 2020). Owing to their antioxidant nature, phenolic compounds have been shown to possess anti-carcinogenic activity and protect DNA against free-radical damage (Wahyuni *et al*. 2020).

As the interest in medicinal plant research continues to soar, so do the possible choices in selecting plants for various applications. Often, very little is known about the phytochemical constituents present in plants selected by traditional medical practitioners for treatment of ailments. Research is then based on hypotheses on the biological activity and a broad spectrum of extraction methodologies may be employed (Gupta, Naraniwal, and Kothari 2012).

1.2.8.1 *Bidens pilosa*

B. pilosa is one of approximately 240 identified species of the *Bidens* genus, growing all over the world (Bartolome, Villaseñor and Yang, 2013). The plant is an upright perennial herb distributed widely throughout the world; with either white or yellow flowers, green opposite leaves and many long, thin, ribbed seeds (Yang 2014). Although some varieties of *B. pilosa* can grow up to 1.5 m, the average height of the plant is 60 cm. With a single plant able to produce up to 6000 seeds, propagation of *B. pilosa* in a favourable environment (tropical or temperate climates) has garnered it a reputation as a weed as not only do the seeds germinate within 3 days, but they remain viable for 3 years or more.

Figure 1.3: **Bidens pilosa.** (https://commons.wikimedia.org/w/index.php?curid=10880484)

All parts of *B. pilosa* have shown to have some medicinal properties and have been in use worldwide to treat a myriad of disorders (Liang *et al*. 2020; Xuan and Khanh 2016). The plant boasts an array of phytocompounds, with 201 reportedly already identified (Bartolome, Villaseñor and Yang, 2013). These compounds are supposedly responsible for its wide array of medicinal applications. Isolated secondary metabolites from *B. pilosa* plant parts have important biological activities that include antibacterial, anti-inflammatory, anti-malarial, antiseptic, anticancer, hypoglycaemic, diuretic, anti-diabetic, and hepato-protective activity (Ajanaku *et al*. 2018; Bilanda *et al*. 2017; Chang *et al*. 2007; Cortés-Rojas *et al*. 2013; Hsu *et al*. 2009; Pegoraro *et al*. 2021)

1.3 MOTIVATION FOR THE STUDY

Recent searches for anticancer agents involve investigating plants currently used for various traditional medicinal purposes and testing these plants for possible drug leads. There are records of the anti-tumour activity of *Bidens pilosa*, yet there are disparities on its use against breast cancer (Arroyo *et al*. 2010; Raimi *et al*. 2020; Shen *et al*. 2018; Steenkamp and Gouws 2006; Yi *et al*. 2016). The rich supply of phytochemicals in *B. pilosa* makes it an attractive candidate for further studies in cancer development

and progression. Due to the important role that epigenetic modulation plays in cancer progression (Stefansson *et al*. 2012), the elucidation of epigenetic mechanisms regulated by anti-cancer therapeutics is receiving increased momentum worldwide. Several studies have reported that phytochemicals such as flavonoids inhibit cancer progression by modulating epigenetic mechanisms (George, Dellaire, and Rupasinghe 2017; Izzo, Naponelli, and Bettuzzi 2020; Selvakumar *et al*. 2020). It has therefore become necessary to further investigate the role plants may play in modulating cancer progression through epigenetic alterations in the search for favourable cancer therapies.

1.4 HYPOTHESIS

Bidens pilosa modifies methylation patterns and modulates telomerase activity in MCF-7 cells in a manner that mitigates proliferation of breast cancer cells.

1.5 AIM

The aim of the study was to investigate the epigenetic alterations effected by *Bidens pilosa* in the MCF-7 breast cancer cell line.

1.5.1 Objectives

The specific objectives of the study were to:

i. Fractionate *Bidens pilosa* using organic solvents of varying polarity;
ii. Quantify phenolic content of the fractions;
iii. Evaluate cytotoxicity of the fractions in the MCF-7 breast cancer cell line;
iv. Assess the effect of the most active fraction on global DNA methylation levels in MCF-7 cells;
v. Assess the effect of the most active fraction on the DNA methylation status of breast cancer-associated genes in MCF-7 cells;
vi. Analyse expression of breast cancer-associated genes known to be regulated by differential methylation in MCF-7 breast cancer cells and
vii. Evaluate alterations in telomerase activity in MCF-7 cells treated with the most active fraction of *B. pilosa*.

CHAPTER 2

MATERIALS AND METHODS

2.1 MATERIALS

2.1.1 Equipment

Waring Commercial Blendor (**Dynamics Corporation, New Hartfort, USA**)

SP-UV 300 spectrophotometer (**Spectrum Instruments, Addison, USA**)

7890N Gas chromatography instrument, J & W capillary column HP-5MS (**Agilent Technologies, Santa Clara, USA**)

LECO Pegasus HT Flight Mass Spectrometry Time (**LECO Corporation, Michigan, USA**)

Carbon dioxide incubator, Nanodrop™ One Microvolume UV-Vis Spectrophotometer, Qubit® fluorometer, Quantstudio 7™ Flex Real-Time PCR System, Thermal Cycler (**Thermo Fisher Scientific, Waltham, USA**)

Glomax®-Multi Detection System (**Promega Corporation, Madison, USA**)

Muse® Cell Analyzer (**Merck, Darmstadt, Germany**)

Heating block (**Labnet International Inc., Edison, USA**)

SpectraMax i3x spectrophotometer (**Molecular Devices LLC, San Jose, USA**)

Trans-Blot® Turbo™ transfer system, ChemiDoc™ MP Imaging System (**Bio-Rad, Hercules, USA**)

Orbital plate shaker (**IKA, Staufen, Germany**)

2.1.2 Chemicals, Kits, Cells and Culture Media

Organic solvents (**Rochelle Chemicals, Johannesburg, RSA**)

Thin layer chromatography plates (**Macherey-Nagel, Düren, Germany**)

Whatman No.1 filter paper, 2,2-Diphenyl-1-picryl-hydrazyl (DPPH), Folin-Ciocalteu's reagent, Sodium carbonate ($NaHCO_3$), Sodium nitrate ($NaNO_3$), Gallic acid,

Quercetin, Aluminium chloride ($AlCl_3$), Sodium hydroxide (NaOH), GC-MS grade organic solvents, Phosphate buffered saline (PBS), 3-(4,5-Dimethylthiazol-2-yl)-2,5-diphenyl tetrazolium bromide (MTT), Skim milk, Imprint® Methylated DNA Quantification kit, Streptavidin sepharose beads, Nuclease-free water, *T*elo*TAGGG*™ Telomerase PCR ELISA kit (**Sigma-Aldrich, Saint Louis, USA**)

Helium (**Afrox, Johannesburg, RSA**)

MCF-7 cell culture (**ATCC, Rockville, USA**)

Dulbecco's Modified Eagle Medium (DMEM) (**Gibco, Auckland, New Zealand**)

Fetal bovine serum (FBS), Trypsin-ethylenediaminetetraacetic acid (Trypsin-EDTA) (**Hyclone, Logan, USA**)

Dimethylsulfoxide (DMSO) (**Merck, Darmstadt, Germany**)

Muse® Mitopotential kit, Muse® Annexin V and Dead Cell kit, Muse® Cell Cycle kit (**Luminex, Austin, USA**)

AllPrep® Mini kit, Human Breast Cancer RT^2 Profiler PCR Array, RT^2 First Strand kit, *BRCA*1*, BRCA*2 *and CDH*1 pyrosequencing primers, EpiTect® Fast Bisulfite Conversion kit, PyroMark PCR kit, PyroMark binding buffer, PyroMark denaturation solution, PyroMark wash buffer, PyroMark annealing buffer, Bisulfite converted control human DNA (**Qiagen, Hilden, Germany**)

TurboDNase kit, Qubit® dsDNA Broad-Range Assay kit, MicroAmp optical adhesive film, Pierce® BCA Protein Assay kit (**Thermo Fisher Scientific, Waltham, USA**)

Quick Start™ Bovine Serum Albumin Standard Set, Laemmli sample buffer, PVDF membranes, Tris-buffered saline (TBS), Clarity™ Western ECL Substrate, (**Bio-Rad, Hercules, USA**)

GAPDH, β-actin, BRCA1, BRCA2 primary antibodies, horseradish peroxidase-conjugated secondary antibody (**Abcam, Cambridge, UK**)

DNA loading dye, Molecular weight marker (**Lonza, Basel. Switzerland**)

2.2 METHODS

2.2.1 Collection and preparation of fractions

Leaves of *Bidens pilosa* were collected in Soekmekaar, Limpopo (GPS coordinates: 23.946°S, 29.929°E) in summer and a specimen was submitted to the Larry Leach Herbarium (University of Limpopo) for verification. The leaves were dried in open air at room temperature. Dried leaves were ground into fine powder with a Waring Commercial Blendor (Model 32BL79, Dynamics Corporation, New Hartfort, USA) and extracted exhaustively with absolute methanol (10 g sample/100 ml solvent). The sample was shaken vigorously at room temperature overnight and filtered with Whatman No.1 filter paper (Sigma-Aldrich, St. Louis, USA). The methanol was evaporated under a stream of air. Thereafter, the dried crude methanol residue was resuspended in chloroform/water (1:1, v/v) and fractionated using solvent/solvent extraction into 6 fractions: *n*-hexane (B1), chloroform (B2), ethyl acetate, (B3), *n*-butanol (B4) fraction, 65% methanol (B5) and water (B6). The fractions were left to dry under a stream of air at room temperature. A schematic representation of the fractionation procedure is illustrated in Figure 2.1.

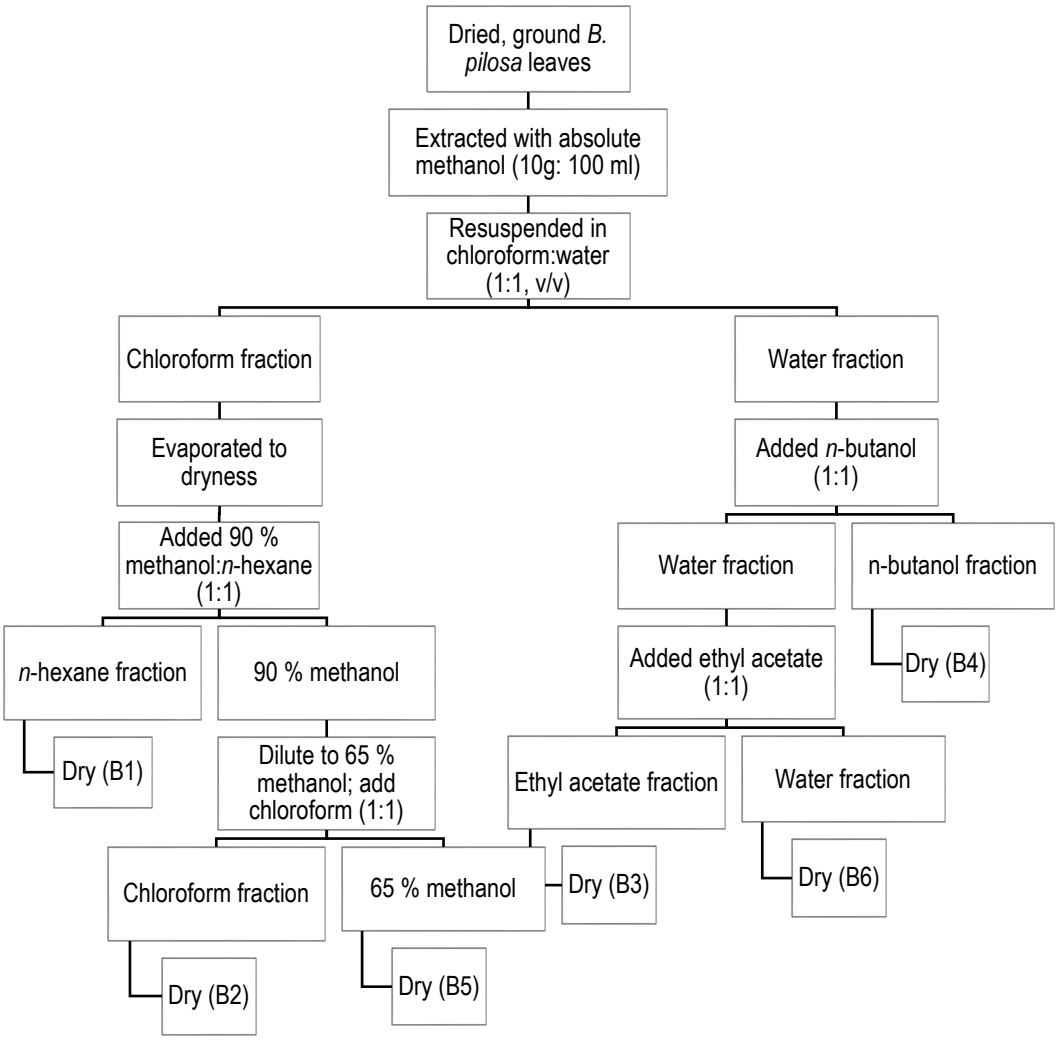

Figure 2.1: Fractionation scheme of *Bidens pilosa* leaves.

2.2.2 TLC analysis of phytoconstituents

The range and distribution of secondary metabolites present in plant extracts can be visualised by a quick, inexpensive method that involves separation of the compounds by thin layer chromatography (TLC) (Marston 2011). To assess the phytocompounds present in *Bidens pilosa*, the crude methanol extract and it six fractions of varying polarity were reconstituted to 10 mg/ml in dimethylsulfoxide (DMSO). Ten microliters of each sample was loaded onto an aluminium-backed, silica gel TLC plate (Macherey-Nagel, Düren, Germany) and the plate was developed in CEF (chloroform: ethylacetate: formic acid; 5: 4: 1, v/v/v). This mobile phase was selected from preliminary TLC trials conducted with numerous mobile phases for analysis of *B. pilosa* phytoconstituents (not included in this document). The plate was sprayed with vanillin (0.1 g vanillin, 28 ml methanol, 1 ml sulphuric acid) and heated at 110°C for 30 minutes in an oven for colour development.

2.2.3 TLC-DPPH antioxidant screening

Rapid screening of plant extracts for compounds with antioxidant activity is commonly performed by assessment of the ability of separated compounds to scavenge free radicals (Agatonovic-Kustrin, Morton, and Ristivojeví 2016). The presence of antioxidant compounds within the crude methanol extract of *B. pilosa* and its six fractions was confirmed by chromatographic separation of the fractions as above (Section 2.2.2) and spraying the plates with 0.2% 2,2-diphenyl-1-picryl-hydrazyl (DPPH) (Sigma-Aldrich, Saint Louis, USA) in absolute methanol. DPPH is reduced from violet to a yellow diphenylpicryl hydrazine in the presence of an antioxidant compound (Pourmorad, Hosseinimehr, and Shahabimajd 2006).

2.2.4. DPPH radical-scavenging activity assay

Antioxidant activity of the crude methanol extract as well as the six fractions of *B. pilosa* was quantified by a spectrophotometric assay where the percentage of DPPH reduced to hydrazine was measured. A serial dilution of each sample (15.625, 31.25, 62.5, 125 and 250 μg/ml in acetone) was prepared in test tubes and 1 ml of 0.2 mM DPPH (Sigma-Aldrich, Saint Louis, USA) in methanol was added to each well. The plate was incubated at room temperature for 30 minutes in the dark and

absorbance was measured at 517 nm in an SP-UV 300 spectrophotometer (Spectrum instruments, Addison, USA). Acetone was used as a blank. The scavenging activity of each sample was calculated as follows:

$$\% \text{ inhibition} = \frac{[A_{517} \text{ of blank} - A_{517} \text{ of sample}]}{A_{517} \text{ of blank}} \times 100$$

2.2.5 Folin-Ciocalteu phenolic content assay

Plant phenolic compounds are a diverse group of secondary metabolites produced during normal development and when the plant experiences unfavourable conditions. They include flavonoids, phenolic acids and tannins, among others, and have excellent antioxidant activity (Cheynier 2012; Niroula et al. 2019). To quantify the total phenolic compounds present in *B. pilosa*, 250 µl of Folin-Ciocalteu's reagent (Sigma-Aldrich, Saint Louis, USA) was added to 500 µl of 20 µg/ml of each sample and incubated for 5 minutes in the dark. Thereafter, 1.25 ml of 7% sodium carbonate ($NaHCO_3$) (Sigma-Aldrich, Saint Louis, USA) was added and incubated for 30 minutes in the dark. Absorbance was read at 550 nm in a SP-UV 300 spectrophotometer (Spectrum instruments, Addison, USA). A serial dilution (0, 0.016, 0.031, 0.0625, 0.125 and 0.25 mg/ml) of gallic acid (Sigma-Aldrich, Saint Louis, USA) was prepared and the above method was used for construction of a standard curve for interpolation of sample concentrations. The total phenolic content of the crude methanol extract and each of the six fractions was expressed as gallic acid equivalents (mg of GAE/g of extract).

2.2.6 Folin-Ciocalteu tannin content assay

The tannins contained within the various fractions prepared from the crude methanol extract of *B. pilosa* were quantified by adding 100 µl of Folin-Ciocalteu's reagent (Sigma-Aldrich, Saint Louis, USA) to 1.5 ml of 133 µg/ml of each sample for 5 minutes in the dark. Two milliliters of 35% $NaHCO_3$ (Sigma-Aldrich, Saint Louis, USA) was added to each reaction and incubated for 30 minutes in the dark. Absorbance was measured at 725 nm in a SP-UV 300 spectrophotometer (Spectrum instruments, Addison, USA). Similarly, a serial dilution (0, 0.016, 0.031, 0.0625, 0.125 and 0.25

mg/ml) of gallic acid (Sigma-Aldrich, Saint Louis, USA) was prepared for construction of a standard curve for interpolation of sample concentrations. Total tannin content of the samples was expressed as gallic acid equivalents (mg of GAE/g of extract).

2.2.7 Aluminium chloride flavonoid content assay

The six fractions of *B. pilosa* were assayed for their flavonoid content alongside the crude methanol extract. Briefly, 300 µl of 5% (w/v) sodium nitrate ($NaNO_3$) (Sigma-Aldrich, Saint Louis, USA) was added to 5 ml of 0.2 mg/ml of each sample and left to react for 5 minutes at room temperature. Thereafter, 300 µl of 10% (w/v) aluminium chloride ($AlCl_3$) (Sigma-Aldrich, Saint Louis, USA) was added and incubated for a further 5 minutes. Two millilitres of 1 M sodium hydroxide (NaOH) (Sigma-Aldrich, Saint Louis, USA) was added and absorbance was measured at 510 nm in a SP-UV 300 spectrophotometer (Spectrum instruments, Addison, USA). A standard curve was constructed by analysis of a serial dilution (0, 0.313, 0.625, 1.25, 2.5, 5 and 10 mg/ml) of quercetin (Sigma-Aldrich, St. Louis, USA) as above. Flavonoid content of the samples was expressed as quercetin equivalents (mg of QE/g of extract).

2.2.8 Gas chromatography-mass spectrometry

The myriad of compounds abundant in the crude methanol extract of *B. pilosa* and its six fractions were identified using gas chromatography performed on a gas chromatography instrument (7890N GC-MS, Agilent Technologies, Santa Clara, USA) coupled to a LECO Pegasus HT Time-of-Flight Mass Spectrometer (TOFMS) (LECO Corporation, Michigan, USA). Briefly, samples were completely dissolved to 0.05 mg/ml in GC-MS grade methanol (Sigma-Aldrich, St. Louis, USA) and a very small volume of the reconstituted samples re-dissolved in acetonitrile (GC-MS grade, Sigma-Aldrich, St. Louis, USA). Thereafter, the samples were loaded into a Gerstel MPS2 Liquid/HS/SPME auto-sampler. For chromatographic separation, 1 µl of each sample was injected at 250ºC with a splitless injector into a J & W capillary column HP-5MS 30 X 0.25 mm I.D with a film thickness of 0.25 µM (Agilent, Technologies, Santa Clara, USA) and 99.99% helium (Afrox, Johannesburg, RSA) was used as a carrier at a constant flow of 1 ml/min. The oven was set to 80ºC for 1 minute, then ramped to 280°C at 10ºC per minute for 20 minutes. The interface temperature of the

GC/TOFMS was set to 280ºC and the mass spectra of samples were obtained in full scan mode at 70 eV (m/z scan varying from 50 to 550). Data was collected with ChromaTOF (Version 5.0, LECO Corporation, Michigan, USA), which contains a NIST 95 library for compound matches.

2.2.9 Cell culture and maintenance

A human breast cancer cell line, MCF-7 (ATCC® HTB-22™), obtained from the American Type Culture Collection (ATCC, Rockville, USA) was used for all cell culture assays. Cells were cultured in Dulbecco's Modified Eagle's Medium (DMEM) (Gibco, Auckland, New Zealand) supplemented with 10% foetal bovine serum (FBS) (Hyclone, Logan, USA). The culture flasks were maintained in a Heracell™ 150i carbon dioxide (CO_2) incubator (Thermo Fisher Scientific, Waltham, USA) at 37°C with 5% CO_2 and 80% humidity.

2.2.10 MTT cell viability assay

Cytotoxicity of the crude methanol *B. pilosa* extract and its fractions in MCF-7 cells was evaluated with the MTT (3-(4,5-dimethylthiazol-2-yl)-2,5-diphenyl tetrazolium bromide) assay. One hundred microliters of cells was seeded at 2.5 x 10^5 cells/ml in 96-well cell culture plates and incubated at 37°C overnight, followed by treatment with varying concentrations (from 25 to 800 μg/ml) of the crude *B. pilosa* plant extract and six fractions of varying polarity. Thereafter, cells were incubated at 37°C and viability was assessed at 24 and 48 hours. Without removing the treatment, cytotoxicity of each fraction was measured by adding 30 μl of 5 mg/ml MTT (Sigma-Aldrich, Saint Louis, USA) in phosphate buffered saline (PBS) (Sigma-Aldrich, Saint Louis, USA) to wells of the 96-well plates, and the plates were incubated at 37°C for 2 hours. The MTT was decanted and replaced with 100 μl of DMSO (Merck, Darmstadt, Germany) to dissolve the violet crystals and absorbance was read on a Glomax®-Multi Detection System (Promega Corporation, Madison, USA) at 560 nm. Results are presented as percentage of viability of untreated cells, calculated as follows:

$$\% \text{ viability} = \frac{C-T}{C} \times 100$$

where **C** (control) is the mean of the absorbance of the wells with untreated cells, and **T** (treated) is the mean of the absorbance of wells containing extract-treated cells.

2.2.11 Mitochondrial membrane potential assay

The cytotoxic effects of *B. pilosa* on MCF-7 cells were further investigated by assessing depolarization of mitochondrial membranes following treatment with the crude methanol extract and its six fractions. A fluorescent, lipophilic cationic dye is used to analyse depolarization of mitochondrial membranes following treatment with test compounds. Compounds that cause apoptosis decrease mitochondrial membrane potential resulting in less dye being able to cross the outer membrane from the cytoplasm, while healthy cells accumulate more dye. Cells were seeded at 2.5 x 10^5 cells/ml in 48-well cell culture plates and incubated at 37°C overnight, followed by treatment with 75, 100 and 125 µg/ml of the crude *B. pilosa* plant extract as well as its six fractions of varying polarity. Cells were incubated at 37°C and mitochondrial membrane depolarization was assessed at 12 and 24 hours by flow cytometry with the Muse® MitoPotential kit (Luminex, Austin, USA). Briefly, cells were detached from the wells by decanting the extract and adding 100 µl of 0.25% trypsin-ethylenediaminetetraacetic acid (trypsin-EDTA) (Hyclone, Logan, USA) and incubating for 5 minutes at 37°C. The reaction was stopped by adding 100 µl of DMEM with 10% FBS to the trypsin-EDTA. Thereafter, 100 µl of cells from 3 pooled wells per concentration were added to 95 µl of Muse® mitopotential working solution and incubated for 20 minutes at 37°C followed by addition of 5 µl of Muse® mitopotential 7-AAD (Luminex, Austin, USA). Samples were incubated for 5 minutes at room temperature and analysed on the Muse® Cell Analyzer (Merck, Darmstadt, Germany).

2.2.12 Annexin V and dead cell assay

Programmed cells death can be detected by differential staining of viable, apoptotic and dead cells by exploiting changes in the integrity of the plasma membrane between these cells (Demchenko 2013). The apoptotic potential of the chloroform fraction of the crude methanol extract of *B. pilosa* in MCF-7 cells was analysed using Muse® Annexin V and Dead Cell kit. Cells were seeded at 2.5 x 10^5 cells/ml in 48-well cell culture plates and incubated overnight at 37°C, followed by treatment with 75, 100 and

125 µg/ml of the chloroform fraction of *B. pilosa.* Cells were detached from the wells by decanting the extract and adding 100 µl of 0.25% trypsin-EDTA (Hyclone, Logan, USA) and incubating for 5 minutes at 37°C. The reaction was stopped by adding 100 µl of DMEM with 10% FBS to the trypsin-EDTA. Thereafter, cells were resuspended in the Annexin V & dead cell assay stain (Luminex, Austin, USA) for 30 minutes in the dark and analysed on the Muse® Cell Analyzer (Merck, Darmstadt, Germany) to obtain the percentage of live, early apoptotic, late apoptotic, total apoptotic, and dead cells.

2.2.13 Cell cycle analysis

Analysis of the cell cycle is crucial in understanding the mechanism of action of many cancer treatments (Williams and Stoeber, 2012). The Muse® Cell Cycle kit utilises propidium iodide to stain DNA, enabling enumeration of cells in each phase of the cell cycle due to differences in DNA content (https://www.luminexcorp.com/muse-cell-cycle-kit). Cells were seeded at 2.5 x 10^5 cells/ml in 48-well cell culture plates and incubated overnight at 37°C. To synchronise the cells in the G_0/G_1 phase of the cell division cycle, the growth medium was aspirated and 500 µl of DMEM without FBS was added to the cells. The serum-starved cells were treated with 75, 100 and 125 µg/ml of the chloroform fraction of *B. pilosa* and incubated 24 hours at 37°C. To harvest the cells, the treatment was decanted, 100 µl of 0.25% trypsin-EDTA (Hyclone, Logan, USA) was added and plates were incubated for 5 minutes at 37°C. Thereafter, 100 µl of DMEM with 10% FBS was added to the trypsin-EDTA. Cells were centrifuged for 5 minutes at 1000 rpm and washed once with 200 µl PBS. One millilitre of ice-cold 70% ethanol was added drop-wise to each sample, incubated for 3 hours at -20°C and centrifuged at 1000 rpm for 5 minutes. Cells were washed by adding 200 µl PBS to the tubes and centrifuging at 1000 rpm for 5 minutes. Two hundred microliters of Muse® cell cycle reagent (Luminex, Austin, USA) was added to each tube and incubated in the dark for 30 min. The percentage of cells in the various phases of the cell division cycle was quantified using the Muse® Cell Analyzer (Merck, Darmstadt, Germany).

2.2.14 Isolation of RNA, DNA and protein

Total RNA, DNA and proteins were isolated using the AllPrep® Mini kit according to the manufacturer's instructions (Qiagen, Hilden, Germany). The AllPrep® kit allows simultaneous extraction of RNA, DNA and proteins from one biological sample, by exploiting the different binding specificities of these molecules Briefly, MCF-7 cells were seeded at a density of 2.5 x 10^5 cells/ml in 6-well cell culture plates and left to attach to the plates for 24 hours. Thereafter, cells were treated with 75, 100 and 125 µg/ml of the *B. pilosa* chloroform fraction for 24 and 48 hours. A volume of 500 µl of 0.25% trypsin-EDTA (Hyclone, Logan, Utah) was added to each well to detach the cells and three wells per concentration were pooled together. Cells were pelleted by centrifugation at 1000 rpm for 5 minutes. The cell pellet was resuspended in 350 µl of buffer RLT, whereafter the mixture was transferred to a QIAshredder spin column in a 2 ml collection tube. Tubes were centrifuged at 13 000 rpm for 2 minutes. The homogenized lysate was transferred to an AllPrep® DNA spin column in a 2 ml collection tube and centrifuged at 13 000 rpm for 30 seconds. Thereafter, the DNA spin column was placed into a new 2 ml collection tube and stored at 4°C for DNA isolation. For RNA extraction, 250 µl of 100 % ethanol was added to the flow-through in the collection tube and the mixture transferred to an RNeasy spin column in a 2 ml collection tube. The tube was centrifuged at 13 000 rpm for 15 seconds and the flow-through transferred to a 2 ml microcentrifuge tube and stored at 4°C until protein extraction. The spin column membrane was washed by adding 700 µl of buffer RW1 to the spin column and centrifugation at 13 000 rpm for 15 seconds, whereafter the flow-through was discarded. A volume of 500 µl of buffer RPE was added to the RNeasy spin column, the tube centrifuged at 13 000 rpm for 15 seconds and the flow-through discarded. Residual ethanol was removed by a second wash step with 500 µl buffer RPE, whereafter tubes were centrifuged at 13 000 rpm for 2 minutes. The RNeasy spin column was placed into a new 1.5 ml collection tube and RNA eluted by adding 50 µl of RNase-free water and centrifugation at 13 000 rpm for 1 minute. RNA was stored at -80°C. For protein extraction, 600 µl of buffer APP was added to the flow-through that was previously kept aside during RNA extraction, tubes vortexed and incubated at room temperature for 10 minutes to precipitate proteins. Tubes were centrifuged at 13 000 rpm for 10 minutes and supernatants were discarded. The pellet was resuspended in 500 µl of 70% ethanol and centrifuged at 13 000 rpm for 1 minute,

whereafter the supernatant was discarded. After drying for 10 minutes, the pellet was dissolved in 100 µl of 5% sodium dodecyl sulphate (SDS) and incubated for 5 minutes at 95°C on a heating block (Labnet International Inc., Edison, USA). Tubes were cooled to room temperature and centrifuged at 13 000 rpm for 1 minute to precipitate undissolved material and the supernatant, which contained proteins, was stored at -20°C. Genomic DNA was purified by adding 500 µl of buffer AW1 to the AllPrep® DNA spin column that was stored at 4°C and the tubes were centrifuged at 13 000 rpm for 15 seconds. The flow-through was discarded and 500 µl buffer AW2 was added to the spin column and centrifuged at 13 000 rpm for 2 minutes. The DNA spin column was transferred to a new 1.5 ml collection tube and 100 µl of buffer EB (preheated to 70°C) was added. The tubes were incubated at room temperature for 2 minutes and centrifuged for 1 minute at 13 000 rpm. The eluted DNA was stored at -20°C.

2.2.15 DNase treatment of RNA samples

Genomic DNA was eliminated from RNA preparations using the TurboDNase kit, according to the manufacturer's instructions (Thermo Fisher Scientific, Waltham, USA). Briefly, 5 µl of DNase buffer was mixed with 46 µl of RNA (20 µg), whereafter 1 µl of DNase was added and mixed by tapping. Tubes were incubated at 37°C for 30 minutes. The contents of the tubes were mixed again by tapping, followed by further incubation for 30 minutes at 37°C. The reaction was stopped by adding 10 µl of DNase inactivating reagent and shaking tubes in an orbital shaker for 5 minutes at 25°C. The tubes were centrifuged at 13 000 rpm for 1.5 minutes and 46 µl of the supernatant was transferred to a 2 ml microcentrifuge tube. Samples were stored at -80°C.

2.2.16 Nucleic acid concentration and purity determination

RNA and DNA concentration and purity were measured using a Nanodrop™ One Microvolume UV-Vis Spectrophotometer (Thermo Fisher Scientific, Waltham, USA) as recommended by the manufacturers. The average of two measurements for each sample was used. Nucleic acids absorb light at 260 nm (A_{260}), while proteins and other contaminants absorb at 280 nm (A_{280}) (Desjardins and Conklin 2010). The ratio of $^{A260}/_{A280}$ was used to assess the purity of RNA and DNA. An $^{A260}/_{A280}$ ratio of ~1.8 and

~2.0 is generally accepted as pure (Desjardins and Conklin 2010). In addition to Nanodrop, DNA for bisulfite conversion and pyrosequencing, were quantified with the Qubit® dsDNA Broad-Range Assay Kit (Thermo Fisher Scientific, Waltham, USA) protocol using a Qubit® fluorometer (Thermo Fisher Scientific, Waltham, USA) according to the manufacturer's instructions.

2.2.17 Human Breast Cancer RT^2 Profiler PCR Array

The Human Breast Cancer RT^2 Profiler PCR Array (Qiagen, Hilden, Germany) was used to investigate whether the chloroform fraction of *B. pilosa*, altered the expression of cancer-associated genes. The array contains 84 genes associated with breast cancer, five endogenous controls to normalise gene expression and genomic DNA, reverse transcription and three positive PCR controls. RNA was reverse transcribed to complimentary DNA (cDNA) using the RT^2 First Strand Kit according to manufacturer's instructions (Qiagen, Hilden, Germany). Briefly, genomic DNA elimination mix was prepared by adding 2 µl of buffer GE to 7 µl of RNA (160 ng) and RNase-free water to a total volume 10 µl. The mixture was incubated at 42°C for 5 minutes, and thereafter placed on ice for 1 minute. For each sample, 10 µl of reverse transcription mix was prepared by adding 1 µl of control P2, 4 µl of 5x buffer BC3, 2 µl of reverse transcriptase and 3 µl of RNase-free water. The reverse transcriptase mix was added to 10 µl of genomic DNA elimination mix and gently mixed by pipetting. Tubes were incubated at 42°C for 15 minutes and 95°C for 5 minutes. Thereafter, 91 µl of RNase-free water was added to each reaction and tubes were placed on ice. For PCR analysis, 102 µl of diluted cDNA was mixed with 650 µl of RT^2 SYBR Green Mastermix and 548 µl of RNase-free water. Thereafter, 10 µl of each sample was aliquoted into wells of the PCR plate. The plate was sealed with MicroAmp optical adhesive film (Thermo Fisher Scientific, Waltham, USA) and centrifuged at 3000 rpm for 1 minute at room temperature. Thereafter, the plate was placed in the Quantstudio 7™ Flex Real-Time PCR System (Thermo Fisher Scientific, Waltham, USA), and the reaction was run using the following cycle conditions: denaturation for 15 minutes at 95°C, and combined annealing and extension for 40 cycles at 60°C for 1 minute. After the run, default settings for the threshold cycle (C_T) and baseline were used, and C_T values were exported to Microsoft Excel (2013) for analysis. The C_T values were

uploaded onto the data analysis web portal for analysis (http://www.qiagen.com/geneglobe). Gene expression was quantified using the delta-delta C_T method and normalised to the housekeeping gene, glyceraldehyde-3-phosphate dehydrogenase (GAPDH), which was identified as the best endogenous control from the PCR array using Norm finder (Vandesompele *et al*., 2002). Samples with C_T values above 35 were removed from the analysis.

2.2.18 Quantification of proteins

Protein concentrations were measured using the Pierce® BCA Protein Assay Kit (Thermo Fisher Scientific, Waltham, USA) according to the manufacturer's instructions. Briefly, protein samples were diluted 1:25, whereafter 25 µl was aliquoted in duplicate into wells of a clear 96-well, flat-bottomed microtiter plate. This was followed by the addition of 200 µl of BCA reagent and incubation at room temperature for 30 minutes in the dark. Eight dilutions between 0.125 mg/ml to 2 mg/ml of the Quick Start™ Bovine Serum Albumin (BSA) Standard Set (Bio-Rad, Hercules, USA) were used as standards and lysis buffer was used as a blank. Absorbance was read at 570 nm on the SpectraMax i3x spectrophotometer (Molecular Devices LLC, San Jose, USA) and protein concentration extrapolated from the standard curve, taking dilution factor into account.

2.2.19 Western blot analysis

The breast cancer susceptibility type 1 protein (BRCA1) plays an important role in the aetiology and progression of breast cancer, as well as how breast cancer cells respond to treatment (Carser *et al*. 2011). Alterations in the expression of BRCA1 after treatment with the chloroform fraction of *B. pilosa* were assessed using Western blot analysis. Thirty micrograms of protein in Laemmli sample buffer (Bio-Rad, Hercules, USA) was boiled for 5 minutes and loaded onto a 12% sodium dodecyl sulphate polyacrylamide gel and electrophoresed at 120 volts for 2 hours. The gel was transferred to a PVDF membrane at 18 volts for 10 minutes using a Trans-Blot® Turbo™ transfer system (Bio-Rad, Hercules, USA). The non-specific binding of antibodies was prevented by blocking the membrane in 3% skim milk (Sigma-Aldrich, St. Louis, USA) in TBS-Tween buffer (1x TBS, 1% Tween-20) for 2 hours on a shaker

before incubation with a 1:1000 dilution of the housekeeping protein, GAPDH (Abcam, Cambridge, UK) in TBS-Tween buffer at 4°C overnight on a shaker. Following incubation, the antibody was removed, and the membrane was washed by shaking in TBS-Tween buffer for 10 minutes at room temperature. The wash step was repeated thrice. Thereafter, the membrane was incubated with a 1:10 000 dilution of horseradish peroxidase-conjugated secondary antibody (Abcam, Cambridge, UK) in 1.5% skim milk for 2 hours, and washed as described previously. Reactive proteins were visualized with the Clarity™ Western ECL Substrate and the ChemiDoc™ MP Imaging System (Bio-Rad, Hercules, USA). To detect BRCA1, the membrane was blocked with 3% skim milk and incubated with 1:250 dilution of BRCA1 (Abcam, Cambridge, UK) and subsequent procedures conducted as described previously. The intensity of each band relative to control was calculated using ImageJ software (Version 1.150i bundled with Java 1.6.0_20, US National Institute of Health, Bethseda, USA).

2.2.20 Global DNA methylation analysis

Global DNA methylation was quantified using the Imprint® Methylated DNA Quantification Kit (Sigma-Aldrich, St. Louis, USA), according to the manufacturer's instructions. Briefly, wells of an assay strip were coated with 30 µl of DNA (50 ng) in DNA binding solution. The assay strips were covered and incubated for 60 minutes at 37°C. This was followed by the addition of 150 µl of block solution and a further incubation for 30 minutes at 37°C. The wells were emptied and washed three times with 150 µl of wash buffer before addition of 50 µl of a 1:1000 dilution of the capture antibody, covered and incubated for 60 minutes at room temperature. The antibody was decanted, and the wells were washed four times with 150 µl of wash buffer. A 1:1000 dilution of detection antibody (50 µl) was added to each well and incubated for 30 minutes at room temperature, followed by its removal and washing of the wells with 150 µl of wash buffer five times. A volume of 100 µl of developing solution was added to each well, covered and incubated at room temperature in the dark until the solution developed a blue colour (approximately 10 minutes), after which 50 µl of stop solution was added to each well and absorbance read at 450 nm in a SpectraMax i3x spectrophotometer (Molecular Devices LLC, San Jose, USA). The percentage of methylation was calculated relative to the 50 ng methylated control DNA.

2.2.21 PCR primer design for pyrosequencing

One CpG island was randomly selected per promoter region of three genes of interest that were identified from the PCR array (breast cancer type 1 susceptibility protein (*BRCA*1), breast cancer type 2 susceptibility protein (*BRCA*2) and epithelial cadherin (*CDH*1)). Primers for each of the genes were designed using the PyroMark Assay Design 2.0 software. DNA sequences were downloaded from Ensembl (https://www.ensembl.org/index.html). As illustrated in Fig. 2.2, the primers designed for *BRCA*1 spanned six CpG sites in the promoter region, 2310 base pairs upstream of the transcription start site on chromosome 17, while that for *BRCA*2 included ten CpG sites 984 base pairs from the transcription start site on chromosome 13. The PCR primers for *CDH*1 extended over seven CpG sites, flanking the transcription start site on exon 1 of chromosome 16 (Fig. 2.2). Primer sequences are tabulated in Table 2.1.

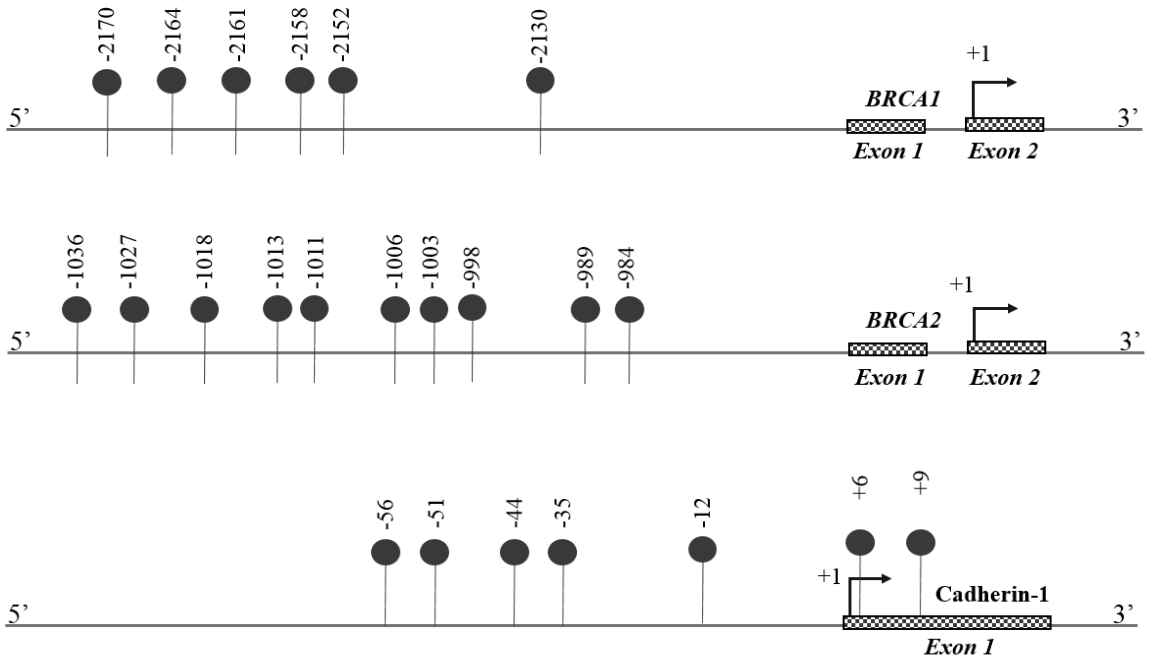

Figure 2.2: Schematic representation of location and number of analysed CpG sites upstream of the transcription start site on *BRCA*1*, BRCA*2 *and CDH*1.

Table 2.1: Pyrosequencing primer sequences for *BRCA*1, *BRCA*2 and *CDH*1

	ID	Sequence	Length (bp)	Tm (°C)	%GC
		***BRCA*1**			
Forward	F1*	5′ TTTGTGGGGTGAATTTAATATGG 3′	23	57.8	34.8
Reverse	R1	5′ ACCCCTCAACCCCAATATTTA 3′	21	60.3	42.9
Sequencing	S1	5′ CAACCCCAATATTTATTATTTTTC 3′	24	45.6	25.0
		***BRCA*2**			
Forward	F2	5′ TGAAGGTTGGGATGTTTGATAAGG 3′	24	58.3	41.7
Reverse	R2*	5′ ATCACAAATCTATCCCCTCAC 3′	21	58.3	42.9
Sequencing	S2	5′ GTAGAGGTTTATTTAGGTTTGATTT 3′	25	44.9	28.0
		***CDH*1**			
Forward	F3	5′ TTGGTTGTGGTAGGTAGGTGAATT 3′	24	59.5	41.7
Reverse	R3*	5′ AACTTCCCCAAACTCACAAATACTTTAC 3′	28	56.8	35.7
Sequencing	S3	5′ GTAGGTGAATTTTTAGTTAATTAG 3′	24	44.2	25.0

bp: base pairs, Tm: Melting temperature, %GC: Guanine/Cytosine content, *BRCA*1: Breast cancer type 1 susceptibility, *BRCA*2: Breast cancer type 2 susceptibility, *CDH*1: Epithelial cadherin, F1: *BRCA*1 forward primer, R1: *BRCA*1 reverse primer, S1: *BRCA*1 sequencing primer, F2: *BRCA*2 forward primer, R2: *BRCA*2 reverse primer, S2: *BRCA*2 sequencing primer, F3: *CDH*1 forward primer, R3:*CDH*1 reverse primer, S3: *CDH*1 sequencing primer, *: Biotinylated.

2.2.22 Bisulfite conversion

Sodium bisulfite deaminates unmethylated cytosine residues to uracil, which are converted to thymine during PCR amplification, while methylated cytosines remain intact (Lee *et al*. 2013). Pyrosequencing of these amplicons allow detection of methylated cytosines residues. Bisulfite conversion was conducted using the EpiTect® Fast Bisulfite Conversion Kit (Qiagen, Hilden, Germany) according to the manufacturer's recommendations. Forty microliters of DNA (500 ng) was incubated with 85 µl of bisulfite solution, 15 µl of DNA protect buffer and RNase-free water in a total volume of 140 µl in PCR tubes. The bisulfite conversion was performed in a Thermal Cycler (Thermo Fisher Scientific, Waltham, USA) with the conditions set out in Table 2.2.

Table 2.2: PCR conditions for bisulfite-converted DNA samples.

Step	Temperature (°C)	Time (min)
1. Denaturation	95	5
2. Incubation	60	20
3. Denaturation	95	5
4. Incubation	60	20
5. Hold	20	∞

∞: indefinite

After bisulfite conversion, DNA samples were purified. Samples were briefly centrifuged and contents were transferred to 1.5 ml Eppendorf tubes. Thereafter, 310 µl of loading buffer (Buffer BL) was added to each sample, followed by 15 seconds of vortexing and brief centrifugation. A volume of 250 µl of ethanol was added to each sample, followed by 15 seconds of vortexing and brief centrifugation. The entire volume of each sample was then transferred to a MinElute DNA spin column. Spin columns were centrifuged at maximum speed for 1 minute and the flow-through from the collection tubes was discarded. Five hundred microlitres of wash buffer (Buffer BW) was added to the spin column and samples were centrifuged at maximum speed for 1 minute. Again, the flow-through from the collection tubes was discarded. This was followed by the addition of 500 µl of desulfonation buffer (Buffer BD) and 15 minutes incubation at room temperature, whereafter tubes were centrifuged at maximum speed for 1 minute. After the flow-through had been discarded, the retained DNA was washed twice with 500 µl of Buffer BW before adding 250 µl of ethanol and centrifuging at maximum speed for 1 minute. The spin columns were transferred to clean microcentrifuge tubes, centrifuged for 1 minute at maximum speed and incubated for 5 minutes in a 60°C heating block (Labnet International Inc., Edison, USA) to remove remaining ethanol. DNA was eluted by transferring spin columns into clean microcentrifuge tubes, incubating each sample in 15 µl elution buffer (Buffer EB) for 1 minute and centrifuging at 16 000 rpm for 1 minute. Bisulfite-converted DNA was stored at -20°C.

2.2.23 PCR amplification of bisulfite-converted DNA

Amplification of bisulfite-converted DNA was carried out using the PyroMark PCR kit (Qiagen, Hilden, Germany), according to the manufacturer's instructions. Each PCR reaction contained the following: 12.5 µl of PyroMark PCR Master Mix, 2.5 µl of CoralLoad® Concentrate, 0.1 µl of forward and reverse primer, and 25 ng of bisulfite

converted DNA. Each sample was made up to 25 µl with RNase free water. The 96-well microtiter plate was sealed and centrifuged at 1000 rpm for 1 minute. DNA was amplified in a Veriti thermal cycler (Thermo Fisher Scientific, Waltham, USA) using the conditions set out in Table 2.3.

Table 2.3: PCR conditions for amplification of bisulfite-converted DNA.

Step	Temperature (°C)	Time (min)	Cycles
1. Activation	95	15	1
2. Denaturation	94	0.5	
3. Annealing of genomic DNA	60	0.5	
4. Annealing of bisulfite-converted DNA	56	0.5	45
5. Extension	72	0.5	
6. Extension	72	10	1

Prior to pyrosequencing, the quality of PCR products was analysed by agarose gel electrophoresis. Briefly, 5 µl of each amplicon was mixed with 2 µl of 6 X DNA Loading Dye (Lonza, Basel, Switzerland), after which samples were loaded on a 1.5% agarose gel alongside 5 µl of a 100 bp molecular weight marker (Lonza, Basel, Switzerland) and electrophoresed at 115 volts for 1 hour. The gel was visualized using the ChemiDoc™ MP Imaging System (Bio-Rad, Hercules, USA).

2.2.24 Pyrosequencing

Pyrosequencing is a sequencing-by-synthesis method that can be applied to measure DNA methylation at CpG sites (Delaney *et al*. 2015). For this procedure, 20 µl of the amplified PCR product was added to each well of a 96-well PCR plate together with 1.5 µl of streptavidin sepharose beads (Sigma-Aldrich, St. Louis, USA), 40 µl of PyroMark binding buffer (Qiagen, Hilden, Germany) and 20.5 µl of nuclease-free water (Sigma-Aldrich, St. Louis, USA). The PCR plate was then tightly sealed with MicroAmp optical adhesive film (Thermo Fisher Scientific, Waltham, USA) and agitated for 10 minutes on an orbital plate shaker (IKA, Staufen, Germany) at 1400 rpm. Meanwhile, the PyroMark Q96 workstation was set up for PCR strand separation by adding 110 ml of 70% ethanol, 90 ml of denaturation solution (Qiagen, Hilden, Germany), 110 ml of wash buffer (Qiagen, Hilden, Germany), 110 ml of deionized water and 180 ml of deionized water separately to the five troughs of the workstation. A concentration of 0.4 µM of sequencing primer; i.e. *BRCA*1, *BRCA*2 and *CDH*1; diluted to a total volume of 40 µl in annealing buffer (Qiagen, Hilden, Germany) was added to wells of a

PyroMark Q96 HS plate low (Qiagen, Hilden, Germany). The PCR plate and the PyroMark Q96 HS plate low were then placed into their respective slots in the workstation, in the same orientation as when samples were loaded. A vacuum was applied to the workstation tool and its filter probes were lowered into the PCR plate to capture the sepharose beads containing immobilized PCR amplicons. The workstation tool was transferred to the trough containing 70% ethanol, followed by transfer to the trough containing denaturation solution to generate single-stranded DNA, and lastly to the trough containing the wash buffer. Between each transfer, the filter probes were flushed for 10-15 seconds. The beads were then released into the PyroMark Q96 HS plate low containing 0.4 µM of sequencing primer. The sequencing primer was annealed to the single stranded DNA by placing the PyroMark Q96 HS plate low in a heating block (Labnet International Inc., Edison, USA) at 80°C for 2 minutes then cooling to room temperature for 5 minutes. To setup the Pyromark Q96 instrument, the reagent cartridge was loaded by pipetting the recommended volume of enzyme, substrate solution and nucleotides (as determined by the PyroMark software) into the corresponding wells; and the cartridge was inserted into the instrument. Thereafter, the PyroMark Q96 HS plate low was placed into the instrument and pyrosequencing was performed using the CpG assay programme of the PyroMark Q96 assay software (version 1.0.10) (Qiagen, Hilden, Germany).

2.2.25 Verification of PCR primers with control methylated DNA

The conversion efficiencies of *BRCA*1, *BRCA*2 and *CDH*1 PCR primers were evaluated using ratios of methylated: unmethylated bisulfite converted control human DNA (0, 10, 25, 50, 75, 90 and 100%) (Qiagen, Hilden, Germany). Pyrosequencing of the different control DNA ratios were performed, and results were used to construct standard curves to determine primer sensitivity as previously described by Willmer *et al.* (2020). Validation of pyrosequencing primers also involved the inclusion of quality controls containing the following: sequencing primer and annealing buffer only; biotinylated PCR-primer and annealing buffer only; sequencing primer, biotinylated PCR-primer and annealing buffer only; PCR amplicon and annealing buffer only; as well as a control containing a PCR no template control, sequencing primer and annealing buffer only. Each pyrosequencing run contained a bisulfite conversion and

PCR no template negative control. Bisulfite conversion controls were also included in all assay sequences to assess conversion efficiency.

2.2.26 Telomerase PCR ELISA

Telomerase is an enzyme that prevents telomere shortening and its increased activity has been implicated in in tumour progression (Hanahan and Weinberg 2000). Telomerase activity was measured using the *T*elo*TAGGG*^{TM} Telomerase PCR ELISA kit (Sigma-Aldrich, St. Louis, USA) according to the manufacturer's instructions. Briefly, of 2.5 x 10^5 cells/ml were pelleted at 1000 rpm for 10 min at 4°C and washed in PBS. Thereafter cells were resuspended in 200 µl of ice-cold lysis reagent and incubated on ice for 30 minutes. The lysate was centrifuged at 16 000 rpm for 20 minutes at 4°C and 175 µl of the supernatant was transferred to a clean tube. For the telomere repeat amplification protocol (TRAP) reaction, 25 µl of reaction mixture was aliquoted into a PCR tube for each sample followed by 3 µl of the sample and 22 µl of sterile deionized water. Amplification was carried out in a Veriti thermal cycler (Thermo Fisher Scientific, Waltham, USA) using the conditions in Table 2.4.

Table 2.4: PCR conditions for telomere repeat amplification protocol (TRAP) reaction.

Step	Temperature (°C)	Time (min)	Cycles
1. Primer elongation	25	30 min	1
2. Telomerase inactivation	94	5 min	1
3. Amplification:			
3.1 Denaturation	94	30 sec	30
3.2 Annealing	50	30 sec	
3.3 Polymerization	72	90 sec	
	72	10 min	1
4. Hold	4	∞	

∞: indefinite

After amplification, 5 µl of PCR product was added to 20 µl of denaturation agent, incubated for 10 minutes at room temperature, followed by the addition of 225 µl hybridization buffer. Tubes were vortexed briefly and 100 µl of each mixture was transferred in duplicate to a microplate, covered and incubated for 2 hours at 37°C, shaking at 300 rpm. After hybridization, the buffer was decanted and each well was washed three times with washing buffer for 30 seconds before addition of 100 µl Anti-DIG-POD working solution and incubation for 30 minutes at room temperature,

shaking at 300 rpm (covered). After the Anti-DIG-POD working solution had been decanted, wells were washed five times with washing buffer for 30 seconds before the addition of 100 µl TMB substrate solution at room temperature. The plate was covered and incubated at room temperature for 20 minutes, shaking at 300 rpm. Without removing the TMB substrate solution, 100 µl stop reagent was added to each well and the absorbance was read at 450 nm (reference 690 nm) on a SpetraMax® i3x Multi-Mode microplate reader (Molecular Devices, San Jose, USA).

2.2.27 Statistical Analysis

The data were analysed using GraphPad Prism statistical software (Version 8.4.2.679, GraphPad Software Inc., San Diego, USA). Measurement data are shown as mean ± standard deviation of three independent experiments. Comparisons between two groups were done using the paired student t-test while those among multiple groups were conducted by one-way analysis of variance (ANOVA) with subsequent Tukey-Kramer's multiple comparison test. A value of $p < 0.05$ indicated significant difference.

CHAPTER 3

RESULTS

3.1 Phytochemical and TLC-DPPH antioxidant screening

Methanol is one of the solvents of choice for preparation of crude plant extracts as this organic solvent results in extraction of phytocompounds over a broad range of polarities (Do *et al*. 2014). This is shown in TLC fingerprint in Fig. 3.1A. The range of polarities of the phytochemicals present in *B. pilosa* is further boasted by the rest of the lanes in Fig. 3.1A, as solvents of increasing polarity were used to fractionate the crude methanol extract. There is an abundance of antioxidant compounds in *B. pilosa*'s crude methanol extract (C); and these compounds were more pronounced in the fractions obtained using solvents of higher polarity (Fig. 3.1B). Polar solvents have been known as good solvents for extraction of antioxidants from plants. Chloroform (B2) extracted antioxidant compounds that were able to migrate further up the thin layer chromatography plate. The mobile phase used for the separation of compounds in this study is both acidic and non-polar containing chloroform, ethyl acetate and formic acid. The composition of the mobile phase enables it to best carry compounds of a similar nature as they dissolve best in it than other compounds within the plant extract. It can, therefore, be inferred that chloroform extracted antioxidant compounds of lower polarity while ethyl acetate (B3), butanol (B4) and methanol (B5) extracted antioxidant compounds of varying polarity. The water fraction (B6), conversely, showed an abundance of antioxidant compounds that are more polar, with lower solubility in the mobile phase and thus poorer migration up the TLC plate.

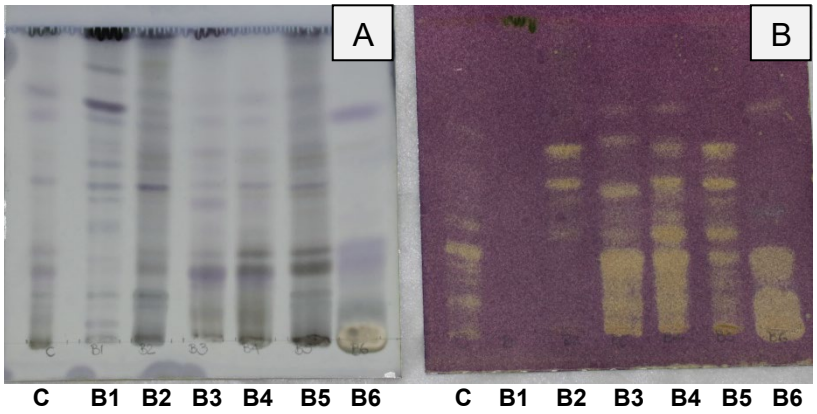

Figure 3.1: **Thin layer chromatography profile of the crude methanol extract and six fractions of *Bidens pilosa* developed in CEF (5:4:1, v/v/v).** Plates were sprayed with (A) vanillin-sulphuric acid and heated at 110°C, and (B) 0.2% 2,2-diphenyl-1-picryl-hydrazyl. Yellow spots on plate (B) are indicative of free-radical-scavenging compounds. C: crude methanol extract, B1: hexane, B2: chloroform, B3: ethyl acetate, B4: butanol, B5: 65 % methanol and B6: water.

3.2 Quantification of antioxidant activity

The antioxidant activity of *Bidens pilosa* was quantified using a spectrophotometric DPPH radical scavenging assay. In this quantitative test, the ethyl acetate and butanol fractions showed great antioxidant potential by quenching more than 50% of the DPPH at 62.5 μg/ml (Fig 3.2). At concentrations above this, the two fractions quenched up to 90% DPPH, exceeding the antioxidant activity of the crude extract in the assay. From Fig. 3.2 the crude extract did not show good radical-scavenging activity, except at the highest concentration tested; i.e. 250 μg/ml. At this concentration, both the crude extract and the 65% methanol fraction also showed impressive scavenging potential, with scavenging of DPPH reaching 82.5 and 27.9%, respectively. The antioxidant activity of all remaining fractions was below 50% for all other fractions at all tested concentrations.

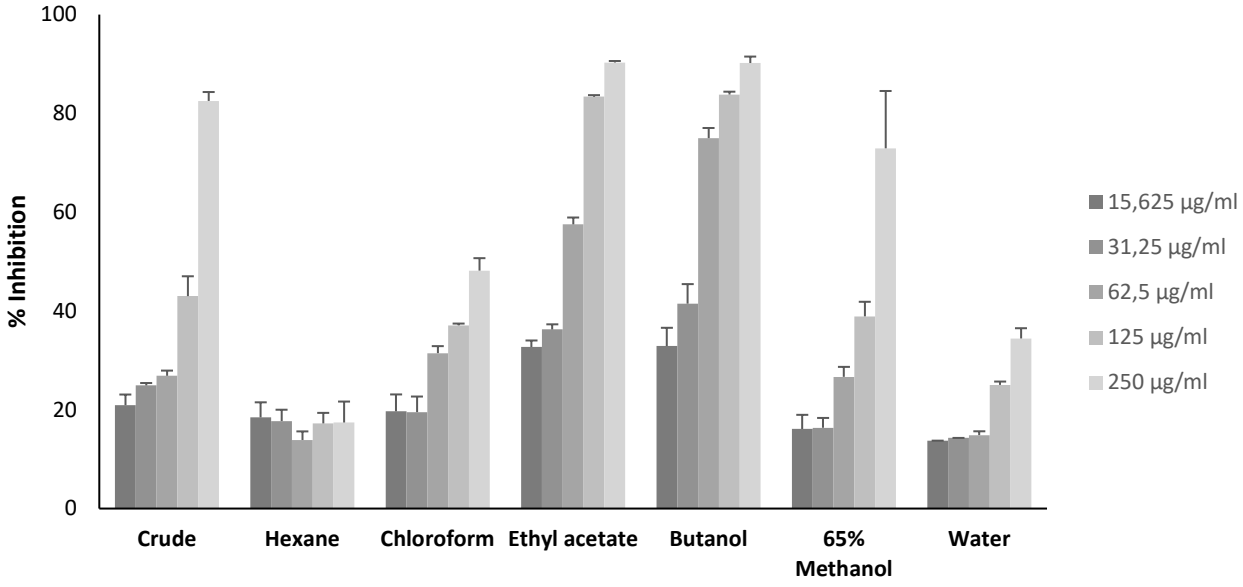

Figure 3.2: DPPH radical scavenging activity of the crude methanol extract and the six fractions of *Bidens pilosa.* Samples were diluted with acetone followed by addition of 0.2% DPPH in methanol (w/v). Absorbance was read at 517 nm after 30 minutes.

3.3 Quantification of the total phenolic content

The total phenolic content of the *B. pilosa* crude methanol extract was quantified and compared to that of its hexane, chloroform, ethyl acetate, butanol, 65% methanol and water fractions. According to Fig. 3.3 the total phenolic content of the water fraction was exceptionally higher than that measured in the other fractions and in the crude extract. This was followed by butanol with 118.54 mg GAE/g. The hexane fraction contained the lowest concentration of phenolic compounds, with only 14.6 mg GAE/g measured.

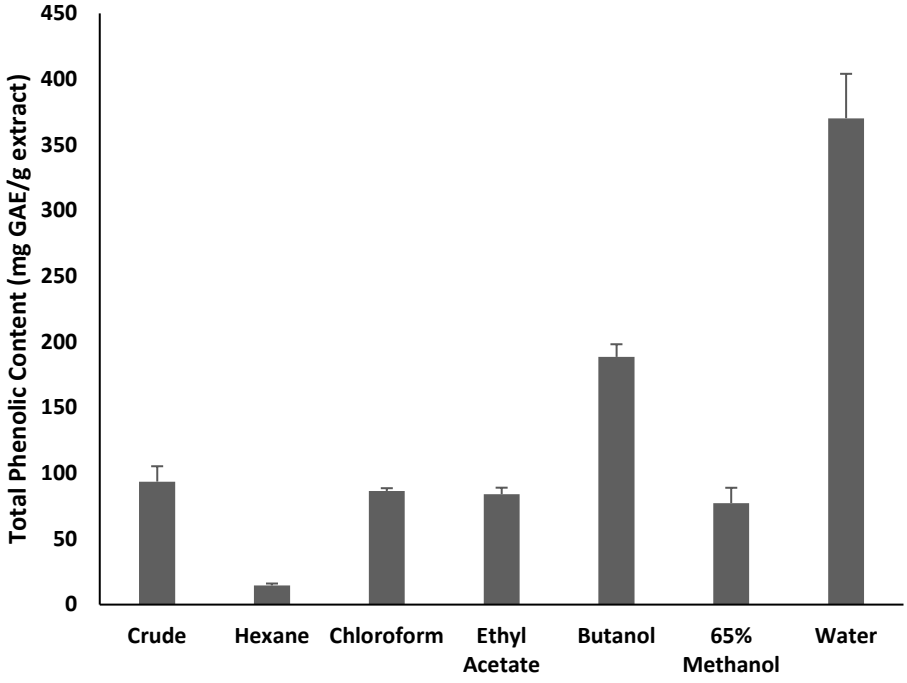

Figure 3.3: **Total phenolic content of the crude methanol extract and six fractions of *Bidens pilosa*.** Folin-Ciocalteu's reagent was used to quantify the total concentration of phenolic compounds colourimetrically at 550 nm. The phenolic content is expressed as gallic acid equivalents.

3.4 Quantification of the total tannin content

More tannins were extracted by butanol, with 59.43 mg GAE/g extract, and the quantity of tannins in the fractions decreased both with an increase as well as a decrease in solvent polarity, as shown by Fig. 3.4. Hexane extracted the lowest amount of tannins with only 2.52 mg GAE/g extract. The crude methanol extract contained more tannins than the hexane, chloroform, 65 % methanol as well as the water fractions.

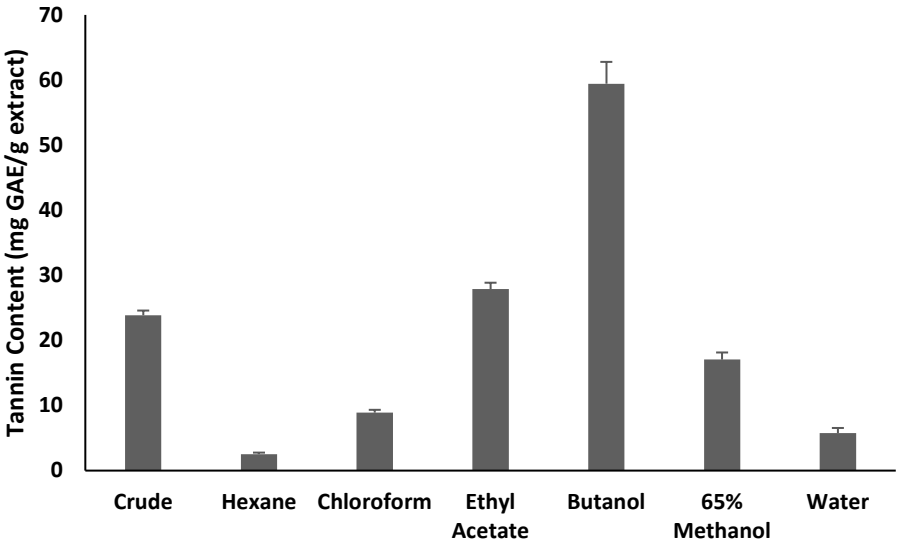

Figure 3.4: **Tannin content of the crude methanol extract and six fractions of *Bidens pilosa*.** Folin-Ciocalteu's reagent was used to quantify the total concentration of phenolic compounds colourimetrically at 725 nm. Tannin content is expressed as gallic acid equivalents.

3.5 Quantification of the total flavonoid content

With a flavonoid content of 2204.09 mg QE/g extract, butanol extracted more flavonoids than all the fractions as well as the crude methanol extract of *B. pilosa* (Fig. 3.5). This was followed by ethyl acetate, albeit with less than half the flavonoid content of the butanol fraction. Both an increase and decrease in solvent polarity from that of butanol resulted in a decrease in the flavonoid content of the fractions. Still, the ethyl acetate and 65 % methanol fractions contained higher flavonoid content that the crude methanol extract from which they were fractionated.

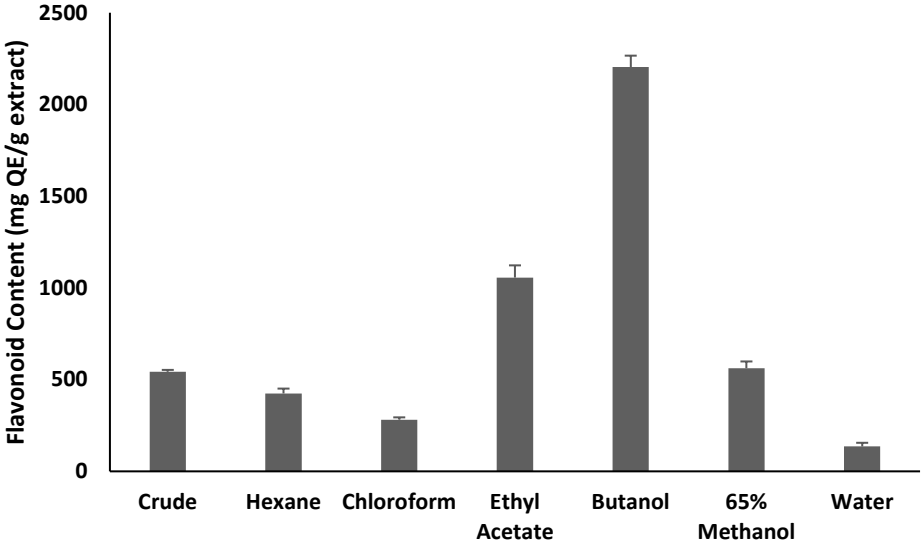

Figure 3.5: Flavonoid content of the crude methanol extract and six fractions of *Bidens pilosa*. Flavonoids in each fraction were quantified colorimetrically at 510 nm. The flavonoid content is expressed as quercetin equivalents.

3.6 Characterisation of *B. pilosa* fractions

Gas chromatography-mass spectrometry analysis of the crude methanol extract of *B. pilosa* as well as its sub-fractions of varying polarity lead to identification of a variety of chemical compounds present in the plant (Tables 3.1 to 3.7). Using ChromaTOF and NIST 95 library for identification, the two most abundant compounds identified in the crude extract were the ester 1-butanol, 3-methyl-, formate and an alkythiol, 1-pentanethiol with % peak areas of 7.6931 and 8.3691, respectively (Table 3.1). Numerous major compounds detected in the crude extract were also abundant in the fractions, with 13 compounds identified as predominant across multiple samples. These compounds belonged to various chemical classes, with 1 aryl aldehyde, 1 ester, 2 sterols, 3 alkanes, 3 fatty acids and 3 terpenes identified as major compounds in multiple samples by the software (Table 3.8). According to Table 3.8, n-hexadecanoic acid (palmitic acid) appeared as an abundant compound in all fractions except the water fraction. Mass spectra of the crude extract and sub-fractions are included as Appendix A.

Table 3.1: Major chemical compounds identified in the crude methanol extract of *Bidens pilosa*.

RT (min:sec)	Compound name	Molecular Formula	% Peak Area
04:00,5	1-Hexen-4-yne, 3-ethylidene-2-methyl-	C_9H_{12}	1.8598
04:00,8	1-Penten-3-yne, 2-methyl-	C_6H_8	1.8598
04:01,7	2-Hexen-4-yne	C_6H_8	1.8598
04:55,3	1-Butanol, 3-methyl-, formate	$C_6H_{12}O_2$	7.6931**
05:00,9	1-Pentanethiol	$C_5H_{12}S$	8.3691**
05:05,3	Undecane, 2-methyl-	$C_{12}H_{26}$	4.3343*
06:07,9	Resorcinol	$C_6H_6O_2$	2.0874*
06:08,1	Tridecane	$C_{13}H_{28}$	2.0693*
08:46,2	Tetradecane	$C_{14}H_{30}$	4.2836*
09:20,1	Benzaldehyde, 2-hydroxy-6-methyl-	$C_8H_8O_2$	3.3858*
11:12,3	Pentadecane	$C_{15}H_{32}$	4.224*
11:12,7	Caryophyllene oxide	$C_{15}H_{24}O$	4.2243*
11:44,2	n-Butyric acid 2-ethylhexyl ester	$C_{12}H_{24}O_2$	1.3427
13:14,2	6-Hydroxy-4,4,7a-trimethyl-5,6,7,7a-tetrahydrobenzofuran-2(4H)-one	$C_{11}H_{16}O_3$	1.6639
13:24,6	Eicosane	$C_{20}H_{42}$	2.7687*
13:25,4	Sebacic acid, heptyl 4-methoxyphenyl ester	$C_{24}H_{38}O_5$	2.8684*
13:49,9	Neophytadiene	$C_{20}H_{38}$	1.6487
15:05,2	n-Hexadecanoic acid	$C_{16}H_{32}O_2$	3.6312*
15:05,7	9-Hexadecenoic acid	$C_{16}H_{30}O_2$	3.6312*
15:25,0	Heneicosane	$C_{21}H_{44}$	1.3389
15:26,3	trans-Sinapyl alcohol	$C_{11}H_{14}O_4$	1.3389
16:30,4	Phytol	$C_{20}H_{40}O$	1.2686
16:46,6	9,12,15-Octadecatrienoic acid, (Z,Z,Z)-	$C_{18}H_{30}O_2$	1.4531
28:30,6	Stigmasterol	$C_{29}H_{48}O$	1.4827

RT: retention time; *: detected in relatively high abundance; **: detected in relatively higher abundance.

Table 3.2: Major chemical compounds identified in the hexane fraction of the crude methanol extract of *Bidens pilosa*.

RT (min:sec)	Compound name	Molecular Formula	% Peak Area
12:45,4	9H-Fluorene, 9-diazo-	$C_{13}H_8N_2$	1.2302
13:51,6	Neophytadiene	$C_{20}H_{38}$	2.3313*
13:55,4	2-Pentadecanone, 6,10,14-trimethyl-	$C_{18}H_{36}O$	1.1775
15:26,6	n-Hexadecanoic acid	$C_{16}H_{32}O_2$	11.946***
16:34,7	Phytol	$C_{20}H_{40}O$	3.6814*
17:10,7	(Z)-18-Octadec-9-enolide	$C_{18}H_{32}O_2$	14.207***
17:12,9	9,12,15-Octadecatrienoic acid, (Z,Z,Z)-	$C_{18}H_{30}O_2$	27.144***
22:25,2	Squalene		1.0817
28:45,9	Stigmasterol	$C_{29}H_{48}O$	4.8186*
29:57,7	β-Sitosterol	$C_{29}H_{50}O$	2.5276*
37:05,5	Phytol, acetate	$C_{22}H_{42}O_2$	2.2696*
37:07,0	Neophytadiene	$C_{20}H_{38}$	2.2696*

RT: retention time; *: detected in relatively high abundance; **: detected in relatively higher abundance; ***: detected in relatively highest abundance.

Table 3.3: Major chemical compounds identified in the chloroform fraction of the crude methanol extract of *Bidens pilosa*.

RT (min:sec)	Compound name	Molecular Formula	% Peak Area
09:17,7	3,6-Nonadien-5-one, 2,2,8,8-tetramethyl-	$C_{13}H_{18}O$	1.7429
09:18,0	β-D-Glucopyranose, 1,6-anhydro-	$C_6H_{10}O_5$	2.9105*
11:01,5	8-(2-Acetyloxiran-2-yl)-6,6-dimethylocta-3,4-dien-2-one	$C_{14}H_{20}O_3$	1.3684
11:03,3	Fumaric acid, ethyl 2,4,5-trichlorophenyl ester	$C_{12}H_9Cl_3O_4$	1.3684
13:28,2	1-Buten-3-one, 1-(2-carboxy-4,4-dimethylcyclobutenyl)-	$C_{11}H_{14}O_3$	3.4408*
13:53,2	Neophytadiene	$C_{20}H_{38}$	2.1564*
13:53,8	3,7,11,15-Tetramethyl-2-hexadecen-1-ol	$C_{20}H_{40}O$	2.1564*
13:54,2	1-(3,3-Dimethyl-1-yl)-2,2-dimethylcyclopropene-3-carboxylic acid	$C_7\ H_{10}O_2$	2.1564*
14:17,4	Platambin	$C_{15}H_{26}O_2$	1.5012
14:18,0	2-n-Octylfuran	$C_{12}H_{20}O$	1.5219
14:19,0	Neophytadiene	$C_{20}H_{38}$	1.5219
15:20,2	l-Phenylalanine, N-(2-hydroxy-1-oxopentyl)-, methyl ester, (S)-	???	3.1578*
15:26,8	n-Hexadecanoic acid	$C_{16}H_{32}O_2$	10.142***
17:10,9	1-Oxacyclopentadecan-2-one, 15-ethenyl-15-methyl	$C_{17}H_{30}O_2$	8.0469**
17:14,2	9,12-Octadecadienoic acid (Z,Z)-	$C_{18}H_{32}O_2$	10.15***
17:17,4	9,12,15-Octadecatrienoic acid, (Z,Z,Z)-	$C_{18}H_{30}O_2$	16.418***

RT: retention time; *: detected in relatively high abundance; **: detected in relatively higher abundance; ***: detected in relatively highest abundance.

Table 3.4: Major chemical compounds identified in the ethyl acetate fraction of the crude methanol extract of *Bidens pilosa*.

RT (min:sec)	Compound name	Molecular Formula	% Peak Area
04:55,2	1-Butanol, 3-methyl-, formate	$C_6H_{12}O_2$	5.7594**
05:05,4	Phenylethyl Alcohol	$C_8H_{10}O$	2.1824*
05:11,9	5-Aminovaleric acid	$C_5H_{11}NO_2$	1.0752
09:22,0	Benzaldehyde, 2-hydroxy-6-methyl-	$C_8H_8O_2$	4.7478*
15:10,4	Phthalic acid, butyl oct-3-yl ester	$C_{20}H_{30}O_4$	10.697***
15:13,2	Ethanol, 2-[4-(1,1-dimethylpropyl)phenoxy]-	$C_{13}H_{20}O_2$	1.3515
15:17,4	Benzoic Acid, TBDMS derivative	$C_{13}H_{20}O_2Si$	8.0195**
15:21,7	n-Hexadecanoic acid	$C_{16}H_{32}O_2$	20.096***
16:14,3	Pyrene	$C_{16}H_{10}$	1.5857
16:15,1	n-Nonadecanol-1	$C_{19}H_{40}O$	1.5857
17:01,2	Eicosane, 1-iodo-	$C_{20}H_{41}I$	1.1499
17:02,2	2-Propenoic acid, 3-(4-methoxyphenyl)-, 2-ethylhexyl ester	$C_{18}H_{26}O_3$	1.7485
17:06,0	Octadecanoic acid	$C_{18}H_{36}O_2$	7.2523**
18:40,0	Methyl dehydroabietate	$C_{21}H_{30}O_2$	3.4608*
18:41,6	Benzyl butyl phthalate	$C_{19}H_{20}O_4$	3.4608*
20:12,2	Bis(2-ethylhexyl) phthalate	$C_{24}H_{38}O_4$	2.6086*

RT: retention time; *: detected in relatively high abundance; **: detected in relatively higher abundance; ***: detected in relatively highest abundance.

Table 3.5: Major chemical compounds identified in the butanol fraction of the crude methanol extract of *Bidens pilosa*.

RT (min:sec)	Compound name	Molecular Formula	% Peak Area
05:51,2	1,4-Diethynylbenzene	$C_{10}H_6$	2.8644*
06:27,0	Benzaldehyde, 4-methyl-	C_8H_8O	4.2972*
06:28,9	Dimethyl sulfone	$C_2H_6O_2S$	1.4398
07:29,9	Indole	C_8H_7N	1.0777
07:45,1	2-Methoxy-4-vinylphenol	$C_9H_{10}O_2$	2.4689*
08:19,2	Phenol, 2-methoxy-3-(2-propenyl)-	$C_{10}H_{12}O_2$	3.48*
09:26,0	4-Fluorobenzoic acid, pent-2-en-4-ynyl ester	$C_{12}H_9FO_2$	2.5547*
09:26,6	Ethanone, 1-(2,3-dihydro-1,1-dimethyl-1H-inden-4-yl)-	$C_{17}H_{24}O$	3.4615*
09:29,3	Benzaldehyde, 2-hydroxy-6-methyl-	$C_8H_8O_2$	12.008***
09:30,3	Ethanone, 1-(2,3-dihydro-1,1-dimethyl-1H-inden-4-yl)-	$C_{17}H_{24}O$	11.852***
10:41,1	Geranyl vinyl ether	$C_{12}H_{20}O$	1.1644
10:43,4	1,6-Heptadien-4-ol, 4-propyl-	$C_{10}H_{18}O$	1.2492
10:47,2	D-Allose	$C_6H_{12}O_6$	2.1573*
10:53,3	2',4'-Dimethoxyacetophenone	$C_{10}H_{12}O_3$	1.179
10:58,5	3-Buten-2-one, 4-(2-hydroxy-2,6,6-trimethylcyclohexyl)-	$C_{13}H_{20}O_3$	1.0867
11:12,5	Heptadecane	$C_{17}H_{36}$	1.3563
11:38,4	23-Methyl-tetracosanoic acid, DMOX derivative	$C_{25}H_{50}O_2$	1.1506
11:39,2	2,7-Octadiene-1,6-diol, 2,6-dimethyl-	$C_{10}H_{18}O_2$	1.1506
11:40,4	Megastigmatrienone	$C_{13}H_{18}O$	1.1506
12:24,0	(3R,3aR,4aR,8aR,9aR)-3,8a-Dimethyl-5-methylene-3,3a,4,4a,5,6,9,9a-octahydronaphtho[2,3-b]furan-2(8aH)-one	$C_{15}H_{20}O_2$	1.0463
12:25,8	Idosan triacetate	$C_{12}H_{16}O_8$	1.0656
13:20,1	6-Hydroxy-4,4,7a-trimethyl-5,6,7,7a-tetrahydrobenzofuran-2(4H)-one	$C_{11}H_{16}O_3$	1.2525
13:25,0	Heneicosane	$C_{21}H_{44}$	1.1494
13:26,1	Maltose	$C_{12}H_{22}O_{11}$	1.1684
15:06,0	n-Hexadecanoic acid	$C_{16}H_{32}O_2$	1.1589
15:50,0	Isoxazole, 3,5-dimethyl-4-nitro-	$C_5H_6N_2O_3$	1.2419
16:05,5	α-D-Glucopyranose, 4-O-β-D-galactopyranosyl-	$C_{12}H_{24}O_{12}$	3.6346*

RT: retention time; *: detected in relatively high abundance; **: detected in relatively higher abundance; ***: detected in relatively highest abundance.

Table 3.6: Major chemical compounds identified in the 65% methanol fraction of the crude methanol extract of *Bidens pilosa*.

RT (min:sec)	Compound name	Molecular Formula	% Peak Area
04:53,2	1-Butanol, 3-methyl-, formate	$C_6H_{12}O_2$	1.8522
05:53,1	Benzoic acid	$C_7H_6O_2$	1.6144
05:53,9	Octanoic acid	$C_8H_{16}O_2$	1.5951
10:35,8	2(4H)-Benzofuranone, 5,6,7,7a-tetrahydro-4,4,7a-trimethyl-, (R)-	$C_{11}H_{16}O_2$	1.0763
11:12,5	Heptadecane	$C_{17}H_{36}$	1.1351
12:20,2	3-Buten-2-one, 4-(4-hydroxy-2,2,6-trimethyl-7-oxabicyclo[4.1.0]hept-1-yl)-	$C_{13}H_{20}O_3$	1.3227
12:21,4	11-Hexadecyn-1-ol	$C_{16}H_{30}O$	1.3227
12:22,3	3-Hydroxy-7,8-dihydro-β-ionol	$C_{13}H_{20}O_2$	1.3227
12:22,7	4-(2,6,6-Trimethylcyclohexa-1,3-dienyl)but-3-en-2-one	$C_{13}H_{18}O$	1.3764
13:19,7	Ylangenal	$C_{15}H_{22}O$	1.7572
13:20,2	9-Octadecenoic acid (Z)-, 2,3-bis(acetyloxy)propyl ester	$C_{25}H_{44}O_6$	2.1748*
13:22,6	6-Hydroxy-4,4,7a-trimethyl-5,6,7,7a-tetrahydrobenzofuran-2(4H)-one	$C_{11}H_{16}O_3$	5.6398**
13:25,1	Eicosane	$C_{20}H_{42}$	1.7417
13:25,6	Cyclopentanone, 2-(2-nitro-2-heptenyl)-	$C_{12}H_{19}NO_3$	1.7941
13:51,0	8-(2-Acetyloxiran-2-yl)-6,6-dimethylocta-3,4-dien-2-one	$C_{14}H_{20}O_3$	3.7159*
13:51,7	Neophytadiene	$C_{20}H_{38}$	3.7253*
13:52,2	Salvial-4(14)-en-1-one	$C_{15}H_{24}O$	3.7253*
14:06,0	Neophytadiene	$C_{20}H_{38}$	1.1835
14:06,4	2-Oxabicyclo[4.4.0]dec-3-en-10-ol, 5-methylene-1,3,7,7-tetramethyl-, acetate	$C_{16}H_{26}O_4$	1.2411
14:17,4	Neophytadiene	$C_{20}H_{38}$	1.9206
15:08,2	Dibutyl phthalate	$C_6H_4(CO_2C_4H_9)_2$	1.2866
15:14,5	n-Hexadecanoic acid	$C_{16}H_{32}O_2$	8.8595**
15:15,2	9-Hexadecenoic acid	$C_{16}H_{30}O_2$	8.2462**
16:31,9	Phytol	$C_{20}H_{40}O$	1.1682
16:51,1	Norbornadieone	$C_7H_{10}O$	1.8485
16:51,4	Z,E-3,13-Octadecadien-1-ol	$C_{18}H_{34}O$	2.0305*
16:55,6	9,12,15-Octadecatrienoic acid, (Z,Z,Z)-	$C_{18}H_{30}O_2$	5.736**

RT: retention time; *: detected in relatively high abundance; **: detected in relatively higher abundance; ***: detected in relatively highest abundance.

Table 3.7: Major chemical compounds identified in the water fraction of the crude methanol extract of *Bidens pilosa*.

RT (min:sec)	Compound name	Molecular Formula	% Peak Area
04:45,6	2-Furanmethanol, 5-ethenyltetrahydro-α,α,5-trimethyl-, cis-	$C_{10}H_{18}O_2$	1.0731
04:51,8	1-Pentanol	$C_5H_{12}O$	1.2166
04:56,7	1-Butanol, 3-methyl-, formate	$C_6H_{12}O_2$	2.9365*
05:00,9	Glycerin	$C_3H_8O_3$	6.355**
05:24,9	1-Butanol, 3-methyl-, formate	$C_6H_{12}O_2$	1.6362
05:30,0	4H-Pyran-4-one, 2,3-dihydro-3,5-dihydroxy-6-methyl-	$C_6H_8O_4$	1.4079
08:46,4	Tetradecane	$C_{14}H_{30}$	1.2363
09:23,9	Benzaldehyde, 2-hydroxy-6-methyl-	$C_8H_8O_2$	3.0805*
11:12,5	Heptadecane	$C_{17}H_{36}$	1.1355
17:05,2	Methoxyacetic acid, 3-tetradecyl ester	$C_{17}H_{34}O_3$	1.1254
17:46,7	Cholesta-4,6-dien-3-ol, (3β)-	$C_{27}H_{44}O$	1.4286
17:54,1	Cyclobutene, 2-propenylidene-	C_7H_8	2.6592*
22:06,3	Tetracosane, 11-decyl-	$C_{34}H_{70}$	17.972***
23:57,2	β-Sitosterol	$C_{29}H_{50}O$	1.5156
23:58,9	Hexatriacontane	$C_{36}H_{74}$	1.5156
25:36,7	Tetracosane, 11-decyl-	$C_{34}H_{70}$	15.904***
29:48,0	Hexatriacontane	$C_{36}H_{74}$	9.6352**
34:31,4	Pentanamide, N-[5-[[4-[2,4-bis(1,1-dimethylpropyl)phenoxy]-1-oxobutyl]amino]-2-chlorophenyl]-4,4-dimethyl-3-oxo-	$C_{33}H_{47}ClN_2O_4$	2.7064*
34:49,6	Tetratetracontane	$C_{44}H_{90}$	5.0887**

RT:retention time; *: detected in relatively high abundance; **: detected in relatively higher abundance; ***: detected in relatively highest abundance.

Table 3.8: Major chemical compounds identified in more than one fraction of *B. pilosa.*

Compound name	Class	C	B1	B2	B3	B4	B5	B6
1-Butanol, 3-methyl-, formate	Ester							
6-Hydroxy-4,4,7a-trimethyl-5,6,7,7a-tetrahydrobenzofuran-2(4H)-one	Terpene							
9, 12, 15-Octadecatrienoic acid, (Z,Z,Z)	Fatty acid							
9-Hexadecenoic acid	Fatty acid							
Benzaldehyde, 2-hydroxy-6-methyl-	Aryl aldehyde							
Eicosane	Alkane							
Heneicosane	Alkane							
Heptadecane	Alkane							
Neophytadiene	Terpene							
n-Hexadecanoic acid	Fatty acid							
Phytol	Terpene							
Stigmasterol	Sterol							
β-Sitosterol	Sterol							

% Peak area: ☐ : Not detected or not a major compound, ☐ : < 1.000, ☐ : 1.000 – 4.999, ☐ : 5.000 – 10.000, ■ : > 10.000. C: crude methanol extract, B1: hexane, B2: chloroform, B3: ethyl acetate, B4: butanol, B5: 65% methanol, B6: water.

3.7 Determination of cytotoxicity

Treatment of MCF-7 breast cancer cells with the crude methanol extract of *B. pilosa* and its fractions of varying polarity resulted in general dose-dependent cytotoxic activity. Some of the fractions induced a decrease in cell viability in a concentration- and time-dependent manner while others appeared to enhance viability of the cells (Figs 3.6). The chloroform fraction exhibited the highest cytotoxic activity among the tested fractions. This fraction induced significant death in MCF-7 cells from 200 μg/ml within 24 hours of treatment. According to Fig. 3.7, IC_{50} of the chloroform fraction was calculated to be 112 μg/ml; 100 μg/ml was used in subsequent assays as the test concentration of the chloroform fraction.

Interestingly, the crude methanol extract as well as the hexane and 65% methanol fractions caused a decrease in cell viability in the first 24 hours of incubation. This was, however, followed by increased viability of the MCF-7 cells, after 48 hours (Fig. 3.6B) and then a decline in viability once again after 72 hours of treatment (Fig 3.6C). Still, after 48 and 72 hours of treatment with the fractions, the MCF-7 cells showed a significant dose-dependent decrease in viability at 400 and 800 μg/ml of the 65% methanol fraction while only responding significantly to 800 μg/ml of the hexane fraction. Treatment of the cell culture with the ethyl acetate fraction at concentrations exceeding 200 μg/ml elicited cell death by up to 80% after 72 hours (Fig. 3.6C). According to Fig. 3.6 the water fraction showed no toxicity towards the MCF-7 cells even at 800 μg/ml after 72 hours of treatment.

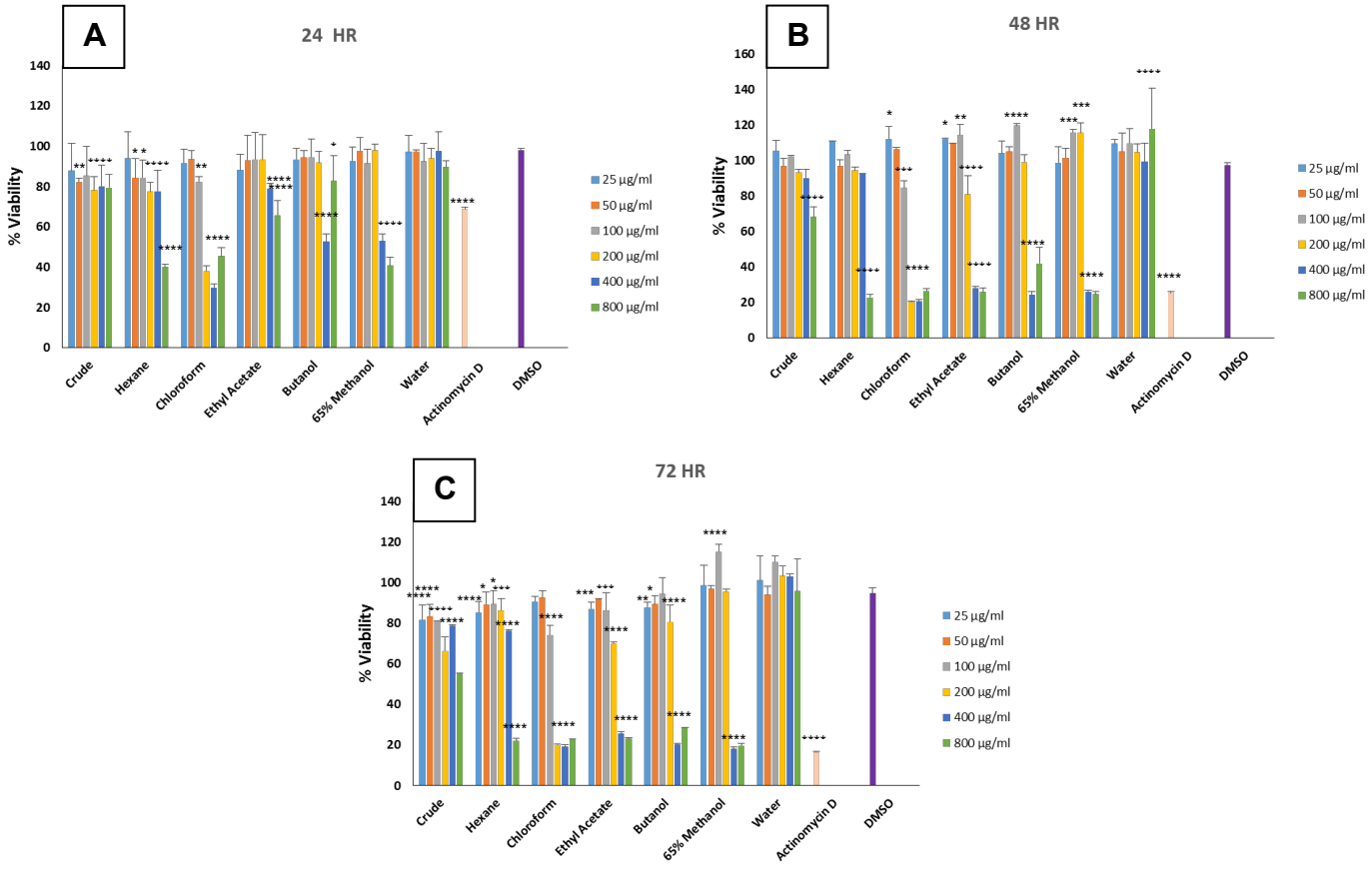

Figure 3.6: The effect of *Bidens pilosa* and its fractions on viability of MCF-7 cells. Cells were treated with various concentrations of the extracts for 24 (A), 48 (B) and 72 (C) hours followed by viability determination by the MTT assay where 2 µg/ml actinomycin D served as a positive control for cell death. Viability was calculated as percentage of untreated control cells. DMSO: 0.05% dimethylsulfoxide. Data is represented as the mean ± standard deviation (SD). *: $p < 0.05$, **: $p < 0.009$, ****: $p < 0.0001$.

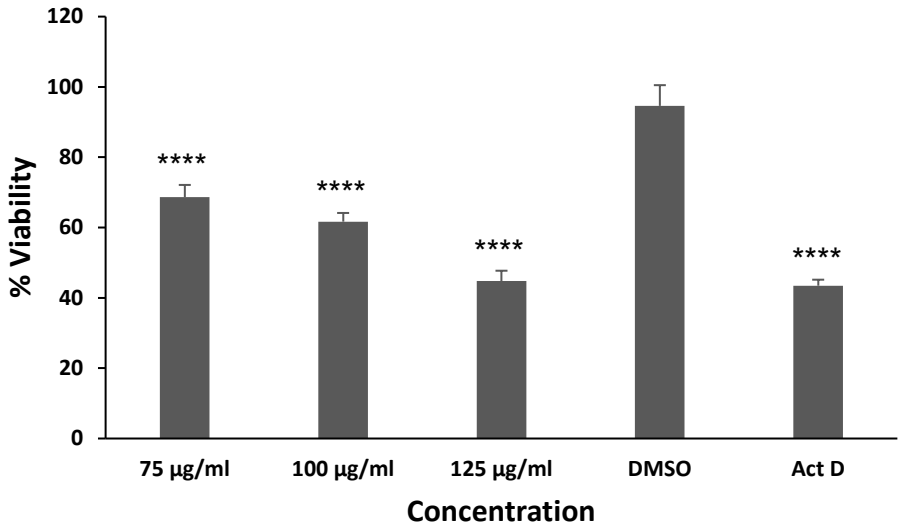

Figure 3.7: The effect of the chloroform fraction of *Bidens pilosa* on viability of MCF-7 cells. Cells were treated with various concentrations of the fraction for 24 hours followed by viability determination by the MTT assay where 2 µg/ml actinomycin D served as a positive control for cell death. Viability was calculated as percentage of untreated control cells. DMSO: 0.8% dimethylsulfoxide, Act D: Actinomycin D. Data is represented as the mean ± standard deviation (SD). ****: $p < 0.0001$.

3.8 Evaluation of mitochondrial membrane depolarisation

The effect of *B. pilosa*'s chloroform fraction on cell health was assessed by measuring the mitochondrial membrane potential of treated MCF-7 cells using the Muse® MitoPotential kit. An increase in concentration of the fraction decreased the viability of cells, after both 12 and 24 hrs, without a significant increase in the number of live cells with depolarised mitochondrial membranes (Figs. 3.8A & 3.8B). At the IC_{50} of 100 μg/ml, 9 % of the viable cells had depolarised mitochondrial membranes after 12 hrs of treatment while 7 % were showed depolarisation after 24 hrs of treatment. However, dead cells showed significant depolarisation of mitochondrial membranes after both 12 and 24 hours of treatment, with up to 27,5% and 26,5% depolarised membranes, respectively.

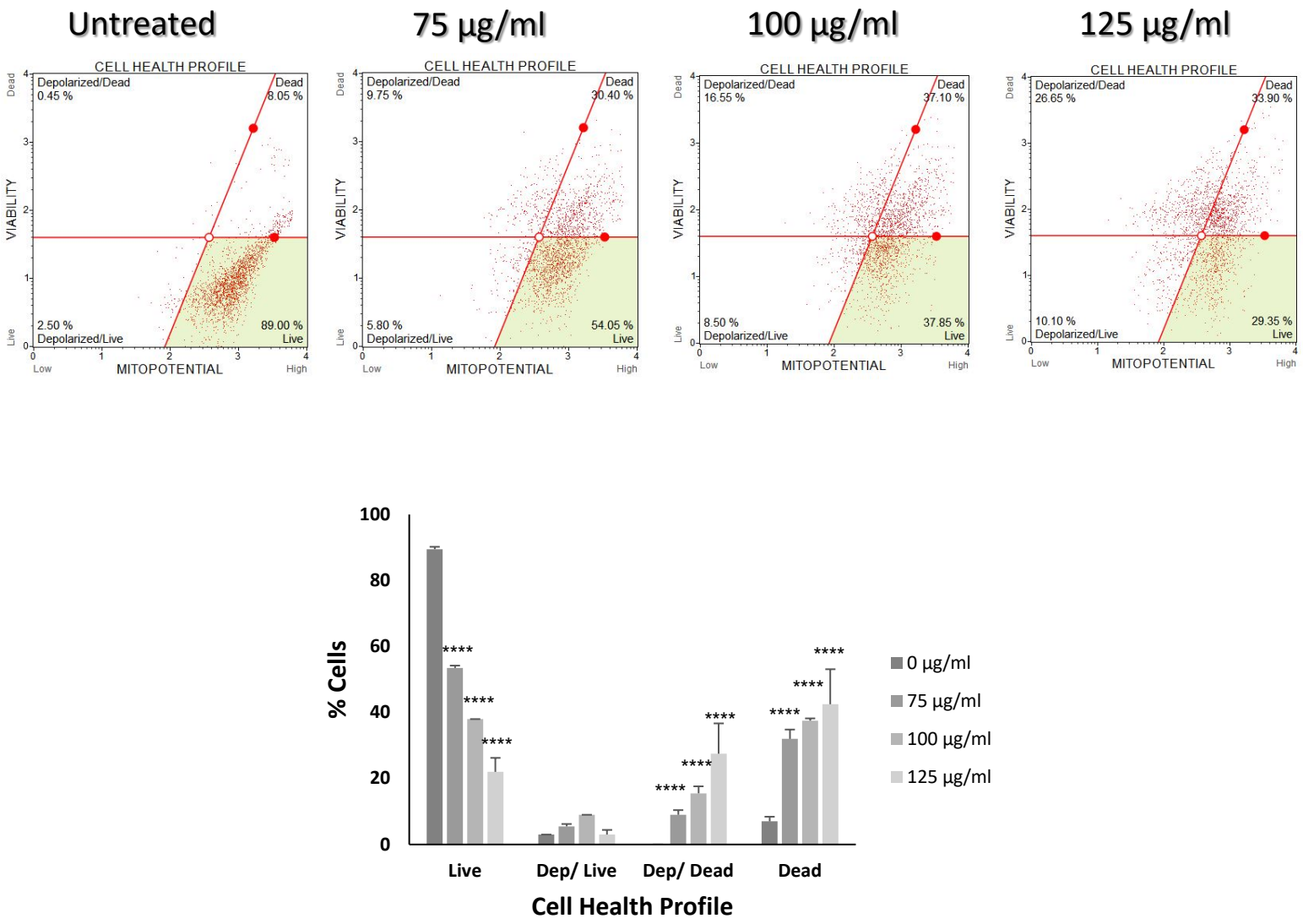

Figure 3.8A: The effect of the chloroform fraction of *Bidens pilosa* on depolarization of MCF-7 mitochondrial membranes after 12 hours. Cells were treated with the fraction for 12 hours before analysis of the mitochondrial membrane potential with a Muse® MitoPotential Kit. Data is represented as the mean ± standard deviation (SD). ****: $p < 0.0001$.

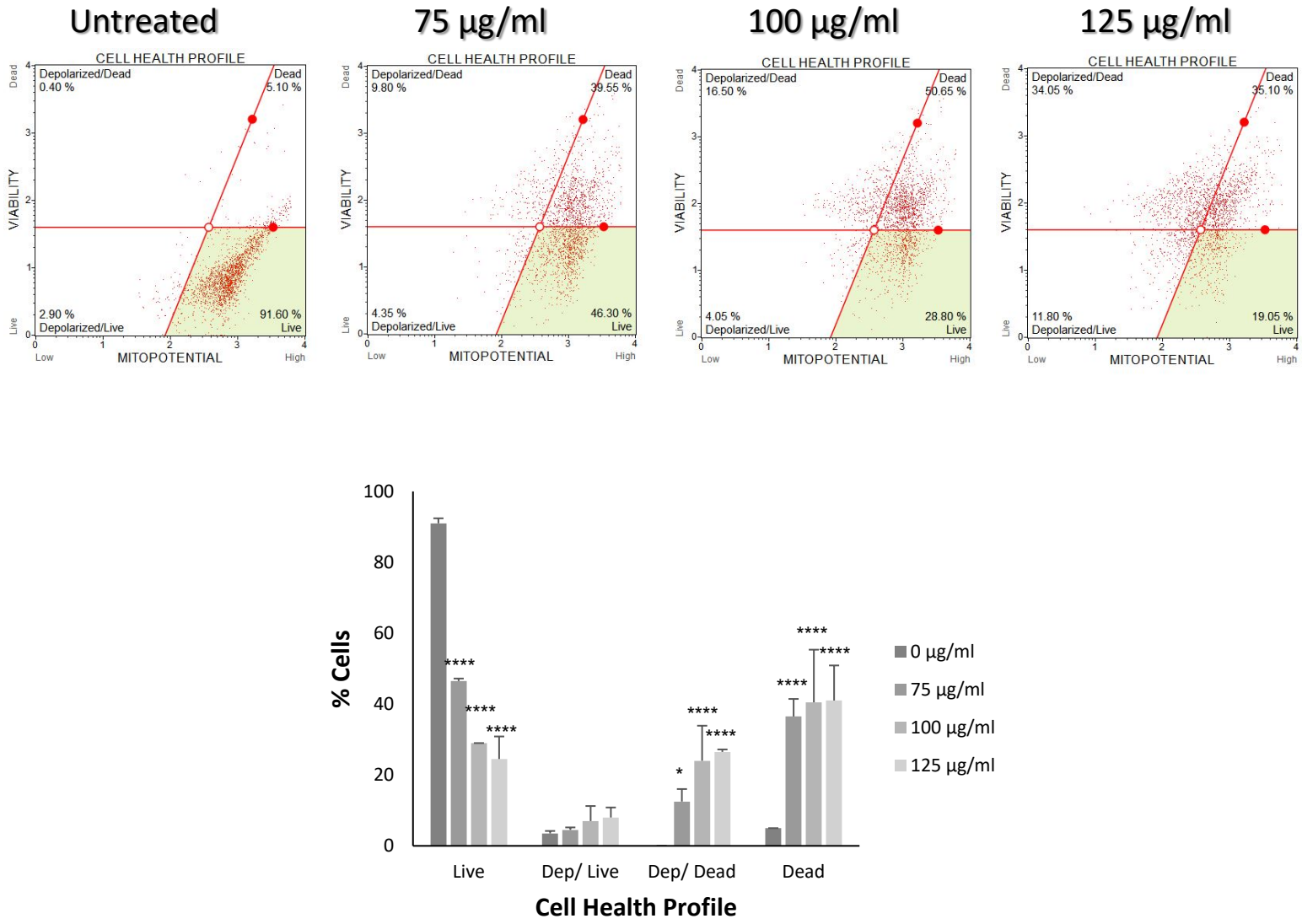

Figure 3.8B: The effect of the chloroform fraction of *Bidens pilosa* on depolarization of MCF-7 mitochondrial membranes after 24 hours. Cells were treated with the fraction for 24 hours before analysis of the mitochondrial membrane potential with a Muse® MitoPotential Kit. Data is represented as the mean ± standard deviation (SD). *: $p < 0.05$; ****: $p < 0.0001$

3.9 Detection of apoptosis

Apoptosis in MCF-7 breast cancer cells could not be verified following 24 hours of treatment with 75, 100 and 125 µg/ml of the *B. pilosa* chloroform fraction using the Muse® Annexin V and Cell Death kit. After 24 hours of incubation with the extract, very few cells were shown to be apoptotic; however, cell death was comparable to that instigated by 100 µg/ml curcumin, known to cause apoptosis in breast cancer cells. (Fig 3.9).

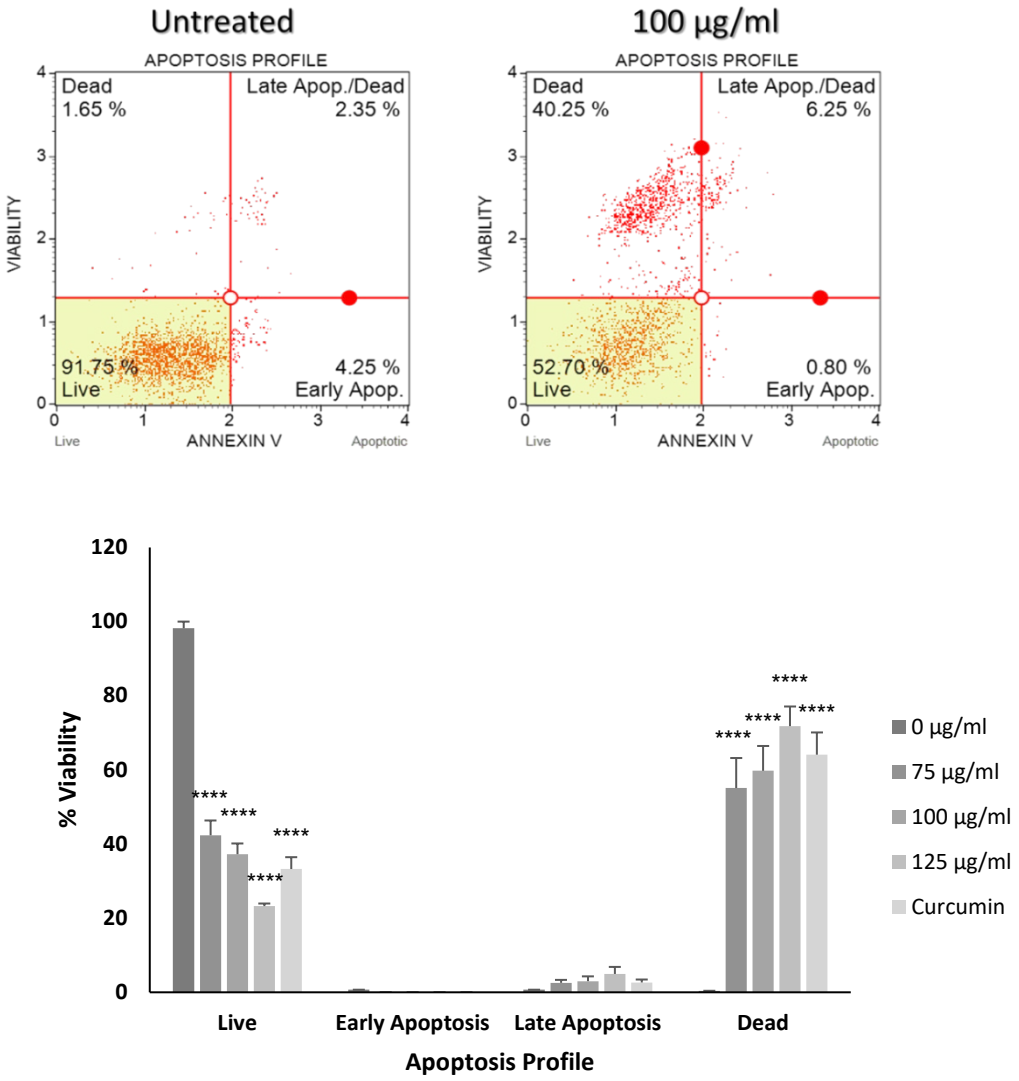

Figure 3.9: The effect of the chloroform fraction of *Bidens pilosa* on MCF-7 cell death. Cells were treated with 75, 100 and 125 µg/ml of the fraction for 24 hours before analysis of apoptosis using a Muse® Annexin V and Cell Death kit. Data is represented as the mean ± standard deviation (SD). ****: P < 0.0001.

3.10 Cell cycle distribution analysis

Analysis of the effects of the chloroform fraction of *B. pilosa* on the cell division cycle in MCF-7 cells indicated a concentration-dependent accumulation of cells in the G_2/M phase of the cycle. Figure 3.10 shows a significant increase in the population of cells in the G_2/M phase of the cell division cycle upon treatment with the fraction, suggesting the chloroform fraction of B. pilosa results in G_2/M cell cycle arrest.

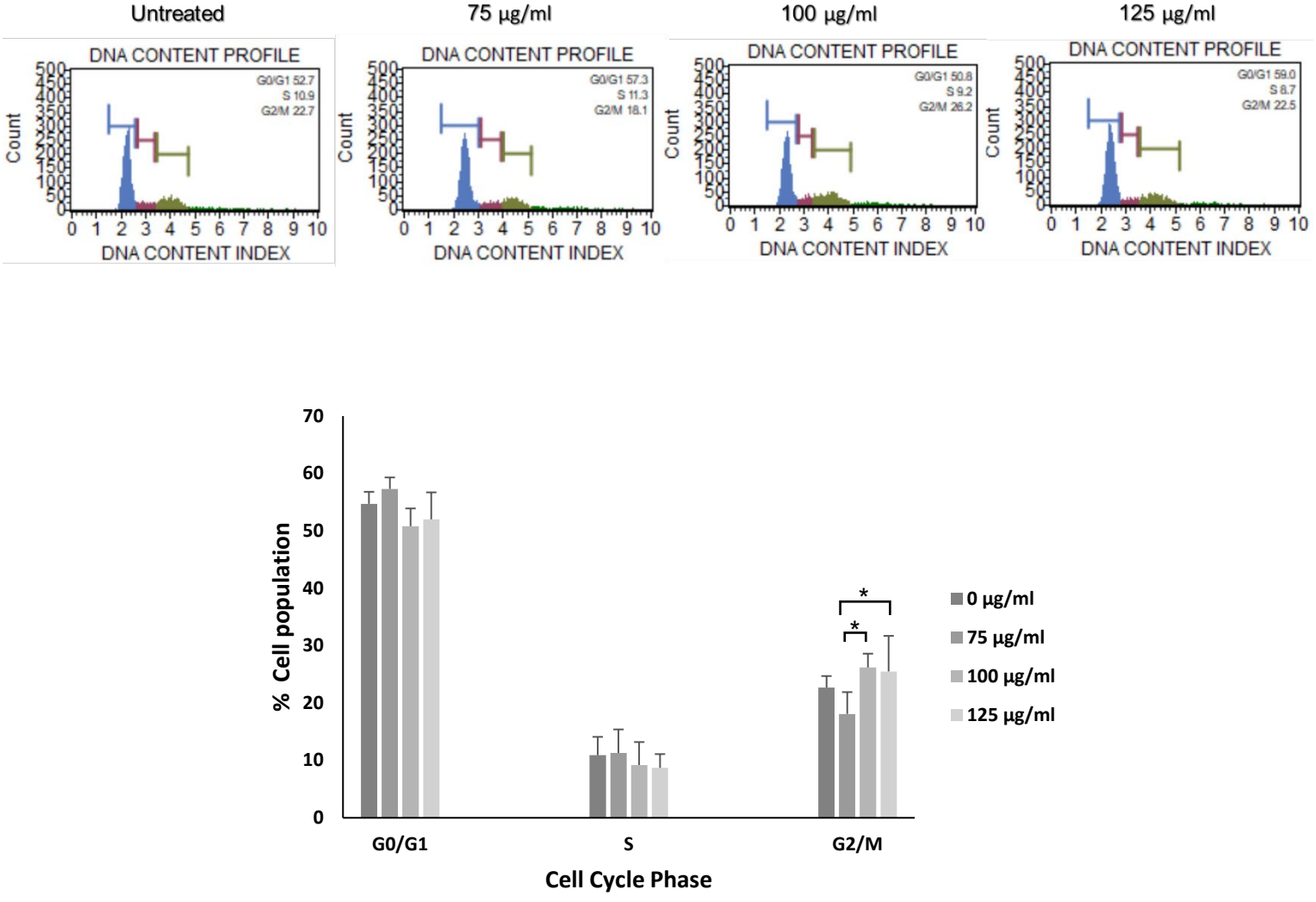

Figure 3.10: The effect of the chloroform fraction of *Bidens pilosa* on MCF-7 cell division cycle. Cells were treated with 75, 100 and 125 µg/ml of the fraction for 24 hours before analysis apoptosis using a Muse® Cell Cycle Kit. Data is represented as the mean ± standard deviation (SD). *: $p < 0.05$.

3.11 Gene expression analysis

Expression of genes on the Human Breast Cancer RT^2 Profiler PCR Array are shown in Fig. 3.11. Treatment of MCF-7 cells with 100 µg/ml of the chloroform fraction of *B. pilosa* up-regulated the expression of 29 genes and down-regulated the expression of 22 genes, using a 2-fold change cut-off and a p value ≤ 0.05 (Table 3.9). Of these, *BRCA*1 and *BRCA*2, tumour suppressor genes that are a hallmark of breast cancer (Atchley *et al*. 2008), were decreased after treatment with this fraction (Table 3.9, Fig. 3.11).

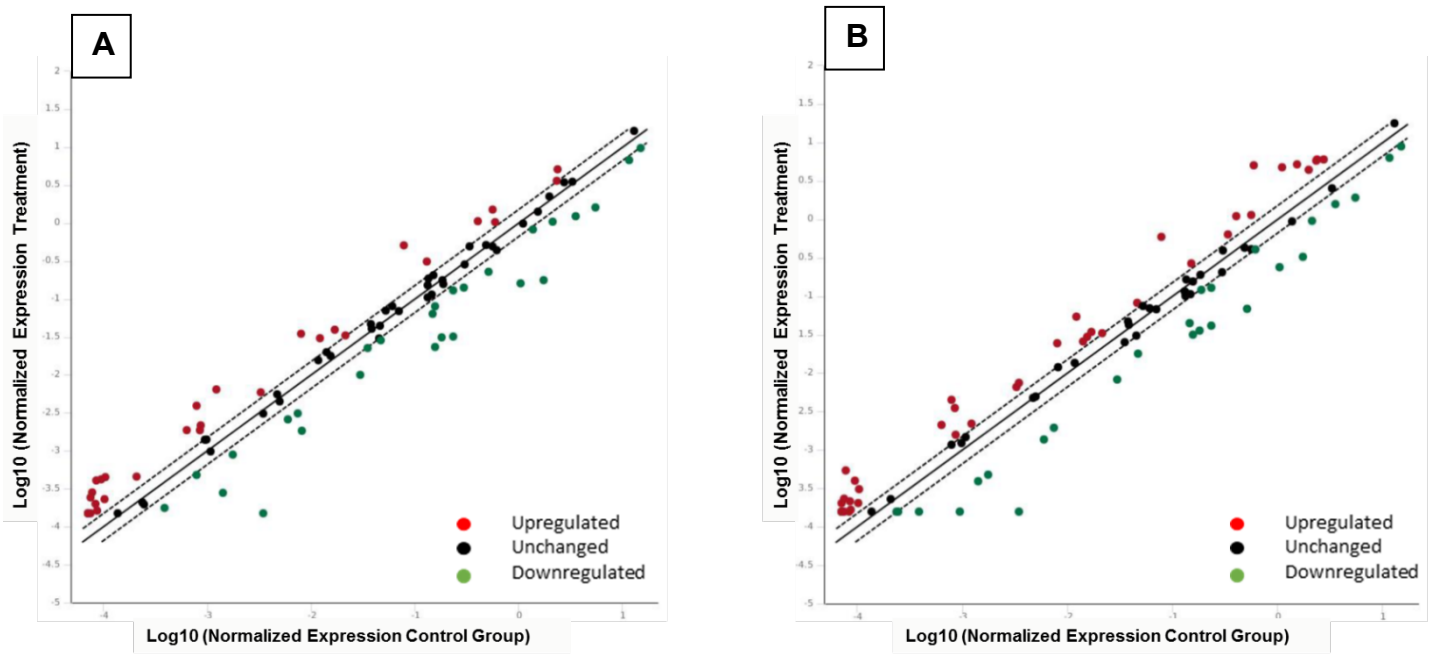

Figure 3.11: Scatter plot of gene expression in MCF-7 cells treated with the chloroform fraction of *B. pilosa*. Cells were seeded at 2.5 x 10^5 cells/ml and treated with 100 µg/ml of the chloroform fraction of *B. pilosa* for 24 (A) and 48 (B) hours before RNA isolation and gene expression analysis using the Human Breast Cancer RT^2 Profiler PCR Array. Each dot represents a gene on the PCR array. Data are presented as the mean of three independent experiments ± standard deviation (SD).

Table 3.9: Differentially expressed genes in MCF-7 cells treated with the chloroform fraction of *B. pilosa.*

Up-regulated				Down-regulated			
24 hr		48 hr		24 hr		48 hr	
Gene	Fold	Gene	Fold	Gene	Fold	Gene	Fold
VEGFA	6.56	*VEGFA*	7.60	*SFRP1*	-22.85	*SFRP1*	-21.75
EGF	5.23	*CDH13*	6.96	*CDH1*	-9.89	*MKI67*	-7.51
CSF1	4.99	*CSF1*	5.72	*MUC1*	-7.28	*SERPINE1*	-6.03
PTGS2	4.83	*GRB7*	4.48	*PGR*	-6.69	*MUC1*	-5.63
ADAM23	4.47	*ADAM23*	4.22	*SLC39A6*	-6.49	*CDH1*	-5.38
NR3C1	4.39	*RARB*	4.16	*THBS1*	-5.83	*THBS1*	-5.09
HIC1	4.34	*GSTP1*	3.33	*SNAI2*	-5.01	*PGR*	-4.93
CDH13	3.65	*GLI1*	3.13	*IGFBP3*	-4.43	*SLC39A6*	-4.36
GLI1	3.27	*NR3C1*	3.08	*CTSD*	-3.45	*EGFR*	-4.33
GSTP1	2.95	*HIC1*	2.98	*BRCA2*	-2.96	*BIRC5*	-3.85
ID1	2.66	*ABCB1*	2.87	*KRT19*	-2.87	*CCNA1*	-3.70
CDKN1A	2.59	*CDKN1A*	2.69	*BIRC5*	-2.41	*BRCA2*	-3.59
GRB7	2.52	*PTGS2*	2.55	*ESR1*	-2.31	*SNAI2*	-3.58
PYCARD	2.51	*XBP1*	2.23	*EGFR*	-2.29	*TFF3*	-3.30
CST6	2.39	*HGDC*	2.23	*MK167*	-2.25	*CTSD*	-2.89
SFN	2.37	*MMP2*	2.23	*KRT5*	-2.20	*BRCA1*	-2.64
ABCG2	2.31	*CDKN2A*	2.23	*IGF1R*	-2.10	*KRT5*	-2.46
IL6	2.25	*IGF1*	2.23	*KRT8*	-2.04	*KRT19*	-2.24
RARB	2.21	*RASSF1*	2.14			*KRT8*	-2.22
ESR2	2.20	*TWIST1*	2.12				
IGF1	2.12	*ATM*	2.03				
CDKN2A	2.12	*ABCG2*	2.01				
HGDC	2.12	*ID1*	2.01				
MMP2	2.12						
ABCB1	2.12						
TWIST1	2.02						

Cells were seeded at 2.5 x 10^5 cells/ml and treated with 100 µg/ml of the chloroform fraction of *B. pilosa* for 24 (A) and 48 (B) hours before RNA isolation and gene expression analysis using the Human Breast Cancer RT^2 Profiler PCR Array. Expression levels were quantified using delta delta C_T formula on GeneGlobe (http://www.qiagen.com/geneglobe), with a 2-fold change cut-off and $p \leq 0.05$. Red: up-regulated at 24 and 48 hours, green: down-regulated at 24 and 48 hours.

Abbreviations: *ABCB1*: ATP-binding cassette, sub-family B, member 1; *ABCG2*: ATP-binding cassette, sub-family G, member 2; *ADAM23*: ADAM metallopeptidase domain 23; *ATM*: Ataxia telangiectasia mutated, *BIRC5*: Baculoviral IAP repeat containing 5; *BRCA1*: Breast cancer 1, early onset; *BRCA2*: Breast cancer 2, early onset; *CCNA1*: Cyclin A1; *CDH1*: Cadherin 1, type 1, epithelial cadherin; *CDH13*: Cadherin 13, heart cadherin; *CDKN1A*: Cyclin-dependent kinase inhibitor 1A, *CDKN2A*: Cyclin-dependent kinase inhibitor 2A; *CSF1*: Colony stimulating factor 1; *CST6*: Cystatin; *CTSD*: Cathepsin D; *EGF*: Epidermal growth factor; *EGFR*: Epidermal growth factor receptor; *ESR1*: Estrogen receptor 1; *ESR2*: Estrogen receptor 2; *GLI1*: GLI family zinc finger 1; *GRB7*: Growth factor receptor-bound protein 7; *GSTP1*: Glutathione S-transferase pi 1; *HGDC*: Human genomic DNA contamination; *HIC1*: Hypermethylated in cancer 1, *ID1:* Inhibitor of DNA binding ; *IGF1*: Insulin-like growth factor 1; *IGF1R*: Insulin-like growth factor 1 receptor; *IGFBP3*: Insulin-like growth factor binding protein 3; *IL6*: Interleukin 6, *KRT19*: Keratin 19; *KRT5*: Keratin 5; *KRT8*: Keratin 8; *MKI67*: Antigen identified by monoclonal antibody Ki67, *MMP2*: Matrix metallopeptidase 2; *MUC1*:

Mucin 1; *NR3C1*: Nuclear receptor sub-family 3, group C, member 1; *PGR*: Progesterone receptor; *PTGS2*: Prostaglandin-endoperoxidase synthase 2; *PYCARD*: PYD and CARD domain containing; *RARB*: Retinoic acid receptor, beta; *RASSF1*: Ras association domain family member 1; *SERPINE1*: Serpin peptidase inhibitor, clade E; *SFN*: Stratifin; *SFRP1*: Secreted frizzled-related protein 1; *SLC39A6*: Solute carrier family 39, member 6; *SNAI2*: Snail homolog 2; *TFF*: Trefoil factor 3; *THBS1*: Thromospondin 1; *TWIST1*: Twist homolog 1; VEGFA: Vascular endothelial growth factor A; *XBP1*: X-box binding protein 1.

3.12 Evaluation of BRCA1 protein expression

Expression levels of BRCA1 in MCF-7 cells treated with the chloroform fraction of the crude methanol extract of *B. pilosa* were evaluated using Western blotting. According to Fig. 3.12 treatment of the cells with the chloroform fraction of *B. pilosa* caused significant down-regulation of BRCA1 expression of about 50% after 24 and 48 hours. Comparison of the expression levels of the protein when cells were treated with various concentrations of the fraction showed a similar effect regardless of the concentration of the plant fraction as well as exposure time. It is, however, interesting to note complete absence of BRCA1 in cells treated with test concentrations exceeding 75 μg/ml of the chloroform fraction of *B. pilosa* for 48 hours. The plant fraction also regulates the housekeeping proteins, GAPDH and β-actin, with observed down-regulation of both proteins after 48 hours of treatment at all tested concentrations.

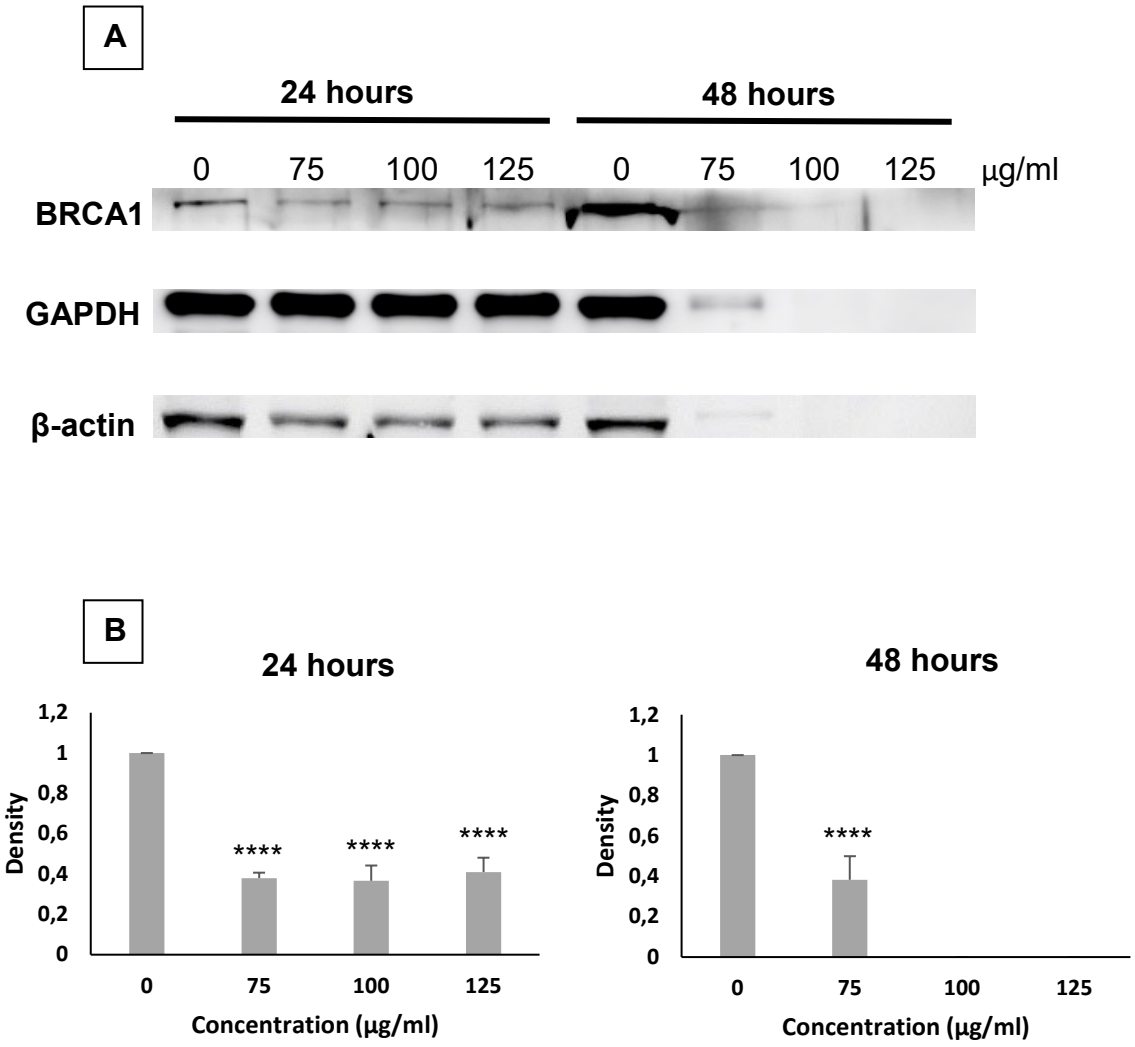

Figure 3.12: Effect of the chloroform fraction of *B. pilosa* on BRCA1 protein expression in MCF-7 cells. A: Cells were exposed to various concentrations of *B. pilosa* for 24 and 48 hours and protein expression was analysed by Western blotting. B: Densitometric band analysis of each BRCA1 band relative to the control was done using ImageJ Software. ****: $p < 0.0001$.

3.13 Quantification of global methylation

The MDQ1 Imprint® Methylated DNA Quantification kit was used to assess the effect of the chloroform fraction of *B. pilosa* on global DNA methylation. Treatment with the extract decreased global DNA methylation by 30% after 24 hours and by 38% after 48 hours of treatment (Fig. 3.13).

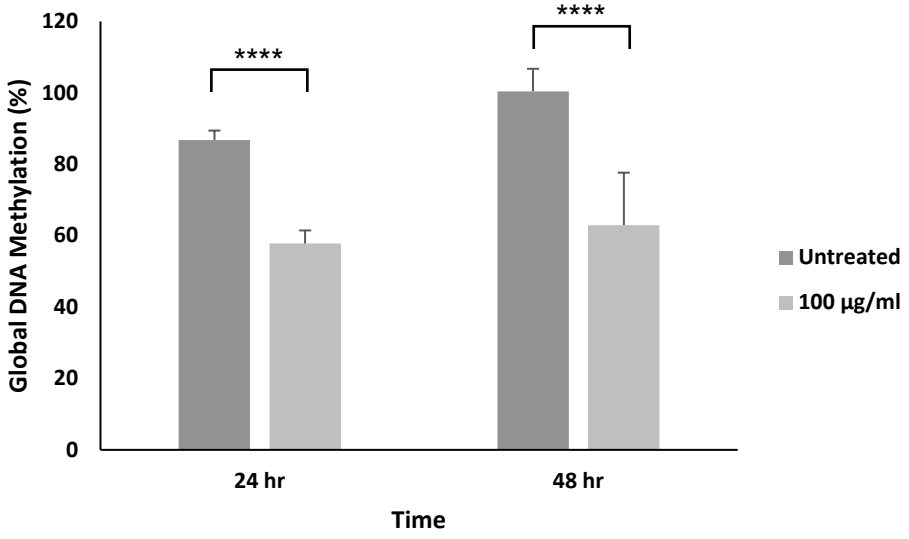

Figure 3.13: Global DNA methylation levels in MCF-7 cells treated with the chloroform fraction of *B. pilosa*. Global DNA methylation was quantified using the MDQ1 Imprint® Methylated DNA Quantification Kit. Methylation levels were calculated relative to a methylated positive control and data represent the mean ± standard deviation (SD) of three independent experiments. ***: $p < 0.005$.

3.14 Confirmation of the quality of bisulfite-converted amplicons

Agarose gels of bisulfite-converted DNA amplified with *BRCA*1, *BRCA*2 and *CDH*1 primers are shown in Fig. 3.14 A, B and C, respectively. Agarose gel electrophoresis show that the expected size amplicons were obtained in both treated and untreated samples, and the absence of bands in the bisulfite and PCR no template controls are indicative of the absence of extraneous nucleic acid contamination.

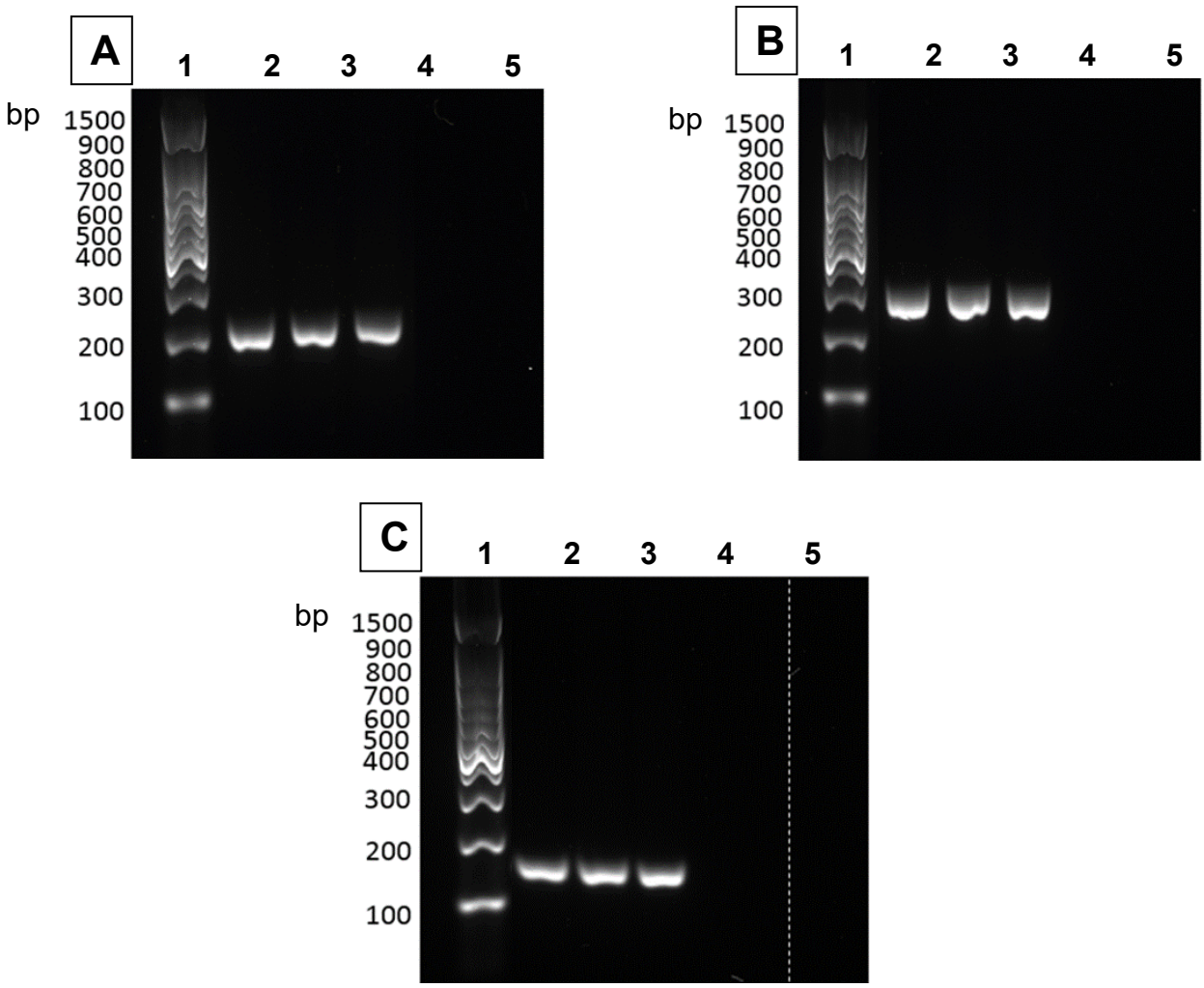

Figure 3.14: Agarose gels of bisulfite-converted amplicons. DNA was extracted from MCF-7 cells treated with 100 µg/ml of the chloroform fraction of *B. pilosa* and bisulfite converted using the EpiTect® Fast Bisulfite Conversion kit. A: *BRCA*1, B: *BRCA*2, C: *CDH*1, lane 1: Molecular weight maker, lane 2: untreated cells, lane 3: cells treated for 24 hours, lane 4: cells treated for 48 hours, lane 5: bisulfite control and lane 6: PCR control, bp: base pairs.

3.15 Analysis of CpG site methylation on *BRCA*1, *BRCA*2 and *CDH*1

Pyrosequencing was conducted to assess the effect of the chloroform fraction of the methanol extract of *B. pilosa* on site-specific methylation of *BRCA*1, *BRCA*2 and *CDH*1. The fraction did not affect the methylation levels of the investigated CpG sites within *BRCA*2 and *CDH*1 (Fig. 3.15B and C), however, 24 hours of treatment with the extract decreased methylation levels at one of the CpGs within *BRCA*1 (Fig. 3.15A). Methylation at this site was lower after 48 hours of treatment as well, but it was not statistically significant.

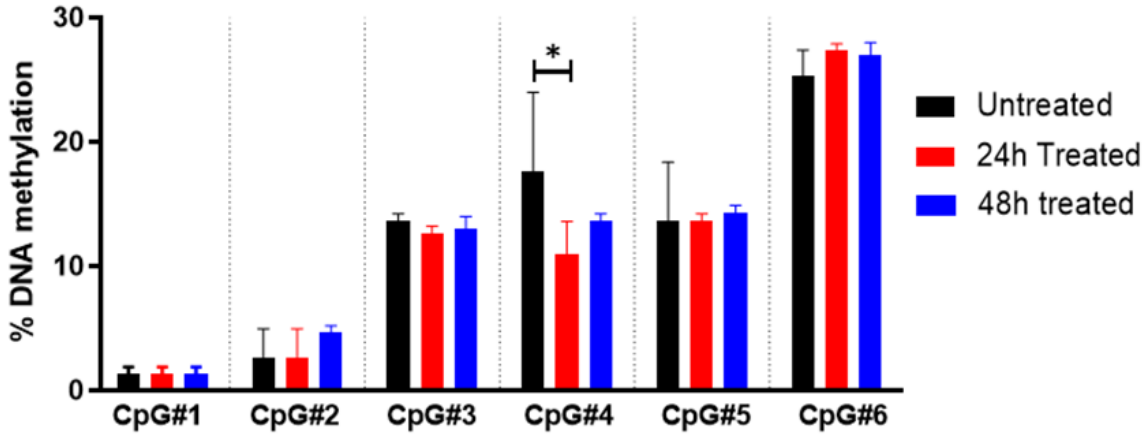

Figure 3.15A: *BRCA*1 CpG site methylation in *B. pilosa* chloroform fraction-treated MCF-7 cells. Human MCF-7 breast cancer cells were treated with 100 µg/ml of the chloroform fraction of *Bidens pilosa* for 24 hours and 48 hours and methylation levels at six CpG sites in the *BRCA*1 gene (-2170,-2164, -2161, -2158, -2152, -2130) assessed using bisulfite pyrosequencing. Data is represented as the mean ± standard deviation (SD) of three independent experiments. *: $p < 0.05$.

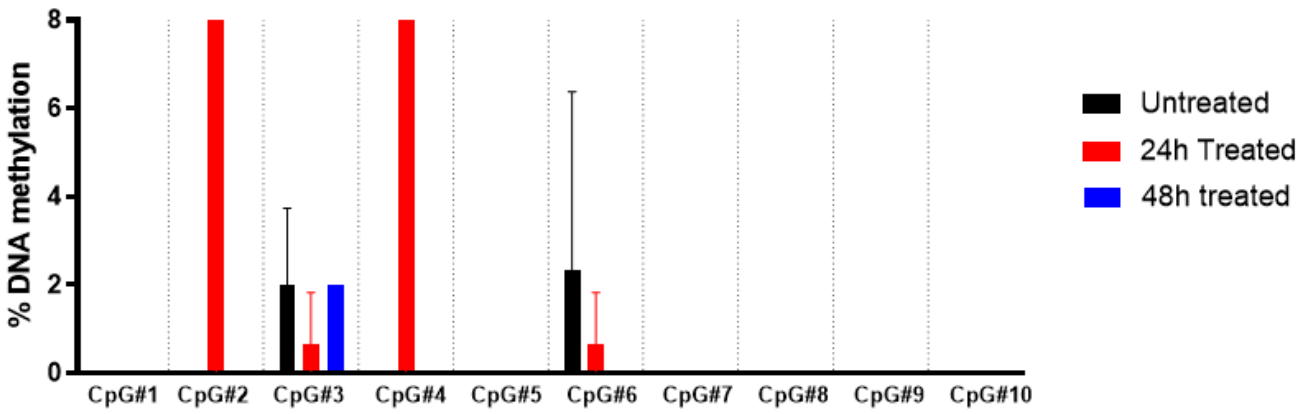

Figure 3.15B: *BRCA2* CpG site methylation in *B. pilosa* chloroform fraction-treated MCF-7 cells. Human MCF-7 breast cancer cells were treated with 100 µg/ml of the chloroform fraction of *Bidens pilosa* for 24 hours and 48 hours and methylation levels at ten CpG sites in the *BRCA2* gene (-1036, -1027, -1018, -1013, -1011, -1006, -1003, -998, -989, -984) assessed using bisulfite pyrosequencing. Data is represented as the mean ± standard deviation (SD) of three independent experiments.

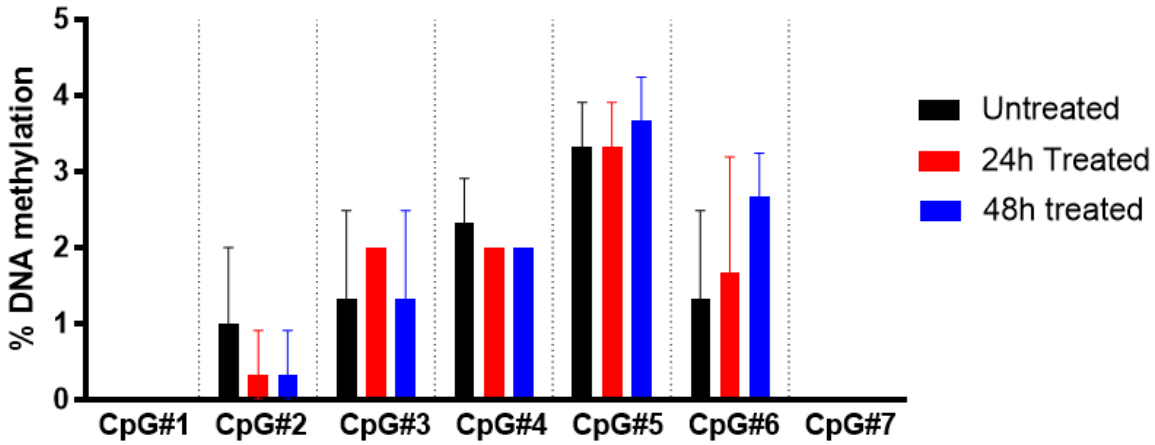

Figure 3.15C: *CDH*1 CpG site methylation in *B. pilosa* chloroform fraction-treated MCF-7 cells. Human MCF-7 breast cancer cells were treated with 100 µg/ml of the chloroform fraction of *Bidens pilosa* for 24 hours and 48 hours and methylation levels at seven CpG sites in the *CDH*1 gene (-56, -51, -44, -35, -12, +6, +9) assessed using bisulfite pyrosequencing. Data is represented as the mean ± standard deviation (SD) of three independent experiments.

3.16 Verification of pyrosequencing primers

Primer efficiency of *BRCA*1 (six CpGs), *BRCA*2 (ten CpGs) and *CDH*1 (seven CpGs) was tested by conducting pyrosequencing with varying percentages (0, 10, 25, 50, 75, 90 and 100 %) of a human methylated DNA control. According to Fig 3.16, the expected percentage of methylation was observed at each of the CpG sites in the probes, confirming that the designed primers were suitable for pyrosequencing. This was true for all sites except CpG6 on *CDH*1, where human (pipetting) error resulted in less than 50% methylation where 75% methylation was expected.

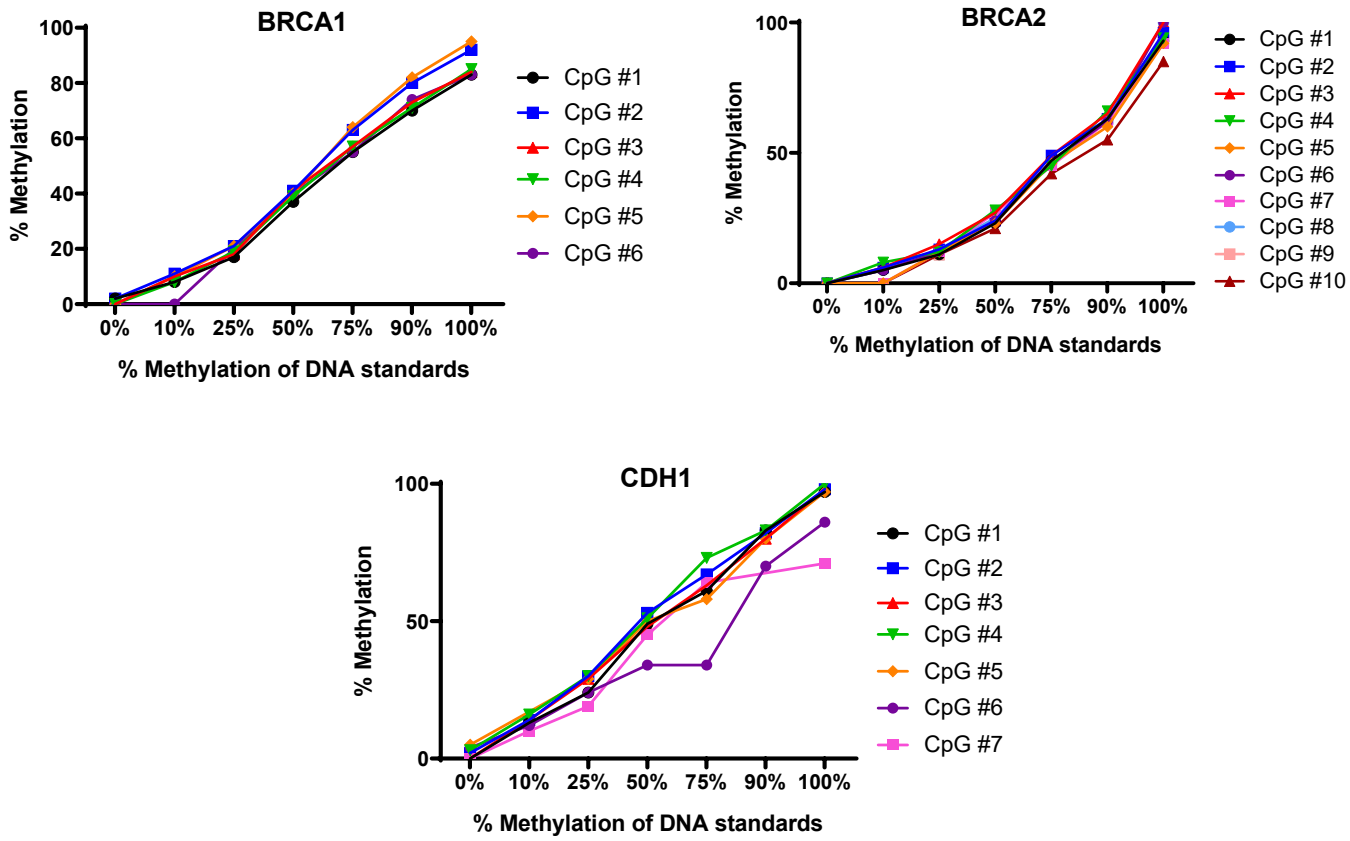

Figure 3.16: **Conversion efficiency of *BRCA*1, *BRCA*2 and *CDH*1 pyrosequencing primers.** Primers were tested for conversion efficiency by performing PCR and pyrosequencing with a methylated DNA control ranging from unmethylated (0%) to completely methylated (100%). Percentage methylation was determined for six CpG sites for *BRCA*1 (-2170,-2164, -2161, -2158, -2152, -2130), ten CpG sites for *BRCA*2 (-1036, -1027, -1018, -1013, -1011, -1006, -1003, -998, -989, -984) and seven CpG sites for *CDH*1 (-56, -51, -44, -35, -12, +6, +9).

3.17 Analysis of telomerase activity

Treatment with the chloroform fraction of *B. pilosa*'s methanol extract decreased telomerase activity of MCF-7 breast cancer cells (Fig. 3.17). In the assay, samples with an absorbance change (A_{450} – A_{690}) below 0.2 are said to have no telomerase activity. According to Fig. 3.17, treatment at all selected concentrations resulted in the absence of telomerase activity after both 24 and 48 hours of exposure to the fraction.

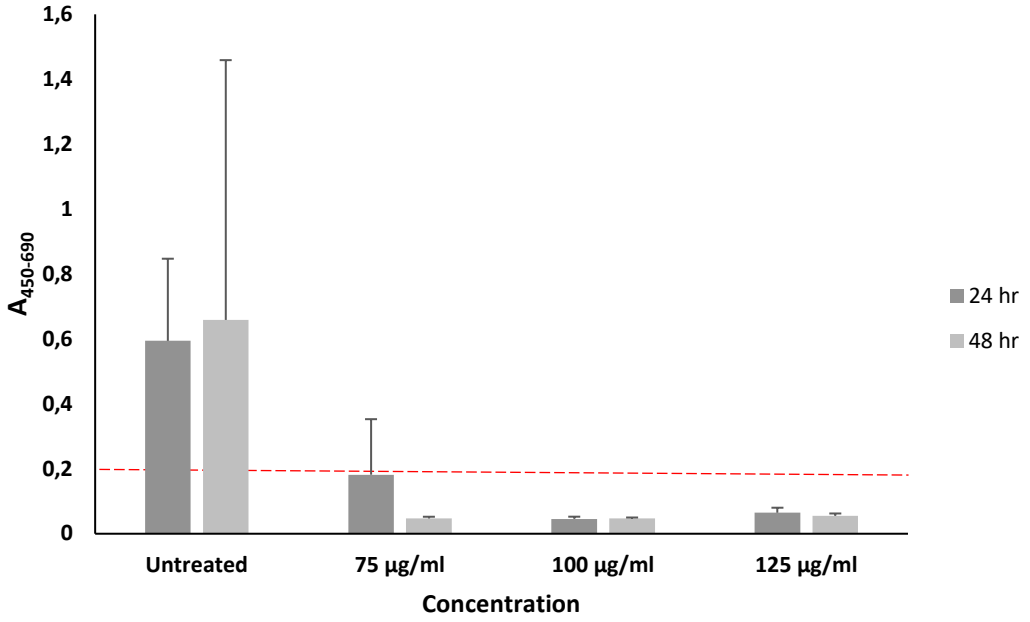

Figure 3.17: Telomerase activity in MCF-7 cells treated with the chloroform fraction of *B. pilosa*. Telomerase activity was measured in 2.5 x 10^5 cells using the *Telo*TAGGG™ Telomerase PCR ELISA kit. Data is represented as the mean ± standard deviation (SD) of three independent experiments.

CHAPTER 4

DISCUSSION AND CONCLUSION

4.1 General Discussion

The global incidence of breast cancer has continued to increase over the years (Rue *et al*. 2009). Conventional therapies for the recalcitrant malignancies are undesirable as they may warrant surgery for their treatment. This method is however invasive and costly, thereby presenting a need for finding alternative options for cancer treatment. Moreover, therapy involving the use of drugs often results in unwanted side effects, thus affecting the overall health of the patient (Hayman, 2008). To this end, the global population is gradually adopting the use of plant extracts as an alternative form of treatment as opposed to the use of synthetic drugs. These plant extracts in turn provide a valuable source for finding new drug leads. So, breast cancer is not excluded from the numerous diseases against which herbal remedies are explored as possible treatment options.

There are numerous reports on the analysis of *B. pilosa* in breast cancer in rats (Arroyo *et al*. 2010; Raimi *et al*. 2020). *B. pilosa* has also been investigated for use as a remedy for a variety of ailments ranging from headaches to ear infections, diarrhoea, ulcers and malaria (Xuan and Khanh 2016). The phytochemical fingerprint analyses carried out in this study corroborate the traditional uses of *B. pilosa* across the globe. Thin layer chromatography was employed to screen the crude methanol extract of *B. pilosa* and its subsequent six sub-fractions of varying polarity for the distribution of secondary metabolites as well as for potential compounds that possess antioxidant activity. The mobile phase (CEF – chloroform, ethyl acetate and formic acid) that was used for developing the TLC plates in Fig. 3.1 was of intermediate polarity and acidic in nature. This mobile phase allowed better separation of chemical compounds of lower polarity as observed in Fig. 3.1A, lane B1, where the compounds were extracted with *n*-hexane. However, the compounds in lane B6 (water sub-fraction) did not separate optimally as they are of higher polarity than the mobile phase and therefore remained adsorbed on to the silica matrix on the TLC plate.

Figure 3.1B underlined the presence of compounds with the ability to quench free radicals by reducing the purple DPPH hydrazyl to a yellow hydrazine. These antioxidant compounds were distributed evenly among the sub-fractions of intermediate polarity as well as polar sub-fractions. It is evident from Fig. 3.1B that the ethyl acetate, *n*-butanol and 65% methanol sub-fractions had the highest distribution of antioxidant compounds, due to their varying polarities. Further, migration of the compounds relative to the solvent front was comparable, alluding to the presence of similar compound groupings in these sub-fractions. Despite the similar distribution of compounds among the various sub-fractions, intensities of the yellow colour of each band against the purple background were different, with many of the bands displaying higher intensity in the *n*-butanol sub-fraction (lane B4). The dissimilarity in intensities was attributed to the different concentrations of the compound in each sub-fraction. Therefore, some of the compounds can be said to be more concentrated and predominant in the *n*-butanol sub-fraction. Since methanol was used as the primary extractant, all the compounds in the sub-fractions were presumed to be present in large quantities in the crude methanol extract. On the contrary, however, Fig 3.1B displayed less intense bands in the methanol crude extract (lane C), suggesting a lower free-radical scavenging activity of its inherent compounds. Indeed, the crude methanol extract is a mixture of a myriad of compounds, some of which may be dampening or masking the activity of key and predominant antioxidant compounds in the crude extract. Therefore, sub-fractionation of the crude methanol extract seemed to have heightened the antioxidant property of these compounds.

TLC-DPPH screening does not give a measure of the reduced DPPH. In order to quantify the antioxidant activity of the crude methanol extract as well as each of the sub-fractions, a spectrophotometric DPPH assay was conducted. Results from this assay has shown both ethyl acetate and *n*-butanol sub-fractions to demonstrate the best antioxidant activity, followed by the 65% methanol and chloroform sub-fractions, as well as the crude methanol extract. When the results of the quantitative assay (Fig. 3.2) are aligned with those from the qualitative assay (Fig. 3.1B), the ethyl acetate and *n*-butanol sub-fractions were found to possess the best antioxidant potential in both assays, while the non-polar (*n*-hexane) and polar (water) solvents displayed little free-radical scavenging activity.

The antioxidant activity of plant extracts is often an attribute of the presence of phenolic compounds, as they have the ability to quench free radicals (Formagio *et al.* 2014). Phenolic compounds have varying polarities and are often best soluble in organic solvents that are less polar than water (Haminiuk *et al*. 2014). It is interesting to note the high total phenolic content of the water sub-fraction (Fig. 3.3), buttressing the traditional medicinal practice of using herbal tinctures that are often prepared by boiling or infusing the plant material in water. The observation that the water sub-fraction contained the highest concentration of phenolic compounds confirms water as an excellent solvent for the preparation of herbal decoctions as phenolic compounds are known to be responsible for many health benefits that are associated with plant-based food (Cheynier 2012). Only the water sub-fraction showed higher total phenolic content than the *n*-butanol sub-fraction (Fig. 3.3). Despite the high total phenolic content observed in Fig. 3.3, the water sub-fraction did not exhibit the anticipated antioxidant activity. This may mean that not all the phenolic compounds present in this sub-fraction possess good antioxidant activity; however, they may still have the excellent biological activities as described (Cheynier 2012). Together with its high content of antioxidant compounds, the *n*-butanol sub-fraction also exhibited the highest tannin and flavonoid content (Figs. 3.4 and 3.5). Tannins and flavonoids are classes of phenolic compounds and they represent a portion of the antioxidant activity of each of the tested sub-fractions of *B. pilosa*. However, flavonoids are of lower molecular weight, but are nonetheless more abundant in the diet than tannins (Palma, 2017).

Although the *n*-butanol sub-fraction displayed better antioxidant potential and a higher content of total phenolic compounds, the chloroform sub-fraction exhibited the highest cytotoxicity against MCF-7 breast cancer cells among all the tested sub-fractions, with an IC_{50} of approximately 100 μg/ml in the MTT assay (Figs. 3.6 and 3.7). At this concentration, the chloroform sub-fraction decreased cell viability with insignificant depolarisation of mitochondrial membranes in live cells (Figs. 3.8A and 3.8B). During apoptosis a series of predictable changes in the cellular morphology and environment take place. Morphological changes occurring during the early stages of apoptosis are accompanied by other transient stages, with the mitochondrial membrane depolarisation being one of the most studied (Christensen *et al.* 2013). Prolonged

mitochondrial depolarisation allows leakage of mitochondrial apoptotic factors into the cytosol (e.g. cytochrome c) which may begin a cascade of events that ultimately trigger the intrinsic pathway of programmed cell death (Zorova *et al*. 2018). According to Figs. 3.8A and 3.8B, the chloroform sub-fraction of *B. pilosa* induced a change in mitochondrial membrane depolarisation, although it was only detected in dead cells. This suggests that, as an early event, the depolarisation occurred prior the 12 hour evaluation period and this led to the detection of mostly cells that had already undergone cell death. Assessment of this transient change in the mitochondria should, therefore, ideally be done early after treatment with the sub-fraction.

The cytotoxic nature of the chloroform sub-fraction could not be strongly linked to the presence of phenolic compounds as its inhibitory effect on MCF-7 cells far exceeded that of the sub-fractions with higher total phenolic, flavonoid and tannin content (Figs. 3.3, 3.4 and 3.5). Indeed, the ethyl acetate, *n*-butanol and 65% methanol sub-fractions contained higher tannin and flavonoid content than the chloroform sub-fraction, yet they exhibited lower cytotoxic effect against MCF-7 breast cancer cells on evaluation with the MTT assay. This finding suggests that the compound(s) responsible for the cytotoxic effect of the chloroform sub-fraction may be of a class of chemical compounds other than the phenolics. Table 3.3 lists the major compounds detected in highest abundance by NIST 95 software in GC-MS in the chloroform sub-fraction as three fatty acids: *n*-hexadecanoic acid (palmitic acid); 9, 12-octadecadienoic acid (Z, Z) (linoleic acid) and 9, 12, 15-octadecatrienoic acid (Z, Z, Z) (α-linolenic acid), with % peak areas of 10.142, 10.15 and 16.418, respectively. Together with many other metabolites identified in this study, these aliphatic compounds are among the 201 compounds identified in the plant in previous studies, summarised by Bartolome, Villaseñor and Yang (2013). Palmitic and linoleic acids were identified in an extract of the aerial parts of *B. pilosa* by Geissberger and Sequin (1991) while α-linolenic acid was first identified by Lee *et al*. (2000) in an extract prepared using the whole plant.

Dietary saturated fatty acids, monounsaturated fatty acids and *trans*-fatty acids have been shown to drastically increase cancer risk while polyunsaturated fatty acids are generally known to possess anticancer activity (Liu and Ma 2014). However, recent research by Zafaryab *et al.* (2019) showed inhibitory effects of palmitic acid (the most common saturated fatty acid) on MCF-7 breast cancer cell growth with upregulation of

pro-apoptotic genes, therefore proposing a treatment option with palmitic acid as a possible therapeutic measure against certain types of malignancies. As observed with palmitic acid, products of *n*-3 polyunsaturated fatty acids have also shown to have anti-carcinogenic potential, while those of *n*-6 polyunsaturated fatty acids stimulate cell proliferation (Corsetto *et al*. 2011). Studies in women with a high consumption of *n*-6 polyunsaturated fatty acids (Western diet) showed a higher incidence of breast cancer than in women with a higher *n*-3 polyunsaturated fatty acid intake (Asian diet) (Murff *et al*. 2011; Straka *et al*. 2015; Zheng *et al*. 2013). As shown in Table 3.3, α-linolenic acid was detected in high abundance in the chloroform sub-fraction. This compound is the precursor of the *n*-3 polyunsaturated fatty acid family and its metabolite, docosahexanoic acid (DHA), which has been shown to induce apoptosis in breast cancer cells by decreasing the expression of the epidermal growth factor receptor, EGFR (Gerber 2012). EGFR is involved in the pathogenesis of cancer as a pivotal driver of the transformation, proliferation and invasion of tumour cells (Ali and Wendt 2017).

Dysregulation of certain genes like *EGFR* is associated with the hallmarks of cancer pathogenesis. These trademarks include uncontrolled replication and proliferation, insensitivity to growth suppressors, sustained angiogenesis, tissue invasion as well as evasion of apoptosis (Hanahan and Weinberg 2011). For the rapid investigation of the genes that are associated with these changes in mammary tumours, the Human Breast Cancer RT^2 Profiler PCR Array that combines real-time PCR with a microarray to analyse differential expression of a panel of genes common to human breast cancer pathways was used. Results of the PCR array in this study showed that the chloroform sub-fraction indeed lowered the expression of *EGFR* (Table 3.9), and this might have been one of the critical contributors to the observed decrease in cell viability (Figs. 3.6 and 3.7). There was a 2.29-fold decrease in *EGFR* expression within 24 hours of treatment of MCF-7 cells with the chloroform sub-fraction and this down-regulation decreased further to 4.33-fold after 48 hours of treatment (Table 3.9). Therefore, the presence of *n*-3 polyunsaturated fatty acids in the chloroform sub-fraction could have played a crucial role in the repression of *EGFR* gene expression, thus contributing to the observed cytotoxic effects of the sub-fraction.

Gene expression analyses also showed an increase in the expression of vascular endothelial growth factor gene (*VEGFA*) and a decrease in *CDH*1 expression after treatment of the cells with the chloroform sub-fraction (Table 3.9). The observed effect in the latter two genes is expected to influence tumour progression. *VEGFA* is involved in angiogenesis – the formation of new blood vessels (Weis and Cheresh 2011). Its importance in cancers is that it enables alterations in endothelial cells that promotes formation of new blood vessels during tumour progression (Zhang *et al*. 2019). However, our results from the viability assays are to the contrary, showing decreased cell viability in treated MCF-7 cells (Figs. 3.8 and 3.9). For the promotion of angiogenesis, VEGFA acts by binding to vascular endothelial growth factor receptor 2 (VEGFR2) on the endothelial cell membrane (Potente, Gerhardt, and Carmeliet 2011), and this binding might have been blocked by the activity of other compounds present in the *B. pilosa* chloroform sub-fraction. However, pathways activated by VEGFA in breast cancer and other cancers are not completely delineated and are mostly not understood (Jang *et al*. 2017). According to Zhang *et al.* (2019) VEGFA may be upregulated in the malignant cell, but yet happen to fail to be transported from tumour cells to bind to VEGFR2 on the neighbouring endothelial cells to initiate angiogenesis. We speculate that this might be the same manner through which the chloroform sub-fraction affected the action of VEGFA, and thus upregulation of the gene is presumed to not play a role in the observed apoptotic effect of the sub-fraction in the MCF-7 cells.

Furthermore, the VEGF family is known to act as survival factors for tumour cells and assist in protecting them from external stresses, e.g. chemo- and radiotherapy (Duffy, Bouchier-Hayes, and Harmey 2004; Mao et al. 2013). The observed upregulation could, therefore, be the cells' adaptive response to the changed environment introduced by the sub-fraction. Interestingly, in the work done by Duffy, Bouchier-Hayes and Harmey (2013), *VEGFR2* mRNA was identified in breast cancer cells, while at the same time the protein was not detectable. A similar increase in *VEGFA* expression levels was also observed at the mRNA level in our study, but we did not evaluate the presence of its corresponding protein due to the observed decrease in cell viability that suggests that no angiogenesis pathways were initiated. It would, therefore, still be necessary to assess the expression levels of the protein as well, as an increase in mRNA synthesis may not necessarily infer an upregulation of the resultant peptide. This could be a critical point of the regulation of *VEGFA* expression,

which warrants further exploration in order to outline the actual molecular mechanism of action.

Similarly, a decrease in the expression of *CDH*1 gene in breast cancer cells is associated with loss of cell-to-cell adhesion and metastasis as the protein encoded by the gene, epithelial cadherin (E-cadherin), functions as a cell invasion suppressor (Corso *et al*. 2016). Interestingly, Table 3.9 shows a marked down-regulation of *CDH*1 at the gene level, with a 10-fold decrease in expression after 24 hour treatment of MCF-7 cells with the chloroform sub-fraction. However, the MCF-7 cell line used in this study is not invasive and, therefore, expresses functional E-cadherin (Eslami Amirabadi *et al*. 2019). Expression of genes may be regulated epigenetically, where the promoter region is rendered inaccessible to transcription factors by methyl groups on cytosine nucleotides in CG-rich sequences (Spencer *et al*. 2017). The *CDH*1 promoter region is unmethylated, allowing efficient transcription of the gene (Shargh *et al*. 2014). Hiraguri *et al.* (1998) showed that in other breast cancer cell lines, the expression of *CDH*1 is modulated by promoter methylation and it was therefore necessary to investigate if the observed repression of *CDH*1 in this study was also a consequence of differential methylation of its promoter region. As shown in Fig. 3.15C, the chloroform sub-fraction did not alter the methylation levels on any of the seven probed CpG sites in the selected CpG island on the promoter of the *CDH*1 gene. After 48 hours of treatment with the sub-fraction, methylation levels remained below 5% on all the investigated seven CpG sites, thus suggesting a different kind of repression mechanism that does not involve hypermethylation at this particular CpG island.

Increased expression of the pro-metastatic gene, *VEGFA*, and a decreased expression of the anti-metastatic gene, *CDH*1, suggest an increase in metastatic potential of the MCF-7 cell line when exposed to the chloroform sub-fraction of the crude methanol extract of *B. pilosa*. However, the gene expression data also suggest that this sub-fraction has a remarkable anti-tumour effect on MCF-7 breast cancer cells. As shown in Table 3.9, it is evident that there is downregulation of the two breast cancer susceptibility genes, *BRCA*1 and *BRCA*2. In normal cells, BRCA1 and BRCA2 proteins are involved in the repair of double-stranded DNA breaks, transcriptional regulation and cell division cycle regulation (Henderson 2012; Wu, Lu, and Yu 2010). Intact BRCA1 is involved in the activation and maintenance of the transition of cells

from G_2 to M phase of the cell division cycle, recruiting other repair proteins to the site of DNA damage. The G_2/M checkpoint is important for inspecting cells before entry into mitosis so as to impede the segregation of broken and faulty chromosomes during mitosis (Simhadri *et al*. 2019). Therefore in the absence of BRCA1, cells are arrested at the G_2/M checkpoint and directed to apoptosis (Sadeghi *et al*. 2020). Table 3.9 and Fig. 3.12 show the repression of *BRCA*1 at both the gene and protein levels following treatment with the chloroform sub-fraction, with consequential accumulation of cells in the G_2/M phase of the cell division cycle (Fig. 3.10). The notable concentration-dependent increase in the population of cells in the G_2/M phase of the cycle suggests that the chloroform sub-fraction effects G_2/M cell division cycle arrest and the subsequent apoptotic demise of the arrested cells. The lack of BRCA1 has been shown to result in higher sensitivity of cells to many chemotherapeutic drugs, e.g. paclitaxel, cisplatin, vincristine (James *et al.*, 2007). A report by Stefansson *et al.* (2012) highlights BRCA1 deficiency to be at the forefront of the sensitivity of cells to cisplatin, with treatment causing excessive DNA damage not observed in cells expressing BRCA1. Therefore, the downregulation of *BRCA*1 in MCF-7 cells treated with the chloroform sub-fraction of *B. pilosa* could be sensitising the cells to other compounds found in the extract that induce apoptosis. This needs further exploration in order to assess if the downregulation of BRCA1 by palmitic acid or DHA sensitises MCF-7 cells to the action of other compounds in the chloroform sub-fraction that results in the DNA damage, culminating in apoptotic cell death.

Both *BRCA*1 and *BRCA*2 have well-characterised CpG islands in their promoter regions. *BRCA*1 promoter methylation plays a critical role in the development and progression of breast cancer (Iwamoto *et al*. 2011). Hypermethylation of the *BRCA*1 and *BRCA*2 promoters is known to lead to repression of the genes early in tumour development (Cai *et al*. 2014; Vos *et al*. 2017). Furthermore, meta-analysis by Zhang and Long (2015) revealed a correlation between aberrant *BRCA*1 promoter methylation and decreased expression of the protein. According to our bisulfite sequencing results, there was a decrease in the percentage of methylation at only one site in the selected CpG island of the *BRCA*1 promoter region following 24 hour treatment of MCF-7 cells with 100 μg/ml of the chloroform sub-fraction (Fig. 3.15A). Although not statistically significant, treatment with the sub-fraction for 48 hours

maintained the hypomethylation status at this CpG site, -2158bp upstream of the transcription start site. However, the other five tested CpG sites upstream of the transcription start site (-2170, -2164, -2161, -2152 and -2130) showed no alteration in the methylation status of this CpG island after treatment with the sub-fraction. Indeed, treatment of MCF-7 cells with the chloroform sub-fraction did not exert significant variation in the methylation status of *BRCA*2 CpG site of the chosen CpG island (Figs. 3.15B). It thus emerged from the current findings that aberrant methylation in the selected CpG islands has no influence on the observed down-regulation of *BRCA*1 and *BRCA*2 genes. However, we acknowledge that the number of CpG sites analysed in this study were few and that other CpG sites or other epigenetic mechanisms may be involved in the regulation of *BRCA*1 and *BRCA*2 genes under the current experimental conditions. It may therefore be worthwhile to analyse other CpG sites on each of these genes to evaluate variations in the methylation status of the entire promoter region following treatment with the chloroform sub-fraction of the methanol extract of *B. pilosa*. Therefore, future studies should assess DNA methylation within larger areas of the gene, as opposed to the small promoter region examined by pyrosequencing in this study.

Together with altered promoter methylation patterns, aberrant methylation of the entire genome is also an epigenetic hallmark of tumours. Loss of global methylation leads to increased instability of the genome (Kuchiba *et al*. 2014). To this end, methylation of the genome in MCF-7 cells was analysed following treatment with the chloroform sub-sub-fraction of *B. pilosa*. The global methylation quantification data showed a notable decrease in DNA methylation after 24 and 48 hours of treatment with the sub-fraction (Fig. 3.13). Further hypomethylation of the genome indicates a decrease in chromosomal stability, thus promoting cancer progression. The genome instability augmented by the treatment with the chloroform sub-fraction may also be contributing to the observed arrest at the G_2/M phase of the cell division cycle (Fig. 3.10), as well as the upregulation of ataxia-telangiectasia-mutated gene, *ATM* (Table 3.9). In fact the protein encoded by *ATM* gene is a key regulator of the DNA damage response and plays a crucial role in maintaining the integrity of the genome through involvement in numerous anti-proliferative pathways that include G_2/M checkpoint activation. Therefore, the instability within chromosomes that is brought about by the action of the

chloroform sub-fraction resulted in an increased G_2/M arrest, possibly directing the cells to an apoptotic death.

In order to retain immortality, breast cancer cells have numerous other epigenetic mechanisms in place. Tumour cells employ the enzyme telomerase to elongate telomeres as shortening of these telomeres during DNA replication limits cellular proliferation (Günes and Rudolph 2013). While most somatic cells lack telomerase, the enzyme is active in 74% of breast cancers and this makes telomerase-inactivating agents a promising approach of destroying cancer cells without affecting the neighbouring normal cells (Kazemi-Lomedasht, Rami, and Zarghami 2013; Sprouse, Steding, and Herbert 2012). Treatment of MCF-7 cells with the chloroform sub-fraction of the crude methanol extract of *B. pilosa* resulted in a decrease in telomerase activity, as measured with the *T*elo*TAGGG*™ Telomerase PCR ELISA assay (Fig. 3.17). Notably, a significant decrease in telomerase activity was noted within 24 hour at all treatment conditions used. The activity of the enzyme was completely absent following 48 hour treatment with 100 μg/ml and 125 μg/ml of the sub-fraction. At these concentrations, none of the treated cells would have had the ability to extend the ends of their chromosomes through the activity of the telomerase. Therefore, the shortening of these telomeres will ultimately limit proliferative capability of the MCF-7 breast cancer cells, resulting in cellular demise.

This study has established the chloroform sub-fraction of *B. pilosa* to possess high content of phenolic compounds and fatty acids. Numerous plant secondary metabolites, especially phenolic compounds, have been shown to modulate telomerase activity in MCF-7 cells. In particular, curcumin, genistein, epigallocatechin gallate and sulforaphane are distinguished phytocompounds with well-documented suppressive effects on the activity of telomerase in breast cancer cells (Kazemi-Lomedasht, Rami, and Zarghami 2013; Lewis *et al*. 2018; Paul, Li, and Tollefsbol 2018). Alpha-linolenic acid and DHA (a metabolite of palmitic acid) have also been shown to reduce telomerase activity with IC_{50} values of 10 and 5 μM, respectively (Eitsuka *et al*. 2018). It is noteworthy to remember that the aforementioned fatty acids have been detected in large quantities in the chloroform sub-fraction of *B. pilosa* (Table 3.3). Furthermore, the *BRCA*1 gene has been implicated in the lengthening of

telomeres in cancer cells with an absence of its cognate protein, resulting in the shortening of telomeres (Rosen 2013). Repression of *BRCA*1 following treatment of MCF-7 cells with the chloroform sub-fraction might have played a pivotal role in the observed decreased telomerase activity in Fig. 3.17. This inhibitory action might have, directly or indirectly, affected the telomerase activity, thus contributing to the observed decrease in cell viability in the MTT cytotoxicity assay.

4.2 Integration and analysis

The observations from this study substantiate the widely reported therapeutic potential ascribed to *B. pilosa.* The wide array of chemical compounds identified in the crude methanol extract alludes to a broad spectrum biological activity of the plant, corroborating previous study findings (Bartolome, Villaseñor and Yang, 2013; Xuan and Khanh, 2016). Although palmitic acid was found in high concentration in the most active sub-fraction of this plant, other compounds may be responsible for the therapeutic action elicited by the chloroform sub-fraction. Plant extracts contain a myriad of compounds, with some enhancing each other's activity and others exerting antagonistic effects. Therefore, the complex nature of plant extracts makes it near impossible to pin-point a specific compound and the pathway that is responsible for the observed response in cells that have undergone treatment. Any cellular response to a plant extract treatment cannot be attributed to one compound and a single pathway in the cell at a given time. Thus, a bioassay-guided isolation will assist in the identification of the compound(s) responsible for the cytotoxicity of the chloroform sub-fraction of *B. pilosa* in MCF-7 cells, as well as the repression of *BRCA*1 expression that led to the resultant cell division cycle arrest and the inactivation of telomerase.

4.3 Novelty and significance

Globally, there is a demand for natural products that are safe and effective for treating a myriad of malignancies and other ailments afflicting human kind. In the current context, a previous study by Kumari *et al.* (2009) has highlighted the anticancer potential of the chloroform extract of *B. pilosa* in breast cancer cells. However, the molecular mechanism of action of the extract in that study was not delineated. Further, many studies investigating the effect of plant extracts on breast cancer still focus

mainly on the bioactivity of the extracts or isolated compounds on the genome, but rarely on the epigenome. Due to the reversibility of epigenetic manifestations, altering the epigenome seems a more promising and ideal approach in the quest for the development of anticancer therapeutics. In the current study, the assessment of the effect of the chloroform sub-fraction of *B. pilosa* in MCF-7 breast cancer cells showed that the plant has the potential of altering epigenetic hallmarks of breast cancer in a manner that ultimately induces apoptosis. Apoptosis is the most ideal way of eliminating cancer cells without damaging the bystander healthy cells. Our study further established that the observed epigenetic modifications are possibly an attribute of the action of palmitic acid, a saturated fatty acid that was previously suspected to increase cancer risk (Liu and Ma 2014). In agreement with findings by Zafaryab *et al.* (2019), the high abundance of this fatty acid in the chloroform sub-fraction of *B. pilosa* may be assumed to have played a critical role in inhibiting MCF-7 cell growth in the present study. Our findings further suggest that the medicinal role of palmitic acid in breast cancer involves the repression of BRCA1 which in turn causes an increase in genome instability as well as the inactivation of telomerase activity in the MCF-7 tumour cells. Indeed, the gradual shortening of the telomeres from the lack of telomerase activity inhibits the cells from indefinite proliferation, thus halting tumour growth, while the faulty DNA resulting from decreased global DNA methylation arrests the cells at the G_2/M checkpoint of the cell division cycle to allow for the repair machinery to initiate. Paradoxically, the G_2/M checkpoint repair is dependent on BRCA1 as an integral component for the recruitment of other repair apparatus to the site of DNA repair. Therefore, in the absence of BRCA1 to initiate the repair process, as observed in our study, the treated cancer cells should subsequently be directed to a programmed cell death. Our findings thus propose a pivotal role of palmitic acid in the development and progression of various types of cancer, and it also most likely has a therapeutic effect in some or all cancers due to its potential to induce apoptosis through alteration of epigenetic mechanisms within tumour cells. Thus, a more though investigation to substantiate this assertion is warranted.

4.4 Strengths and limitations

With every study, resources and time constraints sometimes limit the extent to which investigations can be expanded. As it was in our case, budgetary constraints limited

the extent to which we could have widen the scope of investigation on the effect of the chloroform sub-fraction on the methylation statuses of CpG islands on *BRCA*1, *BRCA*2 and *CDH*1 promoter regions. Although pyrosequencing is a highly sensitive and specific method of DNA methylation analysis, only short sections of DNA can be analysed using this method, and for this reason we might have also missed regions of altered DNA methylation in the genes of interest in this study. As a consequence, therefore, future studies are necessary in order to investigate overlapping primer sets which will allow proper interrogation of larger gene sequences. We cannot also discount the possibility of the involvement of other relevant genetic or epigenetic mechanisms that underlie the regulation of *BRCA*1 and *BRCA*2 expression, such as the involvement of the non-coding micro RNAs and/or histone modifications. These also necessitate future exploration.

The limiting cost of bisulfite pyrosequencing also restricted us to investigate only one CpG island for each of the selected genes, while it could have been interesting to have been able to analyse the methylation status of the entire promoter region of these three genes. By assessing only one CpG island per gene, it is possible that some significant changes occurring in the CpG sites on the other islands in the selected gene could have been missed. These “missed” changes could as well have been some of the critical contributors of the epigenetic modifications effected on the cells by the plant and may have also been some of the regulatory repertoire that are involved in the regulation of these selected genes. Another great limiting factor to what could been achieved in this study was time. It was not possible to analyse the effect of the chloroform sub-fraction of *B. pilosa* on the mitochondrial membrane potential in the treated MCF-7 cells after a shorter incubation period due to time limitations. The effects of the chloroform sub-fraction on mitochondrial membrane depolarisation, gene expression as well as global methylation suggested that apoptosis was induced in the MCF-7 cell line used. Nevertheless, no hallmarks of apoptosis could be verified during the chosen treatment periods. The authentication of the advent of apoptosis would have strengthened the notion of the combined influence of mitochondrial membrane depolarisation and *BRCA*1 down-regulation on cell division cycle arrest with consequential induction of apoptosis when MCF-7 cells are exposed to the chloroform sub-fraction of the methanol extract of *B. pilosa*. Nonetheless, the abundance of palmitic acid in the chloroform sub-fraction and the observed increase in

hypomethylation patterns of the genome following treatment with this sub-fraction strongly support the initiation of an apoptotic cell death in the cells as a result of the action of palmitic acid or its metabolite DHA, with a concomitant repression of both *BRCA* genes. Indeed, gene expression analyses from our study corroborate this hypothesis, with the increase in the expression of *EGFR* also suggesting the induction of apoptosis as a result of the action of palmitic acid present in the chloroform sub-fraction (Gerber 2012). Ultimately, this study was able to demonstrate the involvement of BRCA1 in global DNA hypomethylation leading to cell division cycle arrest and telomere shortening that underpins the importance of epigenetic mechanisms in combating tumour progression.

4.5 Future work

Epigenetic manifestations within cancer cells are broad. Treatment of MCF-7 cells with the chloroform sub-fraction of *B. pilosa* could be affecting multiple pathways leading to alterations in numerous epigenetic hallmarks of cancer. It is, therefore, necessary to investigate the effect of the chloroform sub-fraction on other possible mechanisms such as histone modifications and micro-RNAs, as it may have a multidimensional epigenetic action against MCF-7 breast cancer cells due to the presence of multiple bioactive phytocompounds. Investigating alterations in the methylation patterns of other CpG islands in the *BRCA* genes promoter regions would also provide insight on the epigenetic influence of the sub-fraction on the regulatory dynamics of *BRCA*1 and *BRCA*2 genes. Furthermore, assessment of protein expression of VEGFA and CDH1 will also provide an understanding of whether the observed differential gene expression patterns has a bearing on the inhibitory effect of the sub-fraction in MCF-7 cell viability or not. Finally, the expression of BRCA2 also needs to be evaluated. Treatment of MCF-7 cells with the chloroform sub-fraction of *B. pilosa* down-regulated BRCA1 at both gene and protein levels and it is necessary to assess if the repression of *BRCA*2 at mRNA level is also resonated at the protein level. This will strengthen the hypothesis of the involvement of BRCA proteins in the epigenetic changes observed in MCF-7 cells following treatment with the chloroform sub-fraction of the methanol extract of *B. pilosa*, culminating in apoptosis.

4.6 Conclusion

In conclusion, the large quantities of fatty acids in the chloroform sub-fraction of the methanol extract of *B. pilosa* suggest that the observed repression of *BRCA*1 may be an effect of the action of these lipids, particularly palmitic acid. Palmitic acid, and/or its metabolite DHA, may be responsible for the down-regulation of the *BRCA*1 gene, thus leading to the observed decrease in the global DNA methylation patterns in this study. Hypomethylation of the genome results in chromosomal instability that will have cells arrested at the G_2/M phase of the cell division cycle for repair. However, the absence of BRCA1 at this checkpoint also means that the damaged DNA will not be repaired and the cells will accordingly be directed to apoptosis. Repression of *BRCA*1 gene has a multifaceted consequence on the cells, not only global DNA hypomethylation leading to cell division cycle arrest, but also on the inactivation of telomerase. The lack of telomerase activity results in shortened telomeres which will limit the cells' proliferative capability similar to what is observed in somatic cells. This study has established that modifications in both these epigenetic phenomena play an important role in mitigating cell proliferation in MCF-7 breast cancer cells treated with the chloroform sub-fraction of the methanol extract of *B. pilosa*. Together with its impressive antioxidant activity and wide distribution of phytocompounds that lend it the excellent medicinal properties, the plant has displayed remarkable potential as an anticancer agent, inhibiting tumour cells from immortal proliferation while also directing them to an apoptotic cell death. These attributes, thus make the plant a noteworthy lead in breast cancer drug development.

.

REFERENCES

Agatonovic-Kustrin, Snezana, David W. Morton, and Petar Ristivojeví. 2016. “Assessment of Antioxidant Activity in Victorian Marine Algal Extracts Using High Performance Thin-Layer Chromatography and Multivariate Analysis.” *Journal of Chromatography A* 1468:228–35.

Agrawal, Anshu, Richard F. Murphy, and Devendra K. Agrawal. 2007. “DNA Methylation in Breast and Colorectal Cancers.” *Modern Pathology* 20:711–21.

Ahmed, Ahmed R. H. 2016. “HER2 Expression Is a Strong Independent Predictor of Nodal Metastasis in Breast Cancer.” *Journal of the Egyptian National Cancer Institute* 28(4):219–27.

Ajanaku, Christiana, Johnbull Echeme, Raphael Mordi, Oladotun Bolade, Stella Okoye, Hassana Jonathan, and Oluwaseun Ejilude. 2018. “In-Vitro Antibacterial, Phytochemical, Antimycobacterial Activities and GC-MS Analyses of Bidens Pilosa Leaf Extract.” *Journal of Microbiology, Biotechnology and Food Sciences* 8(1):721–25.

Alba, Luz Helena, Sandra Díaz, Oscar Gamboa, César Poveda, Andrés Henao, Fernando Perry, Catherine Duggan, Fabián Gil, and Raúl Murillo. 2018. “Accuracy of Mammography and Clinical Breast Examination in the Implementation of Breast Cancer Screening Programs in Colombia.” *Preventive Medicine* 115:19–25.

Ali, Remah, and Michael K. Wendt. 2017. “The Paradoxical Functions of EGFR during Breast Cancer Progression.” *Signal Transduction and Targeted Therapy* 2.

Arroyo, Jorge, Pablo Bonilla, Ernesto Ráez, Alejandro Barreda, and Oscar Huamán. 2010. “Bidens Pilosa Chemoprotective Effect on Induced Breast Cancer in Rats.” *An Fac Med* 71(3):153–60.

Asiaf, Asia, Shiekh Tanveer Ahmad, Sheikh Aejaz Aziz, Ajaz Ahmad Malik, Zubaida Rasool, Akbar Masood, and Mohammad Afzal Zargar. 2014. “Loss of Expression and Aberrant Methylation of the CDH1 (E-Cadherin) Gene in Breast Cancer Patients from Kashmir.” *Asian Pacific Journal of Cancer Prevention* 15(15):6397–6403.

Atchley, Deann P., Constance T. Albarracin, Adriana Lopez, Vicente Valero, Christopher I. Amos, Ana Maria Gonzalez-Angulo, Gabriel N. Hortobagyi, and Banu K. Arun. 2008. “Clinical and Pathologic Characteristics of Patients with BRCA-Positive and BRCA-Negative Breast Cancer.” *Journal of Clinical Oncology*

26(26):4282–88.

Babenko, V. N., Yu L. Orlov, Zh T. Isakova, D. A. Antonov, and M. I. Voevoda. 2017. “The Evolution of CpG Islands by Tandem Duplications.” *Russian Journal of Genetics: Applied Research* 7(5):538–49.

Bae, Soo Youn, Sangmin Kim, Jun Ho Lee, Hyun chul Lee, Se Kyung Lee, Won Ho Kil, Seok Won Kim, Jeong Eon Lee, and Seok Jin Nam. 2015. “Poor Prognosis of Single Hormone Receptor- Positive Breast Cancer: Similar Outcome as Triple-Negative Breast Cancer.” *BMC Cancer* 15(1):138.

Barra, V., and D. Fachinetti. 2018. “The Dark Side of Centromeres: Types, Causes and Consequences of Structural Abnormalities Implicating Centromeric DNA.” *Nature Communications* 9:4340.

Bartolome, Arlene P., Irene M. VillaseÃ±or, and Wen-Chin Yang. 2013. “Bidens Pilosa L. (Asteraceae): Botanical Properties, Traditional Uses, Phytochemistry, and Pharmacology.” *Evidence-Based Complementary and Alternative Medicine : ECAM* 2013:340215.

Beetch, Megan, Sadaf Harandi-Zadeh, Tony Yang, Cayla Boycott, Yihang Chen, Barbara Stefanska, and Sulma Mohammed. 2020. “DNA Methylation Landscape of Triple-Negative Ductal Carcinoma in Situ (DCIS) Progressing to the Invasive Stage in Canine Breast Cancer.” *Scientific Reports* 10(1):2415.

Benson, John R., Ismail Jatoi, and Masakazu Toi. 2016. “Treatment of Low-Risk Ductal Carcinoma in Situ: Is Nothing Better than Something?” *The Lancet Oncology* 17:442–51.

Bertrand, Kimberly A., Traci N. Bethea, Lynn Rosenberg, Elisa V. Bandera, Thaer Khoury, Melissa A. Troester, Christine B. Ambrosone, and Julie R. Palmer. 2020. “Risk Factors for Estrogen Receptor Positive Ductal Carcinoma in Situ of the Breast in African American Women.” *Breast* 49:108–14.

Bezerra, Indara Cavalcante, Raimunda Magalhães Da Silva, Cleoneide Paulo Oliveira, Christina César Praça Brasil, Mardênia Gomes Ferreira Vasconcelos, Marli Vilela Mamede, and Marnewton Tadeu Pinheiro De Oliveira. 2018. “Mastectomized Women’s Perception of Breast Cancer Early Detection.” *PLoS ONE* 13:1.

Bhat, Showkat Ahmad, Sabhiya Majid, Hilal Ahmad Wani, and Samia Rashid. 2019. “Diagnostic Utility of Epigenetics in Breast Cancer – A Review.” *Cancer Treatment and Research Communications* 19:100125.

De Biase, Irene, Carmen Gherasim, Sonia L. La'ulu, Alexander Asamoah, Nicola Longo, and Tatiana Yuzyuk. 2020. "Laboratory Evaluation of Homocysteine Remethylation Disorders and Classic Homocystinuria: Long-Term Follow-up Using a Cohort of 123 Patients." *Clinica Chimica Acta* 509:126–34.

Bilanda, Danielle Claude, Paul Désiré D. Dzeufiet, Léontine Kouakep, Bibi Farouck O. Aboubakar, Léonard Tedong, Pierre Kamtchouing, and Théophile Dimo. 2017. "Bidens Pilosa Ethylene Acetate Extract Can Protect against L-NAME-Induced Hypertension on Rats." *BMC Complementary and Alternative Medicine* 17:1.

Bleyer, Archie, and H. Gilbert Welch. 2012. "Effect of Three Decades of Screening Mammography on Breast-Cancer Incidence." *New England Journal of Medicine* 367(21):1998–2005.

Blows, Fiona M., Kristy E. Driver, Marjanka K. Schmidt, Annegien Broeks, Flora E. van Leeuwen, Jelle Wesseling, Maggie C. Cheang, Karen Gelmon, Torsten O. Nielsen, Carl Blomqvist, Päivi Heikkila, Tuomas Heikkinen, Heli Nevanlinna, Lars A. Akslen, Louis R. Bégin, William D. Foulkes, Fergus J. Couch, Xianshu Wang, Vicky Cafourek, Janet E. Olson, Laura Baglietto, Graham G. Giles, Gianluca Severi, Catriona A. McLean, Melissa C. Southey, Emad Rakha, Andrew R. Green, Ian O. Ellis, Mark E. Sherman, Jolanta Lissowska, William F. Anderson, Angela Cox, Simon S. Cross, Malcolm W. R. Reed, Elena Provenzano, Sarah Jane Dawson, Alison M. Dunning, Manjeet Humphreys, Douglas F. Easton, Montserrat García-Closas, Carlos Caldas, Paul D. Pharoah, and David Huntsman. 2010. "Subtyping of Breast Cancer by Immunohistochemistry to Investigate a Relationship between Subtype and Short and Long Term Survival: A Collaborative Analysis of Data for 10,159 Cases from 12 Studies." *PLoS Medicine* 7(5):1.

Bock, Christoph, Eleni M. Tomazou, Arjen Brinkman, and Fabian Müller. 2010. "Genome-Wide Mapping of DNA Methylation: A Quantitative Technology Comparison." *Nature Biotechnology* 28(10):1106–14.

Burger, Kaspar, Ruth F. Ketley, and Monika Gullerova. 2019. "Beyond the Trinity of ATM, ATR, and DNA-PK: Multiple Kinases Shape the DNA Damage Response in Concert With RNA Metabolism." *Frontiers in Molecular Biosciences* 6:61.

Cai, Fengfeng, Isabell Ge, Minghong Wang, Ewelina Biskup, Xiaoyan Lin, and Xiaoyan Zhong. 2014. "Pyrosequencing Analysis of BRCA1 Methylation Level in Breast Cancer Cells." *Tumor Biology* 34(4):3839–44.

Cai, Yuee, Jinming Zhang, Nelson G. Chen, Zhi Shi, Jiange Qiu, Chengwei He, and Meiwan Chen. 2017. “Recent Advances in Anticancer Activities and Drug Delivery Systems of Tannins.” *Medicinal Research Reviews* 37:665–701.

Can Akincilar, Semih, Bilal Unal, and Vinay Tergaonkar. 2016. “Reactivation of Telomerase in Cancer.” *Cellular and Molecular Life Sciences* 73:1659–70.

Carser, Judith E., Jennifer E. Quinn, Caroline O. Michie, Eamonn J. O’Brien, W. Glenn McCluggage, Perry Maxwell, Elisabeth Lamers, Tong F. Lioe, Alistair R. W. Williams, Richard D. Kennedy, Charlie Gourley, and D. Paul Harkin. 2011. “BRCA1 Is Both a Prognostic and Predictive Biomarker of Response to Chemotherapy in Sporadic Epithelial Ovarian Cancer.” *Gynecologic Oncology* 123(3):492–98.

Chaffer, Christine L., and Robert A. Weinberg. 2011. “A Perspective on Cancer Cell Metastasis.” *Science* 331(6024):1559–64.

Chan, Mun Yew Patrick, and Serene Lim. 2010. “Predictors of Invasive Breast Cancer in Ductal Carcinoma in Situ Initially Diagnosed by Core Biopsy.” *Asian Journal of Surgery* 33(2):76–82.

Chang, Shu Lin, Yi Ming Chiang, Cicero Lee Tian Chang, Hsu Hua Yeh, Lie Fen Shyur, Yueh Hsiung Kuo, Tung Kung Wu, and Wen Chin Yang. 2007. “Flavonoids, Centaurein and Centaureidin, from Bidens Pilosa, Stimulate IFN-γ Expression.” *Journal of Ethnopharmacology* 112(2):232–36.

Chen, Wenjing, Andrew D. Hoffmann, Huiping Liu, and Xia Liu. 2018. “Organotropism: New Insights into Molecular Mechanisms of Breast Cancer Metastasis.” *Npj Precision Oncology* 2(1):4.

Chen, Zhiyuan, and Yi Zhang. 2020. “Role of Mammalian DNA Methyltransferases in Development.” *Annual Review of Biochemistry* 89:135–58.

Cheng, Tzu Chun, Shih Hsin Tu, Li Ching Chen, Ming Yao Chen, Wen Ye Chen, Yen Kuang Lin, Chi Tang Ho, Shyr Yi Lin, Chih Hsiung Wu, and Yuan Soon Ho. 2015. “Down-Regulation of α-L-Fucosidase 1 Expression Confers Inferior Survival for Triple-Negative Breast Cancer Patients by Modulating the Glycosylation Status of the Tumor Cell Surface.” *Oncotarget* 6(25):21283–300.

Cheynier, Véronique. 2012. “Phenolic Compounds: From Plants to Foods.” *Phytochemistry Reviews* 11(2–3):153–77.

Cho, Yoon Hee, Hulya Yazici, Hui Chen Wu, Mary Beth Terry, Karina Gonzalez, Mengxue Qu, Nejat Dalay, and Regina M. Santella. 2010. “Aberrant Promoter

Hypermethylation and Genomic Hypomethylation in Tumor, Adjacent Normal Tissues and Blood from Breast Cancer Patients." *Anticancer Research* 30(7):2489–96.

Christensen, Melinda E., Elisa S. Jansen, Washington Sanchez, and Nigel J. Waterhouse. 2013. "Flow Cytometry Based Assays for the Measurement of Apoptosis-Associated Mitochondrial Membrane Depolarisation and Cytochrome c Release." *Methods* 61(2):138–45.

Coleman, Cathy. 2017. "Early Detection and Screening for Breast Cancer." *Seminars in Oncology Nursing* 33(2):141–55.

Corsetto, Paola A., Gigliola Montorfano, Stefania Zava, Ilaria E. Jovenitti, Andrea Cremona, and Angela M. Rizzo. 2011. "Effects of N-3 PUFAs on Breast Cancer Cells through Their Incorporation in Plasma Membrane." *Lipids in Health and Disease* 10:73.

Corso, Giovanni, Mattia Intra, Chiara Trentin, Paolo Veronesi, and Viviana Galimberti. 2016. "CDH1 Germline Mutations and Hereditary Lobular Breast Cancer." *Familial Cancer* 15:215–19.

Cortés-Rojas, Diego F., Daniela A. Chagas-Paula, Fernando B. Da Costa, Claudia R. F. Souza, and Wanderley P. Oliveira. 2013. "Bioactive Compounds in Bidens Pilosa L. Populations: A Key Step in the Standardization of Phytopharmaceutical Preparations." *Revista Brasileira de Farmacognosia* 23(1):28–35.

Cotton, Allison M., E. Magda Price, Meaghan J. Jones, Bradley P. Balaton, Michael S. Kobor, and Carolyn J. Brown. 2015. "Landscape of DNA Methylation on the X Chromosome Reflects CpG Density, Functional Chromatin State and X-Chromosome Inactivation." *Human Molecular Genetics* 24(6):1528–39.

Davalos, Veronica, and Manel Esteller. 2010. "MicroRNAs and Cancer Epigenetics: A Macrorevolution." *Current Opinion in Oncology* 22:35–45.

Dawson, Mark A., and Tony Kouzarides. 2012. "Cancer Epigenetics: From Mechanism to Therapy." *Cell* 150:12–27.

Delaney, Colin, Sanjay K. Garg, and Raymond Yung. 2015. "Analysis of DNA Methylation by Pyrosequencing." Pp. 249–64 in *Methods in Molecular Biology*. Vol. 1343. Humana Press Inc.

Demchenko, Alexander P. 2013. "Beyond Annexin V: Fluorescence Response of Cellular Membranes to Apoptosis." *Cytotechnology* 65(2):157–72.

Demicheli, Romano, Michael W. Retsky, William J. M. Hrushesky, Michael Baum,

Isaac D. Gukas, and Ismail Jatoi. 2007. “Racial Disparities in Breast Cancer Outcome: Insights into Host-Tumor Interactions.” *Cancer* 110(9):1880–88.

Desantis, Carol, Ahmedin Jemal, and Elizabeth Ward. 2010. “Disparities in Breast Cancer Prognostic Factors by Race, Insurance Status, and Education.” *Cancer Causes and Control* 21(9):1445–50.

Desjardins, P., and D. Conklin. 2010. “NanoDrop Microvolume Quantitation of Nucleic Acids.” *J. Vis. Exp* (45):2565.

Do, Quy Diem, Artik Elisa Angkawijaya, Phuong Lan Tran-Nguyen, Lien Huong Huynh, Felycia Edi Soetaredjo, Suryadi Ismadji, and Yi Hsu Ju. 2014. “Effect of Extraction Solvent on Total Phenol Content, Total Flavonoid Content, and Antioxidant Activity of Limnophila Aromatica.” *Journal of Food and Drug Analysis* 22(3):296–302.

Drake, Thomas M., and Kjetil Søreide. 2019. “Cancer Epigenetics in Solid Organ Tumours: A Primer for Surgical Oncologists.” *European Journal of Surgical Oncology* 45:736–46.

Duffy, Angela M., David J. Bouchier-Hayes, and Judith H. Harmey. 2004. “Vascular Endothelial Growth Factor (VEGF) and Its Role in Non-Endothelial Cells: Autocrine Signalling by VEGF.” Pp. 133–44 in *VEGF and Cancer*. Landes Bioscience.

Ehrlich, Kenneth C., Carl Baribault, and Melanie Ehrlich. 2020. “Epigenetics of Muscle- and Brain-Specific Expression of Klhl Family Genes.” *International Journal of Molecular Sciences* 21(21):1–21.

Ehrlich, Melanie. 2002. “DNA Hypomethylation, Cancer, the Immunodeficiency, Centromeric Region Instability, Facial Anomalies Syndrome and Chromosomal Rearrangements.” *Journal of Nutrition* 132:2424S-2429S.

Ehrlich, Melanie. 2009. “DNA Hypomethylation in Cancer Cells.” *Epigenomics* 1:239–59.

Eitsuka, Takahiro, Kiyotaka Nakagawa, Shunji Kato, Junya Ito, Yurika Otoki, Soo Takasu, Naoki Shimizu, Takumi Takahashi, and Teruo Miyazawa. 2018. “Modulation of Telomerase Activity in Cancer Cells by Dietary Compounds: A Review.” *International Journal of Molecular Sciences* 19(2):478.

Engels, Charla C., Mandy Kiderlen, Esther Bastiaannet, Antien L. Mooyaart, Ronald van Vlierberghe, Vincent T. H. B. M. Smit, Peter J. K. Kuppen, Cornelis J. H. van de Velde, and G. J. Liefers. 2016. “The Clinical Prognostic Value of Molecular

Intrinsic Tumor Subtypes in Older Breast Cancer Patients: A FOCUS Study Analysis.” *Molecular Oncology* 10(4):594–600.

Eslami Amirabadi, H., M. Tuerlings, A. Hollestelle, S. SahebAli, R. Luttge, C. C. van Donkelaar, J. W. M. Martens, and J. M. J. den Toonder. 2019. “Characterizing the Invasion of Different Breast Cancer Cell Lines with Distinct E-Cadherin Status in 3D Using a Microfluidic System.” *Biomedical Microdevices* 21(2):101.

Espina, Carolina, Fiona McKenzie, and Isabel Dos-Santos-Silva. 2017. “Delayed Presentation and Diagnosis of Breast Cancer in African Women: A Systematic Review.” *Annals of Epidemiology* 27:659-671.e7.

Esserman, Laura, and Christina Yau. 2015. “Rethinking the Standard for Ductal Carcinoma in Situ Treatment.” *JAMA Oncology* 1(7):881–83.

Esteva, Francisco J., Vanessa M. Hubbard-Lucey, Jun Tang, and Lajos Pusztai. 2019. “Immunotherapy and Targeted Therapy Combinations in Metastatic Breast Cancer.” *The Lancet Oncology* 20:e175–86.

Fang, Fang, Sevin Turcan, Andreas Rimner, Andrew Kaufman, Dilip Giri, Luc G. T. Morris, Ronglai Shen, Venkatraman Seshan, Qianxing Mo, Adriana Heguy, Stephen B. Baylin, Nita Ahuja, Agnes Viale, Joan Massague, Larry Norton, Linda T. Vahdat, Mary Ellen Moynahan, and Timothy A. Chan. 2011. “Breast Cancer Methylomes Establish an Epigenomic Foundation for Metastasis.” *Science Translational Medicine* 3(75):75.

Favaloro, B., N. Allocati, V. Graziano, C. Di Ilio, and V. De Laurenzi. 2012. “Role of Apoptosis in Disease.” *Aging* 4:330–49.

Feeley, Linda P., Anna M. Mulligan, Dushanthi Pinnaduwage, Shelley B. Bull, and Irene L. Andrulis. 2014. “Distinguishing Luminal Breast Cancer Subtypes by Ki67, Progesterone Receptor or TP53 Status Provides Prognostic Information.” *Modern Pathology* 27(4):554–61.

Formagio, Anelise Samara Nazari, Carla Roberta Ferreira Volobuff, Matheus Santiago, Claudia Andrea Lima Cardoso, Maria Do Carmo Vieira, and Zefa Valdevina Pereira. 2014. “Evaluation of Antioxidant Activity, Total Flavonoids, Tannins and Phenolic Compounds in Psychotria Leaf Extracts.” *Antioxidants* 3(4):745–57.

Franco, Rodrigo, Onard Schoneveld, Alexandros G. Georgakilas, and Mihalis I. Panayiotidis. 2008. “Oxidative Stress, DNA Methylation and Carcinogenesis.” *Cancer Letters* 266:6–11.

Fuchs, Yaron, and Hermann Steller. 2011. “Programmed Cell Death in Animal Development and Disease.” *Cell* 147:742–58.

Gall, Tamara M. H., and Adam E. Frampton. 2013. “Gene of the Month: E-Cadherin (CDH1).” *Journal of Clinical Pathology* 66(11):928–32.

Galluzzi, Lorenzo, Ilio Vitale, Stuart A. Aaronson, John M. Abrams, Dieter Adam, Patrizia Agostinis, Emad S. Alnemri, Lucia Altucci, Ivano Amelio, David W. Andrews, Margherita Annicchiarico-Petruzzelli, Alexey V Antonov, Eli Arama, Eric H. Baehrecke, Nickolai A. Barlev, Nicolas G. Bazan, Francesca Bernassola, Mathieu J. M. Bertrand, Katiuscia Bianchi, Mikhail V Blagosklonny, Klas Blomgren, Christoph Borner, Patricia Boya, Catherine Brenner, Michelangelo Campanella, Eleonora Candi, Didac Carmona-Gutierrez, Francesco Cecconi, Francis K. M. Chan, Navdeep S. Chandel, Emily H. Cheng, Jerry E. Chipuk, John A. Cidlowski, Aaron Ciechanover, Gerald M. Cohen, Marcus Conrad, Juan R. Cubillos-Ruiz, Peter E. Czabotar, Vincenzo Dâ€™Angiolella, Ted M. Dawson, Valina L. Dawson, Vincenzo De Laurenzi, Ruggero De Maria, Klaus-Michael Debatin, Ralph J. DeBerardinis, Mohanish Deshmukh, Nicola Di Daniele, Francesco Di Virgilio, Vishva M. Dixit, Scott J. Dixon, Colin S. Duckett, Brian D. Dynlacht, Wafik S. El-Deiry, John W. Elrod, Gian Maria Fimia, Simone Fulda, Ana J. GarcÃ-a-SÃ¡ez, Abhishek D. Garg, Carmen Garrido, Evripidis Gavathiotis, Pierre Golstein, Eyal Gottlieb, Douglas R. Green, Lloyd A. Greene, Hinrich Gronemeyer, Atan Gross, Gyorgy Hajnoczky, J. Marie Hardwick, Isaac S. Harris, Michael O. Hengartner, Claudio Hetz, Hidenori Ichijo, Marja JÃ¤Ã¤ttelÃ¤, Bertrand Joseph, Philipp J. Jost, Philippe P. Juin, William J. Kaiser, Michael Karin, Thomas Kaufmann, Oliver Kepp, Adi Kimchi, Richard N. Kitsis, Daniel J. Klionsky, Richard A. Knight, Sharad Kumar, Sam W. Lee, John J. Lemasters, Beth Levine, Andreas Linkermann, Stuart A. Lipton, Richard A. Lockshin, Carlos LÃ³pez-OtÃ-n, Scott W. Lowe, Tom Luedde, Enrico Lugli, Marion MacFarlane, Frank Madeo, Michal Malewicz, Walter Malorni, Gwenola Manic, Jean-Christophe Marine, Seamus J. Martin, Jean-Claude Martinou, Jan Paul Medema, Patrick Mehlen, Pascal Meier, Sonia Melino, Edward A. Miao, Jeffery D. Molkentin, Ute M. Moll, Cristina MuÃ±oz-Pinedo, Shigekazu Nagata, Gabriel NuÃ±ez, Andrew Oberst, Moshe Oren, Michael Overholtzer, Michele Pagano, Theocharis Panaretakis, Manolis Pasparakis, Josef M. Penninger, David M. Pereira, Shazib Pervaiz, Marcus E. Peter, Mauro Piacentini, Paolo Pinton, Jochen H. M. Prehn,

Hamsa Puthalakath, Gabriel A. Rabinovich, Markus Rehm, Rosario Rizzuto, Cecilia M. P. Rodrigues, David C. Rubinsztein, Thomas Rudel, Kevin M. Ryan, Emre Sayan, Luca Scorrano, Feng Shao, Yufang Shi, John Silke, Hans-Uwe Simon, Antonella Sistigu, Brent R. Stockwell, Andreas Strasser, Gyorgy Szabadkai, Stephen W. G. Tait, Daolin Tang, Nektarios Tavernarakis, Andrew Thorburn, Yoshihide Tsujimoto, Boris Turk, Tom Vanden Berghe, Peter Vandenabeele, Matthew G. Vander Heiden, Andreas Villunger, Herbert W. Virgin, Karen H. Vousden, Domagoj Vucic, Erwin F. Wagner, Henning Walczak, David Wallach, Ying Wang, James A. Wells, Will Wood, Junying Yuan, Zahra Zakeri, Boris Zhivotovsky, Laurence Zitvogel, Gerry Melino, and Guido Kroemer. 2018. “Molecular Mechanisms of Cell Death: Recommendations of the Nomenclature Committee on Cell Death 2018.” *Cell Death and Differentiation* 25(3):486–541.

García-Aranda, Marilina, and Maximino Redondo. 2019. “Immunotherapy: A Challenge of Breast Cancer Treatment.” *Cancers* 11(12):1822.

Geissberger Peter, Sequin Urs. 1991 "Constituents of *Bidens pilosa* L.: do the components found so far explain the use of this plant in traditional medicine?" *Acta Tropica* 48(4):251–261.

George, Vazhappilly Cijo, Graham Dellaire, and H. P. Vasanth. Rupasinghe. 2017. “Plant Flavonoids in Cancer Chemoprevention: Role in Genome Stability.” *Journal of Nutritional Biochemistry* 45:1–4.

Gerber, Mariette. 2012. “Omega-3 Fatty Acids and Cancers: A Systematic Update Review of Epidemiological Studies.” *British Journal of Nutrition* 107:S228–39.

Ginsburg, Ophira, Cheng-Har Yip, Ari Brooks, Anna Cabanes, Maira Caleffi, Jorge Antonio Dunstan Yataco, Bishal Gyawali, Valerie McCormack, Myrna McLaughlin de Anderson, Ravi Mehrotra, Alejandro Mohar, Raul Murillo, Lydia E. Pace, Electra D. Paskett, Anya Romanoff, Anne F. Rositch, John R. Scheel, Miriam Schneidman, Karla Unger-Saldaña, Verna Vanderpuye, Tsu-Yin Wu, Safina Yuma, Allison Dvaladze, Catherine Duggan, and Benjamin O. Anderson. 2020. “Breast Cancer Early Detection: A Phased Approach to Implementation.” *Cancer* 126(S10):2379–93.

Goldar, Samira, Mahmoud Shekari Khaniani, Sima Mansoori Derakhshan, and Behzad Baradaran. 2015. “Molecular Mechanisms of Apoptosis and Roles in Cancer Development and Treatment.” *Asian Pacific Journal of Cancer Prevention* 16:2129–44.

Gómez, Soledad, Giancarlo Castellano, Gemma Mayol, Mariona Suñol, Ana Queiros, Marina Bibikova, Kristopher L. Nazor, Jeanne F. Loring, Isadora Lemos, Eva Rodríguez, Carmen De Torres, Jaume Mora, José I. Martín-Subero, and Cinzia Lavarino. 2015. “DNA Methylation Fingerprint of Neuroblastoma Reveals New Biological and Clinical Insights.” *Epigenomics* 7(7):1137–53.

Goren, Alon, Giora Simchen, Eitan Fibach, Piroska E. Szabo, Keiji Tanimoto, Lyubomira Chakalova, Gerd P. Pfeifer, Peter J. Fraser, James D. Engel, and Howard Cedar. 2006. “Fine Tuning of Globin Gene Expression by DNA Methylation.” *PLoS ONE* 1:e46.

Gottlieb, E., S. M. Armour, M. H. Harris, and C. B. Thompson. 2003. “Mitochondrial Membrane Potential Regulates Matrix Configuration and Cytochrome c Release during Apoptosis.” *Cell Death and Differentiation* 10:709–17.

Green, Douglas R., and Fabien Llambi. 2015. “Cell Death Signaling.” *Cold Spring Harbor Perspectives in Biology* 7(12):1.

Greenlee, Heather, Melissa J. DuPont-Reyes, Lynda G. Balneaves, Linda E. Carlson, Misha R. Cohen, Gary Deng, Jillian A. Johnson, Matthew Mumber, Dugald Seely, Suzanna M. Zick, Lindsay M. Boyce, and Debu Tripathy. 2017. “Clinical Practice Guidelines on the Evidence-Based Use of Integrative Therapies during and after Breast Cancer Treatment.” *CA: A Cancer Journal for Clinicians* 67(3):194–232.

Gujar, Hemant, Daniel J. Weisenberger, and Gangning Liang. 2019. “The Roles of Human DNA Methyltransferases and Their Isoforms in Shaping the Epigenome.” *Genes* 10:172.

Günes, Cagatay, and K. Lenhard Rudolph. 2013. “The Role of Telomeres in Stem Cells and Cancer.” *Cell* 152(3):390–93.

Gupta, Ankit, Madhu Naraniwal, and Vijay Kothari. 2012. “Modern Extraction Methods for Preparation of Bioactive Plant Extracts.” *International Journal of Applied and Natural Sciences* 1(1):8–26.

Hamam, Rimi, Dana Hamam, Khalid A. Alsaleh, Moustapha Kassem, Waleed Zaher, Musaad Alfayez, Abdullah Aldahmash, and Nehad M. Alajez. 2017. “Circulating MicroRNAs in Breast Cancer: Novel Diagnostic and Prognostic Biomarkers.” *Cell Death & Disease* 8(9):e3045.

Hamam, Rimi, Dana Hamam, Khalid A Alsaleh, Moustapha Kassem, Waleed Zaher, Musaad Alfayez, Abdullah Aldahmash, and Nehad M. Alajez. 2017. “Circulating MicroRNAs in Breast Cancer: Novel Diagnostic and Prognostic Biomarkers.” *Cell*

Death & Disease 8(9):e3045.

Haminiuk, Charles Windson Isidoro, Manuel Salvador Vicente Plata-Oviedo, Gisely de Mattos, Solange Teresinha Carpes, and Ivanise Guilherme Branco. 2014. “Extraction and Quantification of Phenolic Acids and Flavonols from Eugenia Pyriformis Using Different Solvents.” *Journal of Food Science and Technology* 51(10):2862–66.

Han, Pei, Wei Li, Jin Yang, Ching Shang, Chiou Hong Lin, Wei Cheng, Calvin T. Hang, Hsiu Ling Cheng, Chen Hao Chen, Johnson Wong, Yiqin Xiong, Mingming Zhao, Stavros G. Drakos, Andrea Ghetti, Dean Y. Li, Daniel Bernstein, Huei sheng Vincent Chen, Thomas Quertermous, and Ching Pin Chang. 2016. “Epigenetic Response to Environmental Stress: Assembly of BRG1-G9a/GLP-DNMT3 Repressive Chromatin Complex on Myh6 Promoter in Pathologically Stressed Hearts.” *Biochimica et Biophysica Acta - Molecular Cell Research* 1863(7):1772–81.

Hanahan, Douglas, and Robert A. Weinberg. 2000. “The Hallmarks of Cancer.” *Cell* 100(1):57–70.

Hanahan, Douglas, and Robert A. Weinberg. 2011. “Hallmarks of Cancer: The next Generation.” *Cell* 144(5):646–74.

Hashimoto, Ko, Shoichi Kokubun, Eiji Itoi, and Helmtrud I. Roach. 2007. “Improved Quantification of DNA Methylation Using Methylation-Sensitive Restriction Enzymes and Real-Time PCR.” *Epigenetics* 2(2):86–91.

Henderson, Beric R. 2012. “The BRCA1 Breast Cancer Suppressor: Regulation of Transport, Dynamics, and Function at Multiple Subcellular Locations.” *Scientifica* 2012:1–15.

Hiraguri, Shunsuke, Tony Godfrey, Haruhiko Nakamura, Jeremy Graff, Collin Collins, Laleh Shayesteh, Norman Doggett, Keith Johnson, Margaret Wheelock, James Herman, Stephen Baylin, Daniel Pinkel, and Joe Gray. 1998. “Mechanisms of Inactivation of E-Cadherin in Breast Cancer Cell Lines.” *Cancer Research* 58(9):1972–77.

Hopkins, Melissa, and Raphael Mkuzi. 2018. “Clinical Breast Examination and Navigation for Early Cancer Detection in Remote Communities Without an Imaging Screening Option.” *Journal of Global Oncology* 4(3):17s.

Hsu, Yi Jou, Tsung Han Lee, Cicero Lee Tian Chang, Yuh Ting Huang, and Wen Chin Yang. 2009. “Anti-Hyperglycemic Effects and Mechanism of Bidens Pilosa Water

Extract.” *Journal of Ethnopharmacology* 122(2):379–83.

Hua, Dong, Yu Hu, Yu Yu Wu, Zhi Hong Cheng, Jian Yu, Xiang Du, and Zhao Hui Huang. 2011. “Quantitative Methylation Analysis of Multiple Genes Using Methylation-Sensitive Restriction Enzyme-Based Quantitative PCR for the Detection of Hepatocellular Carcinoma.” *Experimental and Molecular Pathology* 91(1):455–60.

Huen, Michael S. Y., Shirley M. H. Sy, and Junjie Chen. 2010. “BRCA1 and Its Toolbox for the Maintenance of Genome Integrity.” *Nature Reviews Molecular Cell Biology* 11(2):138–48.

Hughes, Amy L., Jessica R. Kelley, and Robert J. Klose. 2020. “Understanding the Interplay between CpG Island-Associated Gene Promoters and H3K4 Methylation.” *Biochimica et Biophysica Acta - Gene Regulatory Mechanisms* 1863(8):194567.

Hung, Chin Sheng, Sheng Chao Wang, Yi Ting Yen, Tzong Huei Lee, Wu Che Wen, and Ruo Kai Lin. 2018. “Hypermethylation of CCND2 in Lung and Breast Cancer Is a Potential Biomarker and Drug Target.” *International Journal of Molecular Sciences* 19(10):3096.

Ishay-Ronen, Dana, and Gerhard Christofori. 2019. “Targeting Cancer Cell Metastasis by Converting Cancer Cells into Fat.” *Cancer Research* 79:5471–75.

Iwamoto, Takashi, Noriaki Yamamoto, Tetsuya Taguchi, Yasuhiro Tamaki, and Shinzaburo Noguchi. 2011. “BRCA1 Promoter Methylation in Peripheral Blood Cells Is Associated with Increased Risk of Breast Cancer with BRCA1 Promoter Methylation.” *Breast Cancer Research and Treatment* 129(1):69–77.

Izzo, Simona, Valeria Naponelli, and Saverio Bettuzzi. 2020. “Flavonoids as Epigenetic Modulators for Prostate Cancer Prevention.” *Nutrients* 12:1010.

James, Colin R., Jennifer E. Quinn, Paul B. Mullan, Patrick G. Johnston, and D. Paul Harkin. 2007. “BRCA1 , a Potential Predictive Biomarker in the Treatment of Breast Cancer.” *The Oncologist* 12(2):142–50.

Jang, Kibeom, Minsoon Kim, Candace A. Gilbert, Fiona Simpkins, Tan A. Ince, and Joyce M. Slingerland. 2017. “VEGFA Activates an Epigenetic Pathway Upregulating Ovarian Cancer-initiating Cells.” *EMBO Molecular Medicine* 9(3):304–18.

Januškevičienė, Indrė, and Vilma Petrikaitė. 2019. “Heterogeneity of Breast Cancer: The Importance of Interaction between Different Tumor Cell Populations.” *Life*

Sciences 239(July):117009.

Jonasson, Jon G., Olafur A. Stefansson, Oskar T. Johannsson, Helgi Sigurdsson, Bjarni A. Agnarsson, Gudridur H. Olafsdottir, Kristin K. Alexiusdottir, Hrefna Stefansdottir, Rodrigo Munoz Mitev, Katrin Olafsdottir, Kristrun Olafsdottir, Adalgeir Arason, Vigdis Stefansdottir, Elinborg J. Olafsdottir, Rosa B. Barkardottir, Jorunn E. Eyfjord, Steven A. Narod, and Laufey Tryggvadottir. 2016. "Oestrogen Receptor Status, Treatment and Breast Cancer Prognosis in Icelandic BRCA2 Mutation Carriers." *British Journal of Cancer* 115(7):776–83.

Jurrius, Patriek, Thomas Green, Hans Garmo, Matthew Young, Massimiliano Cariati, Cheryl Gillett, Anca Mera, Mark Harries, Anita Grigoriadis, Sarah Pinder, Lars Holmberg, and Arnie Purushotham. 2020. "Invasive Breast Cancer over Four Decades Reveals Persisting Poor Metastatic Outcomes in Treatment Resistant Subgroup – the 'ATRESS' Phenomenon." *Breast* 50:39–48.

Kakumani, Rajasekhar, Omair Ahmad, and Vijay Devabhaktuni. 2012. "Identification of CpG Islands in DNA Sequences Using Statistically Optimal Null Filters Sequence and Genome Analysis." *Eurasip Journal on Bioinformatics and Systems Biology* 12:1.

Kaw, Meenakshi K., and Robert M. Blumenthal. 2010. "Translational Independence between Overlapping Genes for a Restriction Endonuclease and Its Transcriptional Regulator." *BMC Molecular Biology* 11:87.

Kawano, Hiroyuki, Hiroshi Saeki, Hiroyuki Kitao, Yasuo Tsuda, Hajime Otsu, Koji Ando, Shuhei Ito, Akinori Egashira, Eiji Oki, Masaru Morita, Yoshinao Oda, and Yoshihiko Maehara. 2014. "Chromosomal Instability Associated with Global DNA Hypomethylation Is Associated with the Initiation and Progression of Esophageal Squamous Cell Carcinoma." *Annals of Surgical Oncology* 21(4):696–702.

Kazemi-Lomedasht, Fatemeh, Abbas Rami, and Nosratollah Zarghami. 2013a. "Comparison of Inhibitory Effect of Curcumin Nanoparticles and Free Curcumin in Human Telomerase Reverse Transcriptase Gene Expression in Breast Cancer." *Advanced Pharmaceutical Bulletin*.

Kazemi-Lomedasht, Fatemeh, Abbas Rami, and Nosratollah Zarghami. 2013b. "Comparison of Inhibitory Effect of Curcumin Nanoparticles and Free Curcumin in Human Telomerase Reverse Transcriptase Gene Expression in Breast Cancer." *Advanced Pharmaceutical Bulletin* 3(1):127–30.

Ketkar, Shamika, Angela M. Verdoni, Amanda M. Smith, Celia V. Bangert, Elizabeth

R. Leight, David Y. Chen, Meryl K. Brune, Nichole M. Helton, Mieke Hoock, Daniel R. George, Catrina Fronick, Robert S. Fulton, Sai Mukund Ramakrishnan, Gue Su Chang, Allegra A. Petti, David H. Spencer, Christopher A. Miller, and Timothy J. Ley. 2020. “Remethylation of Dnmt3a−/− Hematopoietic Cells Is Associated with Partial Correction of Gene Dysregulation and Reduced Myeloid Skewing.” *Proceedings of the National Academy of Sciences of the United States of America* 117(6):3123–34.

Kim, Min S., Yoo R. Kim, Nam J. Yoo, and Sug H. Lee. 2013. “Mutational Analysis of DNMT3A Gene in Acute Leukemias and Common Solid Cancers.” *APMIS* 121(2):85–94.

Kobayashi, Hiroshi, Sumire Ohno, Yoshikazu Sasaki, and Miyuki Matsuura. 2013. “Hereditary Breast and Ovarian Cancer Susceptibility Genes (Review).” *Oncology Reports* 30:1019–29.

Koo, Minjoung Monica, Christian von Wagner, Gary A. Abel, Sean McPhail, Greg P. Rubin, and Georgios Lyratzopoulos. 2017. “Typical and Atypical Presenting Symptoms of Breast Cancer and Their Associations with Diagnostic Intervals: Evidence from a National Audit of Cancer Diagnosis.” *Cancer Epidemiology*.

Kowal, Krzysztof, Angelika Tkaczyk, Tomasz Ząbek, Mariusz Pierzchała, and Brygida Ślaska. 2020. “Comparative Analysis of CpG Sites and Islands Distributed in Mitochondrial DNA of Model Organisms.” *Animals* 10:665.

Koziel, Jillian E., and Brittney Shea Herbert. 2015. “The Telomerase Inhibitor Imetelstat Alone, and in Combination with Trastuzumab, Decreases the Cancer Stem Cell Population and Self-Renewal of HER2+ Breast Cancer Cells.” *Breast Cancer Research and Treatment* 149(3):607–18.

Kruger, W. M., and J. P. Apffelstaedt. 2007. “Young Breast Cancer Patients in the Developing World: Incidence, Choice of Surgical Treatment and Genetic Factors.” *South African Family Practice* 49(9):19–24.

Kuchiba, A., M. Iwasaki, H. Ono, Y. Kasuga, S. Yokoyama, H. Onuma, H. Nishimura, R. Kusama, S. Tsugane, and T. Yoshida. 2014. “Global Methylation Levels in Peripheral Blood Leukocyte DNA by LUMA and Breast Cancer: A Case-Control Study in Japanese Women.” *British Journal of Cancer* 110(11):2765–71.

Kulis, Marta, Angelika Merkel, Simon Heath, Ana C. Queirós, Ronald P. Schuyler, Giancarlo Castellano, Renée Beekman, Emanuele Raineri, Anna Esteve, Guillem Clot, Néria Verdaguer-Dot, Martí Duran-Ferrer, Nuria Russiñol, Roser Vilarrasa-

Blasi, Simone Ecker, Vera Pancaldi, Daniel Rico, Lidia Agueda, Julie Blanc, David Richardson, Laura Clarke, Avik Datta, Marien Pascual, Xabier Agirre, Felipe Prosper, Diego Alignani, Bruno Paiva, Gersende Caron, Thierry Fest, Marcus O. Muench, Marina E. Fomin, Seung Tae Lee, Joseph L. Wiemels, Alfonso Valencia, Marta Gut, Paul Flicek, Hendrik G. Stunnenberg, Reiner Siebert, Ralf Küppers, Ivo G. Gut, Elías Campo, and José I. Martín-Subero. 2015. “Whole-Genome Fingerprint of the DNA Methylome during Human B Cell Differentiation.” *Nature Genetics* 47(7):746–56.

Kumar, Ashish, Emma Dalan, and Melanie A. Carless. 2020. “Analysis of DNA Methylation Using Pyrosequencing.” Pp. 37–62 in *Epigenetics Methods*. Elsevier.

Kumari, Priyanka, Kanak Misra, Brijesh Singh Sisodia, Uzma Faridi, Suchita Srivastava, Suiab Luqman, Mahendra Pandurang Darokar, Arvind Singh Negi, Madan Mohan Gupta, Subhash Chandra Singh, and Jonnala Kotesh Kumar. 2009. “A Promising Anticancer and Antimalarial Component from the Leaves of Bidens Pilosa.” *Planta Medica* 75(1):59–61.

Landercasper, Jeffrey, Barbara Bennie, Benjamin M. Parsons, Leah L. Dietrich, Caprice C. Greenberg, Lee G. Wilke, and Jared H. Linebarger. 2017. “Fewer Reoperations After Lumpectomy for Breast Cancer with Neoadjuvant Rather than Adjuvant Chemotherapy: A Report from the National Cancer Database.” *Annals of Surgical Oncology* 24(6):1507–15.

Lee, Ching Kuo, Guei J. Wang, Yueh H. Kuo and Ming H. Chang. 2000. "The low polar constituents from *Bidens pilosa* L. var. *minor* (blume) sherff." *Journal of the Chinese Chemical Society* 47(5):1131–1136.

Lee, Eun-Joon, Junfeng Luo, James M. Wilson, and Huidong Shi. 2013. “Analyzing the Cancer Methylome through Targeted Bisulfite Sequencing.” *Cancer Letters* 340(2):1–16.

Lee, Shin Hae, and Kyung Jin Min. 2019. “Phytochemicals.” Pp. 35–47 in *Encyclopedia of Biomedical Gerontology*.

De Leeneer, Kim, Ilse Coene, Brecht Crombez, Justine Simkens, Rudy Van Den Broecke, Alain Bols, Barbara Stragier, Ilse Vanhoutte, Anne De Paepe, Bruce Poppe, and Kathleen Claes. 2012. “Prevalence of BRCA1/2 Mutations in Sporadic Breast/Ovarian Cancer Patients and Identification of a Novel de Novo BRCA1 Mutation in a Patient Diagnosed with Late Onset Breast and Ovarian Cancer: Implications for Genetic Testing.” *Breast Cancer Research and Treatment*

132(1):87–95.

Levitsky, Dmitri O., and Valery M. Dembitsky. 2015. “Anti-Breast Cancer Agents Derived from Plants.” *Natural Products and Bioprospecting* 5:1–16.

Lewis, Kayla, Harrison Jordan, and Trygve Tollefsbol. 2018. “Effects of SAHA and EGCG on Growth Potentiation of Triple-Negative Breast Cancer Cells.” *Cancers* 11(1):23.

Li, Congru, Yong Fan, Guoqiang Li, Xiaocui Xu, Jialei Duan, Rong Li, Xiangjin Kang, Xin Ma, Xuepeng Chen, Yuwen Ke, Jie Yan, Ying Lian, Ping Liu, Yue Zhao, Hongcui Zhao, Yaoyong Chen, Yang Yu, and Jiang Liu. 2018. “DNA Methylation Reprogramming of Functional Elements during Mammalian Embryonic Development.” *Cell Discovery* 4(1):41.

Li, Jian Wei, Miao Mo, Ke Da Yu, Can Ming Chen, Zhen Hu, Yi Feng Hou, Gen Hong Di, Jiong Wu, Zhen Zhou Shen, Zhi Ming Shao, and Guang Yu Liu. 2014. “ER-Poor and HER2-Positive: A Potential Subtype of Breast Cancer to Avoid Axillary Dissection in Node Positive Patients after Neoadjuvant Chemo-Trastuzumab Therapy.” *PLoS ONE* 9(12):e114646.

Liang, Yu Chuan, Chuan Ju Lin, Cheng Ying Yang, Yung Hsiang Chen, Meng Ting Yang, Fu Shiuan Chou, Wen Chin Yang, and Cicero Lee Tian Chang. 2020. “Toxicity Study of Bidens Pilosa in Animals.” *Journal of Traditional and Complementary Medicine* 10(2):150–57.

Library, Wiley Online, Gareth H. Williams, and Kai Stoeber. 2012. “The Cell Cycle and Cancer.” *INVITED REVIEW Journal of Pathology J Pathol* 226:352–64.

Liu, Jiajie, and David W. L. Ma. 2014. “The Role of N-3 Polyunsaturated Fatty Acids in the Prevention and Treatment of Breast Cancer.” *Nutrients* 6:5184–5223.

Liu, Yang, and Xuetao Cao. 2016. “Characteristics and Significance of the Pre-Metastatic Niche.” *Cancer Cell* 30(5):668–81.

Loh, Chin Yap, Jian Yi Chai, Ting Fang Tang, Won Fen Wong, Gautam Sethi, Muthu Kumaraswamy Shanmugam, Pei Pei Chong, and Chung Yeng Looi. 2019. “The E-Cadherin and N-Cadherin Switch in Epithelial-to-Mesenchymal Transition: Signaling, Therapeutic Implications, and Challenges.” *Cells* 8:1118.

Loo, Suet Kee, Suzina Sheikh Suzina, Mustaffa Musa, and Kah Keng Wong. 2018. “DNMT1 Is Associated with Cell Cycle and DNA Replication Gene Sets in Diffuse Large B-Cell Lymphoma.” *Pathology Research and PracticeLoo, Suet Kee, Suzina Sheikh Suzina, Mustaffa Musa, and Kah Keng Wong. 2018. “DNMT1 Is*

Associated with Cell Cycle and DNA Replication Gene Sets in Diffuse Large B-Cell Lymphoma." Pathology Research and Practice. 214(1):134–43.

Loreto, Carla, Giampiero La Rocca, Rita Anzalone, Rosario Caltabiano, Giuseppe Vespasiani, Sergio Castorina, David J. Ralph, Selim Cellek, Giuseppe Musumeci, Salvatore Giunta, Rados Djinovic, Dragoslav Basic, and Salvatore Sansalone. 2014. "The Role of Intrinsic Pathway in Apoptosis Activation and Progression in Peyronie's Disease." *BioMed Research International* 2014:616149.

Mainasara, Muhammad Murtala, Mohd Fadzelly Abu Bakar, and Alona C. Linatoc. 2018. "Malaysian Medicinal Plants' Potential for Breast Cancer Therapy." *Asian Journal of Pharmaceutical and Clinical Research* 11(6):101–17.

Manoochehri, Mehdi, Nasim Borhani, Ashraf Karbasi, Ameneh Koochaki, and Bahram Kazemi. 2016. "Promoter Hypermethylation and Downregulation of the FAS Gene May Be Involved in Colorectal Carcinogenesis." *Oncology Letters* 12(1):285–90.

Mao, Qin, Yu Zhang, Xiaoyue Fu, Jianxin Xue, Wenhao Guo, Maobing Meng, Zongguang Zhou, Xianming Mo, and You Lu. 2013. "A Tumor Hypoxic Niche Protects Human Colon Cancer Stem Cells from Chemotherapy." *Journal of Cancer Research and Clinical Oncology* 139(2):211–22.

Marston, A. 2011. "Thin-Layer Chromatography with Biological Detection in Phytochemistry." *Journal of Chromatography A* 1218:2676–83.

Mattiske, Sam, Rachel J. Suetani, Paul M. Neilsen, and David F. Callen. 2012. "The Oncogenic Role of MiR-155 in Breast Cancer." *Cancer Epidemiology Biomarkers and Prevention* 21:1236–43.

Misek, David E., and Evelyn H. Kim. 2011. "Protein Biomarkers for the Early Detection of Breast Cancer." *International Journal of Proteomics* 2011:1–9.

Moore, Lisa D., Thuc Le, and Guoping Fan. 2013. "DNA Methylation and Its Basic Function." *Neuropsychopharmacology* 38:23–38.

Murata, Takeshi, Hiromitsu Jinno, Maiko Takahashi, Masayuki Shimoda, Tetsu Hayashida, Kaori Kameyama, and Yuko Kitagawa. 2019. "Clinicopathologic Features of Hormone-Receptor-Positive Breast Cancer Patients with Late Recurrence." *Breast Journal* 25(1):9–15.

Murff, Harvey J., Xiao Ou Shu, Honglan Li, Gong Yang, Xiauyan Wu, Hui Cai, Wanqing Wen, Yu Tang Gao, and Wei Zheng. 2011. "Dietary Polyunsaturated Fatty Acids and Breast Cancer Risk in Chinese Women: A Prospective Cohort Study." *International Journal of Cancer* 128(6):1434–41.

N., Nishida, Kudo M., Arizumi T., Hayaishi S., Takita M., Kitai S., Yada N., Inoue T., Hagiwara S., Minami Y., Ueshima K., Sakurai T., and Nagasaka T. 2012. “Novel Association between Global DNA Hypomethylation and Chromosomal Instability Phenotype in Human Hepatocellular Carcinoma.” *Gastroenterology* 8(9):e72312.

Nainu, Firzan, Akiko Shiratsuchi, and Yoshinobu Nakanishi. 2017. “Induction of Apoptosis and Subsequent Phagocytosis of Virus-Infected Cells as an Antiviral Mechanism.” *Frontiers in Immunology* 8:1220.

NCR. 2012. “Cancer in South Africa.” Retrieved (http://www.nicd.ac.za/index.php/centres/national-cancer-registry/cancer-statistics/).

NCR. 2014. “Cancer in South Africa.” Retrieved (http://www.nicd.ac.za/index.php/centres/national-cancer-registry/cancer-statistics/).

Al Nemer, Areej M. 2017. “Histologic Factors Predicting Invasion in Patients with Ductal Carcinoma in Situ (DCIS) in the Preoperative Core Biopsy.” *Pathology Research and Practice* 213(5):429–34.

Nguyen, Kathy C., William G. Willmore, and Azam F. Tayabali. 2013. “Cadmium Telluride Quantum Dots Cause Oxidative Stress Leading to Extrinsic and Intrinsic Apoptosis in Hepatocellular Carcinoma HepG2 Cells.” *Toxicology* 306:114–23.

Niroula, Anuj, Sagar Khatri, Dinesh Khadka, and Rashika Timilsina. 2019. “International Journal of Food Properties Total Phenolic Contents and Antioxidant Activity Profile of Selected Cereal Sprouts and Grasses Total Phenolic Contents and Antioxidant Activity Profile of Selected Cereal Sprouts and Grasses.” *International Journal of Food Properties* 22(1):427–37.

Nowsheen, Somaira, Khaled Aziz, Phuoc T. Tran, Vassilis G. Gorgoulis, Eddy S. Yang, and Alexandros G. Georgakilas. 2014. “Epigenetic Inactivation of DNA Repair in Breast Cancer.” *Cancer Letters* 342:213–22.

Núñez, Cristina, José Luis Capelo, Gilberto Igrejas, Amparo Alfonso, Luis M. Botana, and Carlos Lodeiro. 2016. “An Overview of the Effective Combination Therapies for the Treatment of Breast Cancer.” *Biomaterials* 97:34–50.

O’Brien, Katie M., Jenny Sun, Dale P. Sandler, Lisa A. DeRoo, and Clarice R. Weinberg. 2015. “Risk Factors for Young-Onset Invasive and in Situ Breast Cancer.” *Cancer Causes and Control* 26(12):1771–78.

Odle, Teresa G. 2014. “Adverse Effects of Breast Cancer Treatment.” *Radiologic*

Technology 85(3):297–319.

Ohnishi, Shunsuke, and Hiroshi Takeda. 2015. “Herbal Medicines for the Treatment of Cancer Chemotherapy-Induced Side Effects.” *Frontiers in Pharmacology* 6:14.

Olas, Beata. 2018. “Berry Phenolic Antioxidants - Implications for Human Health?” *Frontiers in Pharmacology* 9:78.

Olver, Ian, Mariko Carey, Allison Boyes, Alix Hall, Natasha Noble, Jamie Bryant, Justin Walsh, and Rob Sanson-Fisher. 2018. “The Timeliness of Patients Reporting the Side Effects of Chemotherapy.” *Supportive Care in Cancer* 26(10):3579–86.

Onyancha, Jared M., Nicholas K. Gikonyo, Sabina W. Wachira, Peter G. Mwitari, and Michael M. Gicheru. 2018. “Anticancer Activities and Safety Evaluation of Selected Kenyan Plant Extracts against Breast Cancer Cell Lines.” *Journal of Pharmacognosy and Phytotherapy* 10(2):21–26.

Orouji, Elias, and Jochen Utikal. 2018. “Tackling Malignant Melanoma Epigenetically: Histone Lysine Methylation.” *Clinical Epigenetics* 10:145.

Ozcan, T., A. Akpinar-Bayizit, L. Yilmaz-Ersan, and B. Delikanli. 2014. “Phenolics in Human Health.” *International Journal of Chemical Engineering and Applications* 5(5):393–96.

De Paepe, C., A. Aberkane, D. Dewandre, W. Essahib, K. Sermon, M. Geens, G. Verheyen, H. Tournaye, and H. Van de Velde. 2019. “BMP4 Plays a Role in Apoptosis during Human Preimplantation Development.” *Molecular Reproduction and Development* 86(1):53–62.

Palma, Manuel. 2017. “Flavonoid Antioxidants: Chemistry, Metabolism and Structure-Activity Relationships.” *Journal of the American Oil Chemists’ Society* 94(9):572–84.

Park, Jong Woo, and Jeung Whan Han. 2019. “Targeting Epigenetics for Cancer Therapy.” *Archives of Pharmacal Research* 42:159–70.

Pasculli, Barbara, Raffaela Barbano, and Paola Parrella. 2018. “Epigenetics of Breast Cancer: Biology and Clinical Implication in the Era of Precision Medicine.” *Seminars in Cancer Biology* 51:22–35.

Paul, Bidisha, Yuanyuan Li, and Trygve O. Tollefsbol. 2018. “The Effects of Combinatorial Genistein and Sulforaphane in Breast Tumor Inhibition: Role in Epigenetic Regulation.” *International Journal of Molecular Sciences* 19(6):1754.

Pegoraro, Cristiane Martinez Ruiz, Gisele Alborghetti Nai, Leonardo Alves Garcia, Fernanda de Maria Serra, Juliana Apolônio Alves, Pedro Henrique Nahas

Chagas, Décio Gomes de Oliveira, and Marcos Alberto Zocoler. 2021. “Protective Effects of Bidens Pilosa on Hepatoxicity and Nephrotoxicity Induced by Carbon Tetrachloride in Rats.” *Drug and Chemical Toxicology* 44(1):64–74.

Pfeffer, Claire M., and Amareshwar T. K. Singh. 2018. “Apoptosis: A Target for Anticancer Therapy.” *International Journal of Molecular Sciences* 19:448.

Potente, Michael, Holger Gerhardt, and Peter Carmeliet. 2011. “Basic and Therapeutic Aspects of Angiogenesis.” *Cell* 146:873–87.

Pourmorad, F., S. J. Hosseinimehr, and N. Shahabimajd. 2006. “Antioxidant Activity, Phenol and Flavonoid Contents of Some Selected Iranian Medicinal Plants.” *African Journal of Biotechnology* 5(11):1142–45.

Prabhu, T. P., P. Panneerselvam, S. Selvakumari, Ubaidulla Udhumansha, and A. Shantha. 2012. “Anticancer Activity of Merremia Emarginata (Burm.F) against Human Cervical and Breast Carcinoma.” *International Journal of Research and Development in Pharmacy and Life Sciences* 1(October):189–92.

Raimi, Idris O., Boikanyo G. Kopaopa, Liziwe L. Mugivhisa, Francis B. Lewu, Stephen O. Amoo, and Joshua O. Olowoyo. 2020. “An Appraisal of Documented Medicinal Plants Used for the Treatment of Cancer in Africa over a Twenty-Year Period (1998–2018).” *Journal of Herbal Medicine* 23:100371.

Rajshekar, Srivarsha, Jun Yao, Paige K. Arnold, Sara G. Payne, Yinwen Zhang, Teresa V. Bowman, Robert J. Schmitz, John R. Edwards, and Mary G. Goll. 2018. “Pericentromeric Hypomethylation Elicits an Interferon Response in an Animal Model of ICF Syndrome.” *ELife Research Communication* (7):e39658.

Rakha, Emad A., Arjun Patel, Des G. Powe, Ahmed Benhasouna, Andrew R. Green, Maryou B. Lambros, Jorge S. Reis-Filho, and Ian O. Ellis. 2010. “Clinical and Biological Significance of E-Cadherin Protein Expression in Invasive Lobular Carcinoma of the Breast.” *American Journal of Surgical Pathology* 34(10):1472–79.

Rao, Satyanarayan, Tsu Pei Chiu, Judith F. Kribelbauer, Richard S. Mann, Harmen J. Bussemaker, and Remo Rohs. 2018. “Systematic Prediction of DNA Shape Changes Due to CpG Methylation Explains Epigenetic Effects on Protein-DNA Binding.” *Epigenetics and Chromatin* 11(1):6.

Reis, I. M., K. Ramachandran, C. Speer, E. Gordian, and R. Singal. 2015. “Serum GADD45a Methylation Is a Useful Biomarker to Distinguish Benign vs Malignant Prostate Disease.” *British Journal of Cancer* 113(3):460–68.

Richard, Tagne Simo, Armel Herve, Nwabo Kamdje, and Farah Mukhtar. 2015. “Medicinal Plants in Breast Cancer Therapy.” *Journal of Diseases and Medicinal Plants*.

Robinson, Mark D., Clare Stirzaker, Aaron L. Statham, Marcel W. Coolen, Jenny Z. Song, Shalima S. Nair, Dario Strbenac, Terence P. Speed, and Susan J. Clark. 2010. “Evaluation of Affinity-Based Genome-Wide DNA Methylation Data: Effects of CpG Density, Amplification Bias, and Copy Number Variation.” *Genome Research* 20(12):1719–29.

Rohilla, Manish, Amanjit Bal, Gurpreet Singh, and Kusum Joshi. 2015. “Phenotypic and Functional Characterization of Ductal Carcinoma in Situ-Associated Myoepithelial Cells.” *Clinical Breast Cancer* 15(5):335–42.

Roleira, Fernanda M. F., Elisiário J. Tavares-Da-Silva, Carla L. Varela, Saul C. Costa, Tiago Silva, Jorge Garrido, and Fernanda Borges. 2015. “Plant Derived and Dietary Phenolic Antioxidants: Anticancer Properties.” *Food Chemistry* 183:235–58.

Rosen, Eliot M. 2013. “BRCA1 in the DNA Damage Response and at Telomeres.” *Frontiers in Genetics* 4(JUN):85.

Röth, Alexander, Calvin B. Harley, and Gabriela M. Baerlocher. 2010. “Imetelstat (GRN163L) - Telomerase-Based Cancer Therapy.” *Recent Results in Cancer Research* 184:221–34.

Rousseaux, Sophie, and Saadi Khochbin. 2015. “Histone Acylation beyond Acetylation: Terra Incognita in Chromatin Biology.” *Cell Journal* 17:1–6.

Sadeghi, Fatemeh, Marzieh Asgari, Mojdeh Matloubi, Maral Ranjbar, Nahid Karkhaneh Yousefi, Tahereh Azari, and Majid Zaki-Dizaji. 2020. “Molecular Contribution of BRCA1 and BRCA2 to Genome Instability in Breast Cancer Patients: Review of Radiosensitivity Assays.” *Biological Procedures Online* 22(1):23.

Sandoval, Juan, and Manel Esteller. 2012. “Cancer Epigenomics: Beyond Genomics.” *Current Opinion in Genetics and Development* 22:50–55.

Savage, Kienan I., and D. Paul Harkin. 2015. “BRCA1, a ‘complex’ Protein Involved in the Maintenance of Genomic Stability.” *FEBS Journal* 630–46.

Schneider, Katrin, Christiane Fuchs, Akos Dobay, Andrea Rottach, Weihua Qin, Patricia Wolf, José M. Álvarez-Castro, Marcus M. Nalaskowski, Elisabeth Kremmer, Volker Schmid, Heinrich Leonhardt, and Lothar Schermelleh. 2013.

"Dissection of Cell Cycle-Dependent Dynamics of Dnmt1 by FRAP and Diffusion-Coupled Modeling." *Nucleic Acids Research* 41(9):4860–76.

Selvakumar, Priyanga, Aja Badgeley, Paige Murphy, Hina Anwar, Urvashi Sharma, Katharine Lawrence, and Ashakumary Lakshmikuttyamma. 2020. "Flavonoids and Other Polyphenols Act as Epigenetic Modifiers in Breast Cancer." *Nutrients* 12:761.

Sen, Tuhinadri, and Samir Kumar Samanta. 2014. "Medicinal Plants, Human Health and Biodiversity: A Broad Review." *Advances in Biochemical Engineering/Biotechnology* 147:59–110.

Senger, Jenna Lynn, Scott J. Adams, and Rani Kanthan. 2017. "Invasive Lobular Carcinoma of the Male Breast – A Systematic Review with an Illustrative Case Study." *Breast Cancer: Targets and Therapy* 9:337–45.

Sestak, Ivana, Mitch Dowsett, Lila Zabaglo, Elena Lopez-Knowles, Sean Ferree, J. Wayne Cowens, and Jack Cuzick. 2013. "Factors Predicting Late Recurrence for Estrogen Receptor-Positive Breast Cancer." *Journal of the National Cancer Institute* 105(19):1504–11.

Shah, Mrinal Y., and Jonathan D. Licht. 2011. "DNMT3A Mutations in Acute Myeloid Leukemia." *Nature Genetics* 43(4):289–90.

Shaikh, Junaid R., and MK Patil. 2020. "Qualitative Tests for Preliminary Phytochemical Screening: An Overview." *International Journal of Chemical Studies*.

Shargh, Shohreh Alizadeh, Meral Sakizli, Vahid Khalaj, Abolfazl Movafagh, Hamidreza Yazdi, Elmira Hagigatjou, Aresou Sayad, Neda Mansouri, Seyed Abdolreza Mortazavi-Tabatabaei, and Hamid Reza Khorram Khorshid. 2014. "Downregulation of E-Cadherin Expression in Breast Cancer by Promoter Hypermethylation and Its Relation with Progression and Prognosis of Tumor." *Medical Oncology* 31(11):1–6.

Shen, Yiwei, Zhouliang Sun, Peiying Shi, Gang Wang, Youjia Wu, Shaoguang Li, Yanjie Zheng, Liying Huang, Liqing Lin, Xinhua Lin, and Hong Yao. 2018. "Anticancer Effect of Petroleum Ether Extract from Bidens Pilosa L and Its Constituent's Analysis by GC-MS." *Journal of Ethnopharmacology* 217:126–33.

Shinjo, Keiko, and Yutaka Kondo. 2015. "Targeting Cancer Epigenetics: Linking Basic Biology to Clinical Medicine." *Advanced Drug Delivery Reviews* 95:56–64.

Si, Ho Choi, Scott Worswick, Hyang Min Byun, Talia Shear, John C. Soussa, Erika M.

Wolff, Dan Douer, Guillermo Garcia-Manero, Gangning Liang, and Allen S. Yang. 2009. “Changes in DNA Methylation of Tandem DNA Repeats Are Different from Interspersed Repeats in Cancer.” *International Journal of Cancer* 125(3):723–29.

Sierra, Amanda, Juan M. Encinas, Juan J. P. Deudero, Jessica H. Chancey, Grigori Enikolopov, Linda S. Overstreet-Wadiche, Stella E. Tsirka, and Mirjana Maletic-Savatic. 2010. “Microglia Shape Adult Hippocampal Neurogenesis through Apoptosis-Coupled Phagocytosis.” *Cell Stem Cell* 7(4):483–95.

Simhadri, Srilatha, Gabriele Vincelli, Yanying Huo, Sarah Misenko, Tzeh Keong Foo, Johanna Ahlskog, Claus S. Sørensen, Gregory G. Oakley, Shridar Ganesan, Samuel F. Bunting, and Bing Xia. 2019. “PALB2 Connects BRCA1 and BRCA2 in the G2/M Checkpoint Response.” *Oncogene* 38(10):1585–96.

Siraj, Abdul K., P. Pratheeshkumar, Sandeep Kumar Parvathareddy, Rong Bu, T. Masoodi, Kaleem Iqbal, Maha Al-Rasheed, F. Al-Dayel, Saif S. Al-Sobhi, A. S. Alzahrani, Mohammed Al-Dawish, and Khawla S. Al-Kuraya. 2019. “Prognostic Significance of DNMT3A Alterations in Middle Eastern Papillary Thyroid Carcinoma.” *European Journal of Cancer* 117:133–44.

Soares, Susana, Elsa Brandão, Carlos Guerreiro, Sónia Soares, Nuno Mateus, and Victor De Freitas. 2020. “Tannins in Food: Insights into the Molecular Perception of Astringency and Bitter Taste.” *Molecules* 25:2590.

Song, Won Jong, Kwan Il Kim, Sang Hyun Park, Mi Seon Kwon, Tae Hoon Lee, Heung Kyu Park, and Jung Suk An. 2012a. “The Risk Factors Influencing between the Early and Late Recurrence in Systemic Recurrent Breast Cancer.” *Journal of Breast Cancer* 15(2):218–23.

Song, Won Jong, Kwan Il Kim, Sang Hyun Park, Mi Seon Kwon, Tae Hoon Lee, Heung Kyu Park, and Jung Suk An. 2012b. “The Risk Factors Influencing between the Early and Late Recurrence in Systemic Recurrent Breast Cancer.” *Journal of Breast Cancer* 15(2):218–23.

Speight, Beverley, and Marc Tischkowitz. 2017. “When to Consider Risk-Reducing Mastectomy in BRCA1/BRCA2 Mutation Carriers with Advanced Stage Ovarian Cancer: A Case Study Illustrating the Genetic Counseling Challenges.” *Journal of Genetic Counseling* 26(6):1173–78.

Spencer, David H., David A. Russler-Germain, Shamika Ketkar, Nichole M. Helton, Tamara L. Lamprecht, Robert S. Fulton, Catrina C. Fronick, Michelle O’Laughlin, Sharon E. Heath, Marwan Shinawi, Peter Westervelt, Jacqueline E. Payton,

Lukas D. Wartman, John S. Welch, Richard K. Wilson, Matthew J. Walter, Daniel C. Link, John F. DiPersio, and Timothy J. Ley. 2017. “CpG Island Hypermethylation Mediated by DNMT3A Is a Consequence of AML Progression.” *Cell* 168(5):801-816.e13.

Sprouse, Alyssa A., Catherine E. Steding, and Brittney Shea Herbert. 2012. “Pharmaceutical Regulation of Telomerase and Its Clinical Potential.” *Journal of Cellular and Molecular Medicine* 16(1):1–7.

Steenkamp, V., and M. C. Gouws. 2006. “Cytotoxicity of Six South African Medicinal Plant Extracts Used in the Treatment of Cancer.” *South African Journal of Botany* 72(4):630–33.

Stefansson, Olafur A., Alberto Villanueva, August Vidal, Lola Martí, and Manel Esteller. 2012. “BRCA1 Epigenetic Inactivation Predicts Sensitivity to Platinum-Based Chemotherapy in Breast and Ovarian Cancer.” *Epigenetics* 7(11):1225–29.

Straka, Shana, Joanne L. Lester, Rachel M. Cole, Rebecca R. Andridge, Sarah Puchala, Angela M. Rose, Steven K. Clinton, Martha A. Belury, and Lisa D. Yee. 2015. “Incorporation of Eicosapentaenioic and Docosahexaenoic Acids into Breast Adipose Tissue of Women at High Risk of Breast Cancer: A Randomized Clinical Trial of Dietary Fish and n-3 Fatty Acid Capsules.” *Molecular Nutrition and Food Research* 59(9):1780–90.

Sung, Hyuna, Jacques Ferlay, Rebecca L. Siegel, Mathieu Laversanne, Isabelle Soerjomataram, Ahmedin Jemal, and Freddie Bray. 2021. “Global Cancer Statistics 2020: GLOBOCAN Estimates of Incidence and Mortality Worldwide for 36 Cancers in 185 Countries.” *CA: A Cancer Journal for Clinicians* 0:1–41.

Tan, E. Jean, Kaoru Kahata, Oskar Idås, Sylvie Thuault, Carl Henrik Heldin, and Aristidis Moustakas. 2015. “The High Mobility Group A2 Protein Epigenetically Silences the Cdh1 Gene during Epithelial-to-Mesenchymal Transition.” *Nucleic Acids Research* 43(1):162–78.

Tang, Jianing, Qiuxia Cui, Dan Zhang, Xing Liao, Jian Zhu, and Gaosong Wu. 2019. “An Estrogen Receptor (ER)-Related Signature in Predicting Prognosis of ER-Positive Breast Cancer Following Endocrine Treatment.” *Journal of Cellular and Molecular Medicine* 23(8):4890–4990.

Tong, Adrian S., J. Lewis Stern, Agnel Sfeir, Melissa Kartawinata, Titia de Lange, Xu Dong Zhu, and Tracy M. Bryan. 2015. “ATM and ATR Signaling Regulate the

Recruitment of Human Telomerase to Telomeres." *Cell Reports* 13(8):1633–46.

Tsai, Hsing Chen, and Stephen B. Baylin. 2011. "Cancer Epigenetics: Linking Basic Biology to Clinical Medicine." *Cell Research* 21:502–17.

Turashvili, Gulisa, and Edi Brogi. 2017. "Tumor Heterogeneity in Breast Cancer." *Frontiers in Medicine* 4:227.

Varela-Rey, Marta, Ashwin Woodhoo, Maria Luz Martinez-Chantar, José M. Mato, and Shelly C. Lu. 2012. "Alcohol, DNA Methylation, and Cancer." *Alcohol Research: Current Reviews* 35:25–35.

Virani, Shama, Shami Virani, Justin A. Colacino, Jung H. Kim, and Laura S. Rozek. 2012. "Cancer Epigenetics: A Brief Review." *ILAR Journal / National Research Council, Institute of Laboratory Animal Resources* 53:359–69.

Visser, Lindy L., Emma J. Groen, Flora E. Van Leeuwen, Esther H. Lips, Marjanka K. Schmidt, and Jelle Wesseling. 2019. "Predictors of an Invasive Breast Cancer Recurrence after DCIS: A Systematic Review and Meta-Analyses." *Cancer Epidemiology Biomarkers and Prevention* 28(5):835–45.

Voduc, K. David, Maggie C. U. Cheang, Scott Tyldesley, Karen Gelmon, Torsten O. Nielsen, and Hagen Kennecke. 2010. "Breast Cancer Subtypes and the Risk of Local and Regional Relapse." *Journal of Clinical Oncology* 28(10):1684–91.

Volpe, Caroline Maria Oliveira, Pedro Henrique Villar-Delfino, Paula Martins Ferreira dos Anjos, and JosÃ© Augusto Nogueira-Machado. n.d. "Cellular Death, Reactive Oxygen Species (ROS) and Diabetic Complications." *Cell Death & Disease* 9(2):119.

Vos, Shoko, Cathy Beatrice Moelans, and Paul Joannes van Diest. 2017. "BRCA Promoter Methylation in Sporadic versus BRCA Germline Mutation-Related Breast Cancers." *Breast Cancer Research* 19(1):64.

Voss, Anne K., and Andreas Strasser. 2020. "The Essentials of Developmental Apoptosis." *F1000Research* 9:148.

Wahyuni, R., W. Wignyanto, S. Wijana, and S. Sucipto. 2020. "Optimization of Protein and Tannin Extraction in Moringa Oleifera Leaf as Antioxidant Source." *Food Research*.

Waks, Adrienne G., and Eric P. Winer. 2019. "Breast Cancer Treatment: A Review." *JAMA - Journal of the American Medical Association* 321:288–300.

Wang, Keh Yang, Chun Chang Chen, and Che Kun James Shen. 2014. "Active DNA Demethylation of the Vertebrate Genomes by DNA Methyltransferases:

Deaminase, Dehydroxymethylase or Demethylase?" *Epigenomics* 6:353–63.

Weis, Sara M., and David A. Cheresh. 2011. "Tumor Angiogenesis: Molecular Pathways and Therapeutic Targets." *Nature Medicine* 17:1359–70.

Wendt, Michael K., Molly A. Taylor, Barbara J. Schiemann, and William P. Schiemann. 2011. "Down-Regulation of Epithelial Cadherin Is Required to Initiate Metastatic Outgrowth of Breast Cancer." *Molecular Biology of the Cell* 22(14):2423–35.

Willmer, Tarryn, Julia H. Goedecke, Stephanie Dias, Johan Louw, and Carmen Pheiffer. 2020. "DNA Methylation of FKBP5 in South African Women: Associations with Obesity and Insulin Resistance." *Clinical Epigenetics* 12:141.

Wong, Sonia How Ming, Chee Mun Fang, Lay Hong Chuah, Chee Onn Leong, and Siew Ching Ngai. 2018. "E-Cadherin: Its Dysregulation in Carcinogenesis and Clinical Implications." *Critical Reviews in Oncology/Hematology* 121:11–22.

Wu, Jiaxue, Lin Yu Lu, and Xiaochun Yu. 2010. "The Role of BRCA1 in DNA Damage Response." *Protein and Cell* 1:117–23.

van Wyk, A. S., and G. Prinsloo. 2018. "Medicinal Plant Harvesting, Sustainability and Cultivation in South Africa." *Biological Conservation* 227:335–42.

Xu, Jinhua, Dezheng Huo, Yinghua Chen, Chika Nwachukwu, Cindy Collins, Janelle Rowell, Dennis J. Slamon, and Olufunmilayo I. Olopade. 2010. "CpG Island Methylation Affects Accessibility of the Proximal BRCA1 Promoter to Transcription Factors." *Breast Cancer Research and Treatment* 120(3):593–601.

Xuan, Tran Dang, and Tran Dang Khanh. 2016a. "Chemistry and Pharmacology of Bidens Pilosa: An Overview." *Journal of Pharmaceutical Investigation*.

Xuan, Tran Dang, and Tran Dang Khanh. 2016b. "Chemistry and Pharmacology of Bidens Pilosa: An Overview." *Journal of Pharmaceutical Investigation* 46(2):91–132.

Yagi, Masaki, Mio Kabata, Akito Tanaka, Tomoyo Ukai, Sho Ohta, Kazuhiko Nakabayashi, Masahito Shimizu, Kenichiro Hata, Alexander Meissner, Takuya Yamamoto, and Yasuhiro Yamada. 2020. "Identification of Distinct Loci for de Novo DNA Methylation by DNMT3A and DNMT3B during Mammalian Development." *Nature Communications* 11(1):3199.

Yang, Wen Chin. 2014. "Botanical, Pharmacological, Phytochemical, and Toxicological Aspects of the Antidiabetic Plant Bidens Pilosa L." *Evidence-Based Complementary and Alternative Medicine* 2014:698617.

Yi, Jun, Jian Guo Wu, Yan Bin Wu, and Wei Peng. 2016. "Antioxidant and Anti-

Proliferative Activities of Flavonoids from Bidens Pilosa L Var Radiata Sch Bip." *Tropical Journal of Pharmaceutical Research* 15(2):341–48.

Zafaryab, Md., K. U. Fakhri, Md. A. Khan, Krishnan Hajela, and M. Rizvi. 2019. "In Vitro Assessment of Cytotoxic and Apoptotic Potential of Palmitic Acid for Breast Cancer Treatment." *International Journal of Life Sciences Research* 7(1):166–74.

Zhang, Chunfu, Kui Liu, Tao Li, Jie Fang, Yanling Ding, Lingxian Sun, Tao Tu, Xinyi Jiang, Shanmei Du, Jiabo Hu, Wei Zhu, Huabiao Chen, and Xiaochun Sun. 2016. "MiR-21: A Gene of Dual Regulation in Breast Cancer." *International Journal of Oncology* 48(1):161–72.

Zhang, Jiayu, Cheng Yang, Chunfu Wu, Wei Cui, and Lihui Wang. 2020. "DNA Methyltransferases in Cancer: Biology, Paradox, Aberrations, and Targeted Therapy." *Cancers* 12:1–22.

Zhang, Li, and Xinghua Long. 2015a. "Association of BRCA1 Promoter Methylation with Sporadic Breast Cancers: Evidence from 40 Studies." *Scientific Reports* 5(1):17869.

Zhang, Li, and Xinghua Long. 2015b. "Association of BRCA1 Promoter Methylation with Sporadic Breast Cancers: Evidence from 40 Studies." *Scientific Reports*.

Zhang, Qi, Sihong Lu, Tianfu Li, Liang Yu, Yunjian Zhang, Huijuan Zeng, Xueke Qian, Jiong Bi, and Ying Lin. 2019. "ACE2 Inhibits Breast Cancer Angiogenesis via Suppressing the VEGFa/VEGFR2/ERK Pathway." *Journal of Experimental and Clinical Cancer Research* 38(1):1–12.

Zheng, Ju Sheng, Xiao Jie Hu, Yi Min Zhao, Jing Yang, and Duo Li. 2013. "Intake of Fish and Marine N-3 Polyunsaturated Fatty Acids and Risk of Breast Cancer: Meta-Analysis of Data from 21 Independent Prospective Cohort Studies." *BMJ (Online)* 346:3706.

Zheng, Yinan, Brian T. Joyce, Lei Liu, Zhou Zhang, Warren A. Kibbe, Wei Zhang, and Lifang Hou. 2017. "Prediction of Genome-Wide DNA Methylation in Repetitive Elements." *Nucleic Acids Research* 45(15):8697–8711.

Zhu, X., L. Shan, F. Wang, J. Wang, F. Wang, G. Shen, X. Liu, B. Wang, Y. Yuan, J. Ying, and H. Yang. 2015. "Hypermethylation of BRCA1 Gene: Implication for Prognostic Biomarker and Therapeutic Target in Sporadic Primary Triple-Negative Breast Cancer." *Breast Cancer Research and Treatment* 150(3):479–86.

Zhu, Zaihua, Weida Meng, Peiru Liu, Xiaoxia Zhu, Yun Liu, and Hejian Zou. 2017.

"DNA Hypomethylation of a Transcription Factor Binding Site within the Promoter of a Gout Risk Gene NRBP1 Upregulates Its Expression by Inhibition of TFAP2A Binding." *Clinical Epigenetics* 9(1):99.

Zhu, Zhong Zheng, David Sparrow, Lifang Hou, Letizia Tarantini, Valentina Bollati, Augusto A. Litonjua, Antonella Zanobetti, Pantel Vokonas, Robert O. Wright, Andrea Baccarelli, and Joel Schwartz. 2011. "Repetitive Element Hypomethylation in Blood Leukocyte DNA and Cancer Incidence, Prevalence, and Mortality in Elderly Individuals: The Normative Aging Study." *Cancer Causes and Control* 22(3):437–47.

Ziech, Dominique, Rodrigo Franco, Aglaia Pappa, and Mihalis I. Panayiotidis. 2011. "Reactive Oxygen Species (ROS)--Induced Genetic and Epigenetic Alterations in Human Carcinogenesis." *Mutation Research - Fundamental and Molecular Mechanisms of Mutagenesis* 711:167–73.

Zorova, Ljubava D., Vasily A. Popkov, Egor Y. Plotnikov, Denis N. Silachev, Irina B. Pevzner, Stanislovas S. Jankauskas, Valentina A. Babenko, Savva D. Zorov, Anastasia V Balakireva, Magdalena Juhaszova, Steven J. Sollott, and Dmitry B. Zorov. 2018. "Mitochondrial Membrane Potential." *Analytical Biochemistry* 552:50–59.

APPENDIX A

GC-MS CHROMATOGRAMS

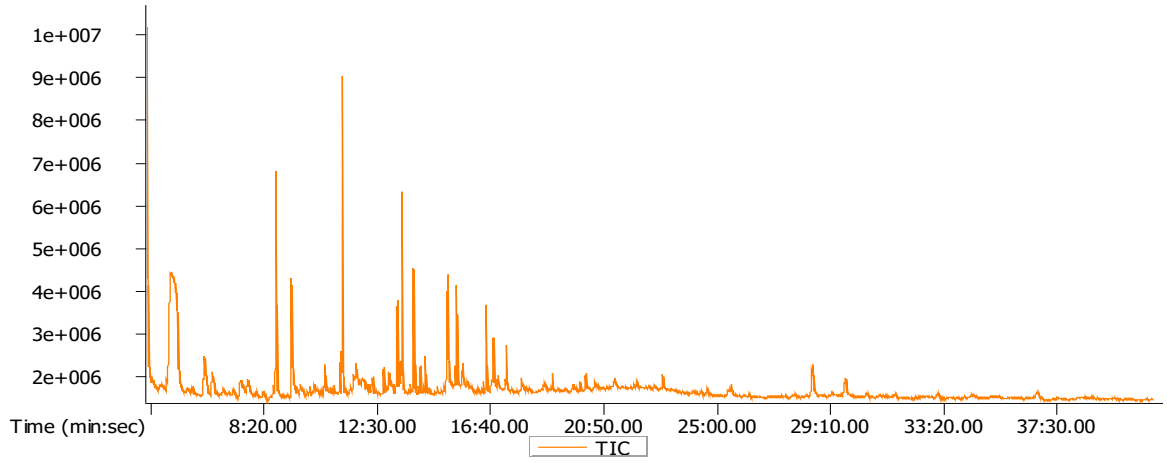

Figure A1: GC-MS chromatogram of the crude methanol extract of *Bidens pilosa.*

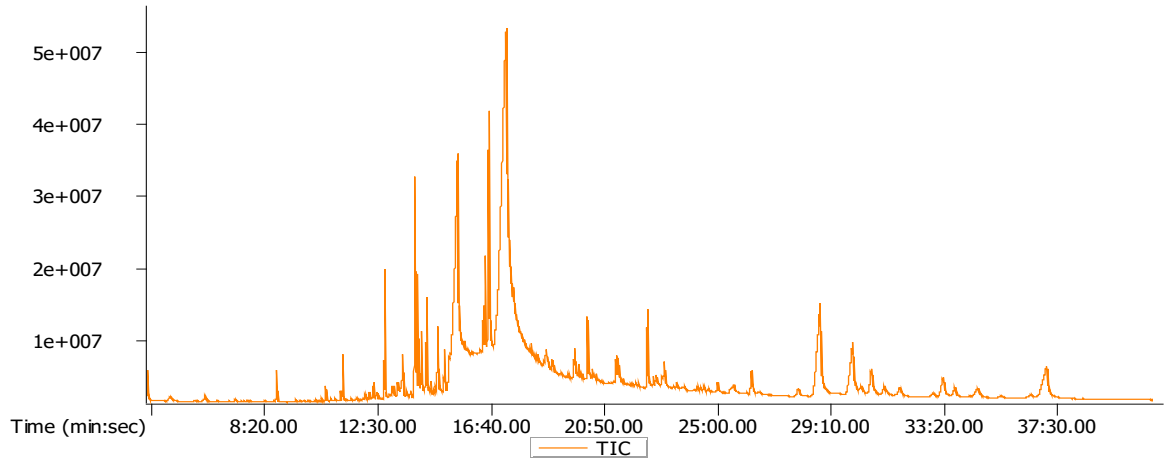

Figure A2: GC-MS chromatogram of the hexane fraction of the crude methanol extract of *Bidens pilosa.*

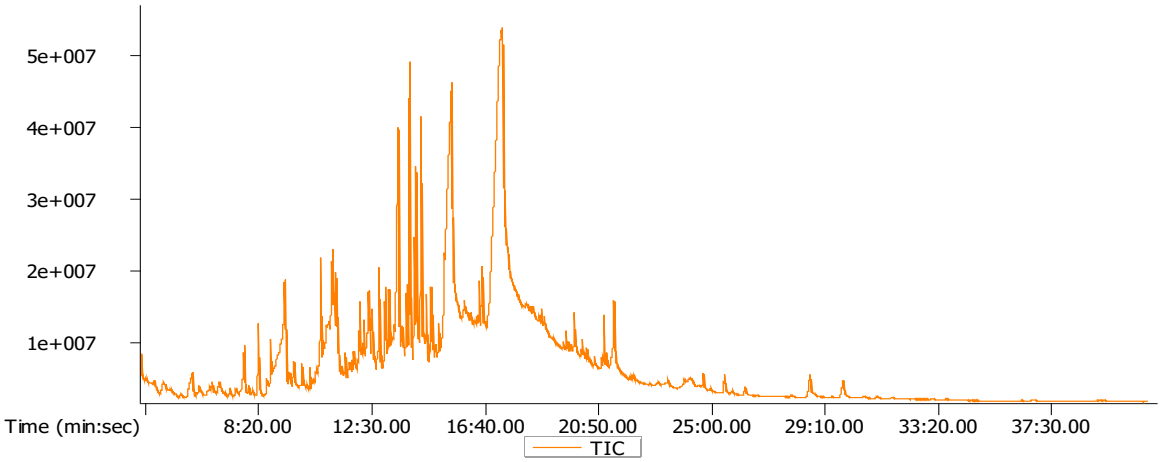

Figure A3: GC-MS chromatogram of the chloroform fraction of the crude methanol extract of *Bidens pilosa.*

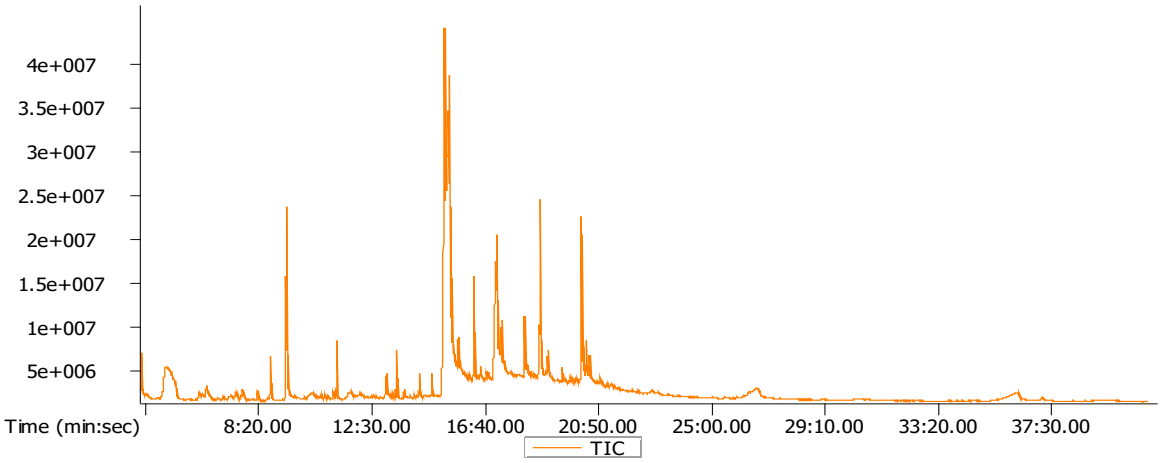

Figure A4: GC-MS chromatogram of the ethyl acetate fraction of the crude methanol extract of *Bidens pilosa.*

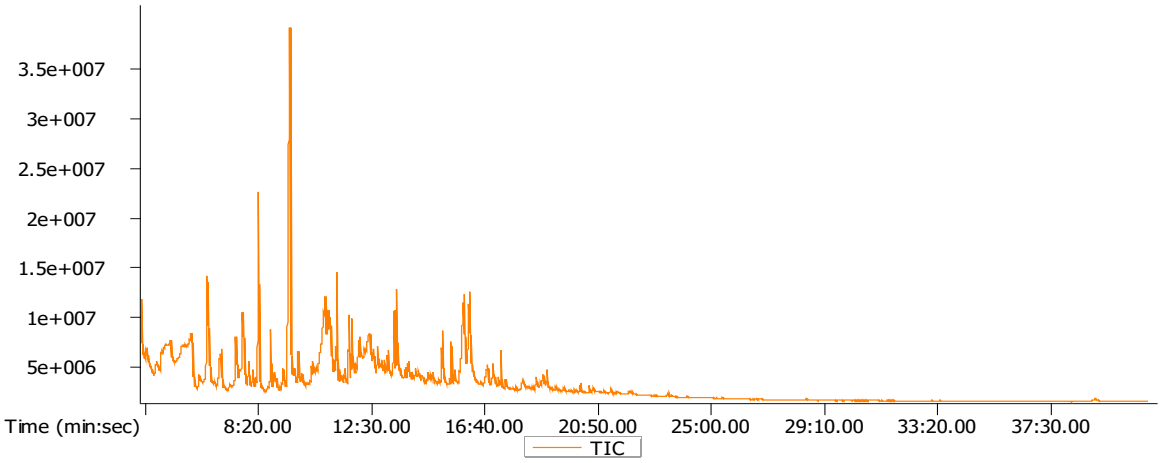

Figure A5: GC-MS chromatogram of the butanol fraction of the crude methanol extract of *Bidens pilosa.*

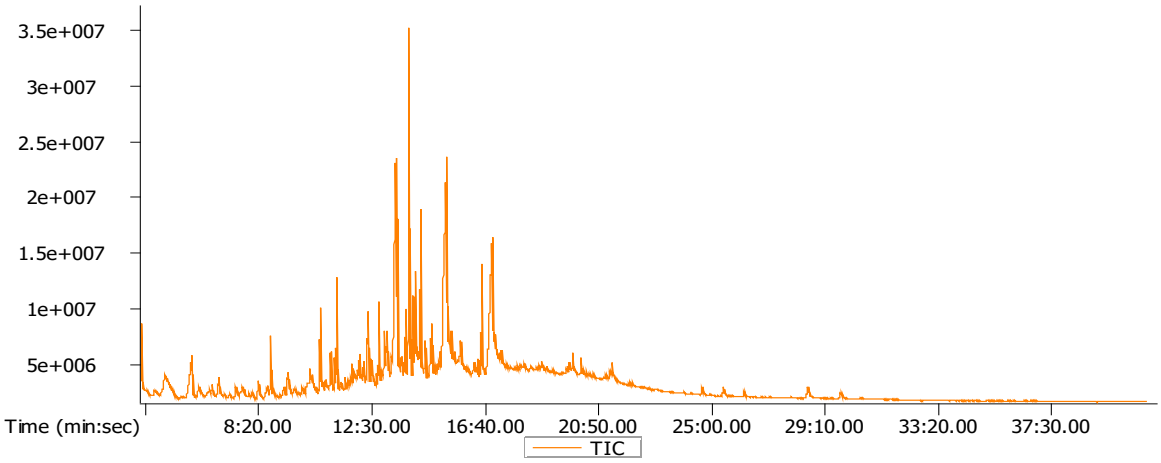

Figure A6: GC-MS chromatogram of the 65% methanol fraction of the crude methanol extract of *Bidens pilosa.*

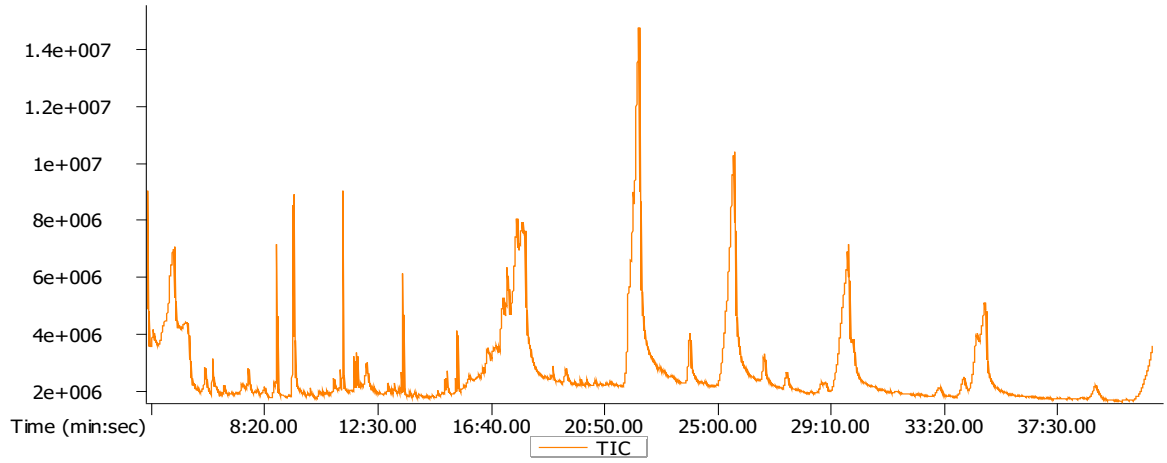

Figure A7: GC-MS chromatogram of the water fraction of the crude methanol extract of *Bidens pilosa*.